European Journal of Taxonomy 1120: 1–54
https://doi.org/10.5852/ejt.2026.1120.3355
This work is licensed under a Creative Commons Attribution License (CC BY 4.0)
europeanjournaloftaxonomy.eu
ISSN 2118-9773
2026 · Jaime S. *et al.*

Received: 11 November 2025 • *Accepted: 25 June 2026* • *Published: 10 November 2026*

Topic editor: Magalie Castelin • *Section editor: Fabio Stoch* • *Desk editor: Pepe Fernández*

Monograph

urn:lsid:zoobank.org:pub:B3C63D37-4F5C-46EA-810F-941EA5BD2940

A reevaluation of the North and Central American *Arctodiaptomus dorsalis* (Marsh, 1907) (Calanoida, Diaptomidae), with reallocation to the genus *Mastigodiaptomus* and description of a new species

Sarahi JAIME [1], Martha A. GUTIÉRREZ-AGUIRRE [2,*], Adrián CERVANTES-MARTÍNEZ [3], Eduardo SUÁREZ-MORALES [4] & Manuel ELÍAS-GUTIÉRREZ [5]

[1,2,3] División de Ciencias Multidisciplinarias, Universidad Autónoma del Estado de Quintana Roo. Av. Andrés Quintana Roo s/n Cozumel, Quintana Roo, 77600, México.
[4,5] Departamento de Sistemática y Ecología Acuática, El Colegio de la Frontera Sur (ECOSUR). Avenida del Centenario km 5.5, Chetumal, Quintana Roo, 77014, México.

[*] Corresponding author: margutierrez@uqroo.edu.mx
[1] Email: 1518305@uqroo.mx
[3] Email: adcervantes@uqroo.edu.mx
[4] Email: esuarez@ecosur.mx
[5] Email: melias@ecosur.mx

Abstract. The freshwater genus *Arctodiaptomus* Kiefer, 1932 is a Palaearctic genus, and comprises nearly 75 nominal species. *Arctodiaptomus dorsalis* (Marsh, 1907), a diaptomid species originally described within the genus *Diaptomus*, has long been reported throughout the Americas. Its morphology diverges from the generic diagnostic features; thus, its taxonomic position has been doubtful. Furthermore, its phenotypic variability has resulted in local synonymies and suggested it as a species complex. In this study, we reassign the taxonomic position of "*A. dorsalis*" based on the examination of type and non-type material from North and Central America, the analyses of mitochondrial *COI*, and biogeographic affinities. Our results show that the American populations attributed *to* "*A. dorsalis*" in the study area diverge genetically from the genus *Arctodiaptomus* by 27–29%, and share key diagnostic features with *Mastigodiaptomus* Light, 1939, therefore, this species should be transferred to that genus. Furthermore, the synonymized species *Diaptomus alter* Herbst, 1960 (Nicaragua), and *D. dampfi* Brehm, 1932 (Guatemala) were examined from type locality material and found to share the diagnostic characters of "*A.*" *dorsalis*. In addition, we describe *Mastigodiaptomus cucapa* sp. nov. linked before to "*A*". *dorsalis*, thus contributing to disentangle this taxonomic problem.

Keywords. *Arctodiaptomus*, free-living copepods, freshwater zooplankton, *Mastigodiaptomus*, mtCOI.

Jaime S., Gutiérrez-Aguirre M.A., Cervantes-Martínez A., Suárez-Morales E. & Elías-Gutiérrez M. 2026. A reevaluation of the North and Central American *Arctodiaptomus dorsalis* (Marsh, 1907) (Calanoida, Diaptomidae), with reallocation to the genus *Mastigodiaptomus* and description of a new species. *European Journal of Taxonomy* 1120: 1–54. https://doi.org/10.5852/ejt.2026.1120.3355

Introduction

Arctodiaptomus Kiefer, 1932 is a Palearctic (PA) genus of freshwater calanoid copepods. It included 75 valid species worldwide (Walter & Boxshall 2021), classified into five subgenera (Reddy 1994; Błędzki & Rybak 2016). Some species have been reported for the Nearctic region, including *A.* (*Rhabdodiaptomus*) *arapahoensis* (Dodds, 1915), *A.* (*R.*) *novosibiricus* (Kiefer, 1971), and *A.* (*Haplodiaptomus*) *kurilensis* Kiefer, 1937. Other representatives such as *A. floridanus* (Marsh, 1926), *A. asymmetricus* (Marsh, 1907), *A. saltillinus* (Brewer, 1898), and *A. dorsalis* (Marsh, 1907) are known from the Nearctic (NA), Mexican Transition Zone (MTZ), and Neotropical (NT) regions (Reid & Williamson 2010).

The present study revises the taxonomic position of "*A. dorsalis*", originally described within the genus *Diaptomus.* Previously, Dussart & Defaye (1983) suggested that "*A. dorsalis*" and its American congeners (i.e., *A. floridanus*, *A. asymmetricus*, *A. saltillinus*) may not belong to the genus *Arctodiaptomus*. Reddy (1994), excluded these species from his global revision of the genus without further clarification. The inclusion of *D. dorsalis* in *Arctodiaptomus* was based on the pincer-like spinous process on the male left P5 Exp2 according to Light (1939), who recommended a more detailed revision of its morphological characters; later, Dussart & Fernando (1985) referred to this species as "*Arctodiaptomus dorsalis*". Subsequent studies began naming this species *A. dorsalis* (i.e., Suárez-Morales *et al.* 1996; Suárez-Morales & Elías-Gutiérrez 2001; Reid 2007; Elías-Gutiérrez *et al.* 2008a, 2008b; Brandorff 2012; Papa *et al.* 2012; Hairston *et al.* 2025).

"*Arctodiaptomus dorsalis*" was originally described from Slidell County in Louisiana, USA (locality now disappeared). The species name refers to the keel-like dorsal projections on female's fourth and fifth pedigers (Marsh 1907; Reid 2007). It has been considered a widespread species across the Americas, from the USA to Colombia (Reid 2007). It has also been reported from Hawaii and the Phillipines, where it is considered an invasive introduced species (Papa *et al.* 2012; de Leon *et al.* 2020; Hairston *et al.* 2025).

Because of its morphological variability, "*A. dorsalis*" has long been regarded as a species complex, leading to taxonomic ambiguities and synonymies in different regions, such as *Diaptomus proximus* Kiefer, 1936 from Haiti, *D. alter* Herbst, 1960 from Nicaragua according with Dussart & Fernando (1985), and *D. dampfi* Brehm, 1932, from Guatemala, based on the taxonomical revision of Suárez-Morales & Elías-Gutiérrez (2001). Elías-Gutiérrez *et al.* (2008a) explored the genetic diversity of the freshwater cladocerans and copepods from Mexico and Guatemala, revealing that "*A. dorsalis*" is a species with high genetic diversity, suggesting that it might constitute a species complex

Considering that the genus *Arctodiaptomus* is primarily distributed in the PA, we hypothesize that this species may be more accurately assigned to a genus whose endemic American taxa share morphological distribution and morphological characters. In this study we propose to reassign "*A. dorsalis*" to the genus *Mastigodiaptomus* Light, 1939 based on the descriptions of the world-wide known copepods by Kiefer (1932) and Dussart & Defaye (1995), *COI* barcodes available for the studied area, and detailed morphological analysis of type material. We also describe a new species associated with the species complex.

Material and methods

This study includes seven American ecoregions as defined by Morrone (2015, 2017) and Escalante *et al.* (2021): Baja Californian, Sonoran, Austroriparian, Veracruzan, Yucatan Peninsula, Pacific Lowlands, and the Sierra Madre Occidental, distributed across two bioregions, the NA and NT, including the MTZ (Fig. 1).

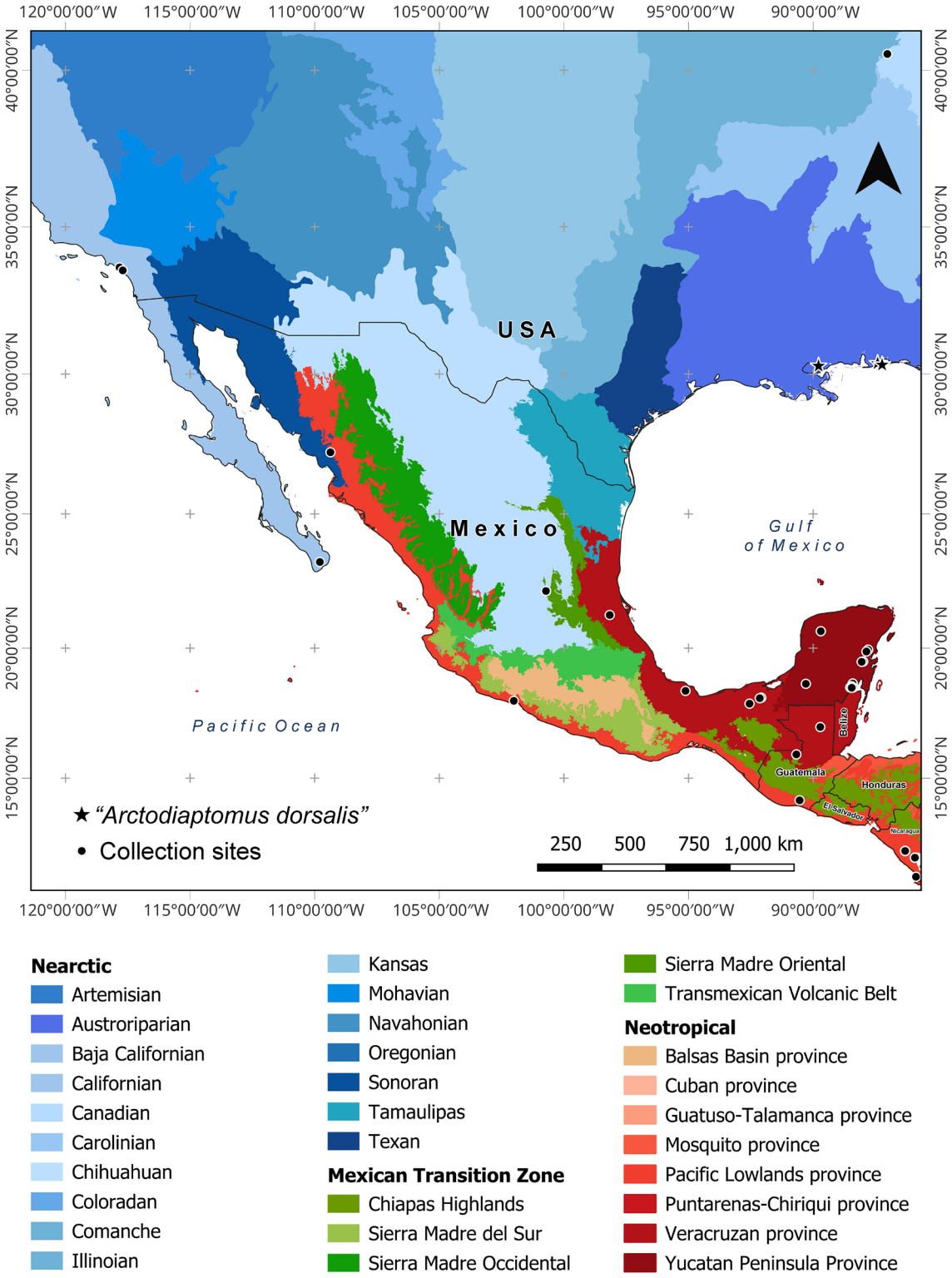


Fig. 1. Collection sites of analyzed specimens of "*Arctodiaptomus dorsalis*". Stars indicate specimens of "*A. dorsalis*" s. str. Ecoregions for both bioregions and the Mexican Transition Zone are based on Morrone (2015, 2017) and Escalante *et al*. (2021).

Taxonomic analysis

The nomenclatural history of the taxa related to "*A. dorsalis*" is presented in chronological order, taking into account previous analyses and descriptions by Marsh (1907, 1959), Brehm (1932, 1939), Kiefer (1936), Light (1939), Wilson (1959), Herbst (1960), Dussart & Defaye (1983), Collado *et al.* (1984), Dussart & Fernando (1985), Reddy (1994), Reed (1994), Suárez-Morales & Elías-Gutiérrez (2001), Reid (2007), Elías-Gutiérrez *et al.* (2008a, 2008b); in order to highlight the longstanding taxonomic uncertainty and problematic position of this species.

To address this uncertainty, an integrative approach combining molecular and morphological evidence was implemented to re-evaluate both the generic placement of "*A. dorsalis*" and its species-level identification.

A total of 222 mitochondrial Cytochrome Oxidase Subunit 1 (*COI*) DNA sequences were obtained from the Barcode of Life Data Systems (www.boldsystems.org, accession date: 2 Mar. 2026). This data includes genetic sequences from the Austroriparian ecoregion, the area were syntypes of "*A. dorsalis*" were recorded (Supp. file 1). These sequences were used to explore the genetic divergence within and between one Nearctic, one Neotropical, and two Palaearctic genera.

In order to re-evaluate the generic placement of "*A. dorsalis*", *COI* barcodes from Mexican representatives of the family Diaptomidae Baird, 1850 of *Mastigodiaptomus* and *Leptodiaptomus* Light, 1938 were included because of their geographical distributions overlap with previous records of "*A. dorsalis*" in the study area. Furthermore, genetic divergence was compared between the above mentioned genera, and some Palaearctic species of *Arctodiaptomus*: *A.* (*Arctodiaptomus*) *laticeps* (Sars G.O., 1863) and *A.* (*Stenodiaptomus*) *stewartianus* (Brehm, 1925), and *Metadiaptomus asiaticus* (Uljanin, 1875): this latter classified in Paradiaptominae Kiefer, 1932. A curated dataset named "*Mastigodiaptomus dorsalis* Taxonomic Revision" was created, including all compiled sequences available at https://doi.org/10.5883/DS-MDTS.

Subsequently, *COI* sequences were aligned to 575 base pairs (bp) with CLUSTAL W and default parameters. Pairwise genetic distances within and between groups (intra-, inter-specific, and intra-, intergeneric) were computed using the Kimura 2 Parameter (K2P) distance model. A Maximum Likelihood (ML) tree was inferred from the aligned sequences, and nodal support was assessed with 1000 bootstrap replicates. The tree was rooted with *M. asiaticus* as the outgroup. Five discrete Gamma categories with Invariant sites (G+I) were used to model distribution rate differences among sites (Kimura 1980). These analyses were performed using MEGA ver. 7. Both analyses together allowed the construction of generic identification to estimate between and within taxa, identify coherent sequence clusters, and determine the generic affinity of "*A. dorsalis*".

To complement the ML tree, multi-rate Poisson Tree Processes (mPTP) and Assemble Species by Automatic Partitioning (ASAP) species delimitation analyses (Kapli *et al*. 2017; Puilliandre *et al*. 2020) were carried out. Both methods provided an independent model-based evaluation of species boundaries, enabling us to detect separation between species and determine whether the American populations attributed to "*A. dorsalis*" correspond to a single or more species. These analyses supported and complemented the anatomical characteristics observations of biological material classified as "*A. dorsalis*", including examinations of syntype material, and to validate the separation of one new species described in this study.

The sequences of *A.* (*A.*) *laticeps* and *A.* (*S.*) *stewartianus* were excluded from the ASAP analysis to avoid algorithmic under-partitioning caused by their high genetic divergence. ASAP was performed using the software available in iTaxoTools (https://itaxotools.org/) (accession date: 13 Mar. 2026), whereas mPTP

was conducted at https://mptp.h-its.org/#/tree (accession date: 13 Mar. 2026), selecting *Metadiaptomus asiaticus* as outgroup (Saetang *et al.* 2022).

The morphological descriptions are based on the examination of type material and specimens deposited in the National Museum of Natural History, Washington D.C. (USNM), and the Colección de Zooplancton held at El Colegio de la Frontera Sur – ECOSUR, Chetumal, Quintana Roo, Mexico (ECO-CH-Z) (Supp. file 2).

Specimens from preserved samples were isolated and mounted on semipermanent slides showing the body and dissected appendages. Illustrations were made with a Nikon Y-IDT camera lucida attached to a Nikon Eclipse i50 light microscope.

Selected specimens were dehydrated through increasing ethanol concentrations up to absolute ethanol, followed by hexamethyl-disilazane (HMDS) drying for Scanning Electron Microscopy (SEM) with a JEOL JSM6010 microscope at ECOSUR-Chetumal, Mexico.

The morphological terminology follows Huys & Boxall (1991), with the following abbreviations:

A1 = antennule
A2 = antenna
ae = aesthetasc
Bs = basis
CR = caudal rami
Cx = coxa
Enp = endopod
Exp = exopod
LP5 = left fifth leg
Md = mandible
Mx1 = maxillule
Mx2 = maxilla
Mxp = maxilliped
P1–P5 = first to fifth legs
RP5 = right fifth leg
s = seta
sp = spine

Identification keys were constructed following the revisions of the genus *Mastigodiaptomus* by Wilson (1959), Elías-Gutiérrez *et al.* (2008b, 2023), Gutiérrez-Aguirre & Cervantes-Martínez (2013, 2016), Gutiérrez-Aguirre *et al.* (2014, 2020) and Suárez-Morales *et al.* (2020).

Results

Nomenclatural History of "Arctodiaptomus dorsalis"

The nomenclatural history of *Arctodiaptomus dorsalis* begins with Marsh (1907), who described *Diaptomus dorsalis* from material collected in Guzman and Slidell lakes in Louisiana. The species was diagnosed by the presence of dorsal processes on the female pedigers and a hyaline process on RP5 Bs. Marsh placed it within the *albuquerquensis* group (with *D. albuquerquensis* Herrick, 1895, *D. asymmetricus* Marsh, 1907, *D. purpureus* Marsh, 1907, and *D. saltillinus* Brewer, 1898, species currently ascribed as *Mastigodiaptomus albuquerquensis* (Herrick, 1895), *Arctodiaptomus asymmetricus*, *Mastigodiaptomus purpureus* (Marsh, 1907), and *Arctodiaptomus saltillinus*) based on shared morphological characters and overlapping distributions in the southern United States.

For Central America, Brehm (1932, 1939) described *D. dampfi* from Lake Petén, Guatemala, distinguishing it from *D. dorsalis* by the absence of dorsal processes on the female pedigers and a symmetrical urosome. Kiefer (1936) later described "*Diaptomus*" *proximus* from Haiti, noting its similarity to *D. dorsalis* but differing in the robustness of the distal spines on the P5.

A conceptual shift occurred with Light (1939); he proposed that several species, including *D. dorsalis*, *D. asymmetricus*, *D. saltillinus*, *D. floridanus* Marsh, 1926, and *D. proximus*, could be assigned to the subgenus *Arctodiaptomus*, although he emphasized the need for further study to confirm this placement.

Marsh (1959) and Wilson (1959) treated the species as *Diaptomus* (*Arctodiaptomus*) *dorsalis*. Marsh maintained *D.* (*A.*) *dorsalis* as distinct from *D.* (*A.*) *saltillinus* and *D.* (*A.*) *asymmetricus*, whereas Wilson considered *D.* (*A.*) *proximus* a synonym of *D.* (*A.*) *dorsalis* but retained *D.* (*A.*) *dampfi* as a valid species.

Herbst (1960) described *D. alter*, distinguishing it from related species based on genital somite asymmetry and male P5 morphology, including thick distal spines on the Cx and an aculeus on Exp2 of the RP5 lacking denticles.

Dussart & Defaye (1983) questioned the placement of several American species within *Arctodiaptomus* and assigned *D. dampfi* to *Mastigodiaptomus dampfi*, mentioning that a detailed generic revision was needed.

Dussart & Fernando (1985) first synonymized *Diaptomus alter* with *D. proximus*, thereby reducing the number of taxa within this group. Subsequently, they synonymized *D. proximus* with *D. dorsalis*. Following these taxonomic decisions, Collado *et al.* (1984) and Dussart & Fernando (1985) supported the combination "*Arctodiaptomus*" *dorsalis* based on morphological characters of P5, particularly the structure of the RP5 Enp, and the presence of a pincer-like process on the LP5 Exp2.

Reed (1994) placed this species within *Arctodiaptomus* (*Arctodiaptomus*) in his American classification of the genus, whereas Reddy (1994) excluded it from his global key to the genus.

Suárez-Morales and Elías-Gutiérrez (2001) synonymized *A. dampfi* with *A. dorsalis*, based on type material and morphological similarities among both species.

Reid (2007) and Elías-Gutiérrez *et al.* (2008b) documented a broad distribution of "*A. dorsalis*" from North to northern South America. Molecular evidence (Elías-Gutiérrez *et al.* 2008a) suggested that *A. dorsalis* represents a species complex.

The nomenclatural history of "*Arctodiaptomus dorsalis*" reveals a pattern of taxonomic uncertainity associated with its genus status. Given this context, the diagnostic morphological features defining the *Mastigodiaptomus* and *Arctodiaptomus* genera were reviewed based on the generic descriptions of Kiefer (1932), Light (1939), Reddy (1994), and Dussart & Defaye (1995), to provide a comparative framework for evaluating the taxonomic placement of "*A. dorsalis*".

Mastigodiaptomus Light, 1939: 1) Male RA1 with spiniform processes on segments 10, 11, 13, 14, 15, sometimes 16; antepenultimate segment with a small extension. 2) Male RP5 Bs with hyaline membrane caudally; Exp 1 short, posterior edge of inner margin with chitinous membrane; Exp2 longer than wide, with caudal hyaline membrane; aculeus inserted at distal third of outer margin, terminal claw long, curved. 3) Male LP5 Exp2 shorter than Exp1 and tapering gradually, ending in short process and inner spiniform seta inserted terminally; short Enp with row of fine hair-setae and two short setae. 4) Female P5 Exp3 with long spiniform seta and vestigial small seta. 5) Female P5 Enp ending in two curved rows of setules and two subapical setae.

Arctodiaptomus Kiefer, 1932: 1) Females A1 and males LA1 with two setae on segment 11. 2) Females and males with well-developed rostrum, with two more or less blunt spines. 3) Males RP5 Bs with hyaline lamella on inner side and proximal chitinous lobe. 4) Males LP5 Bs with hyaline lamella on inner margin, Exp2 ending in elongated digitiform process, with terminal pair of pincer spines. 5) Females with large wings on fifth pediger. 6) Female P5 Enp short, bearing only setules.

Genetic divergence within and between the analyzed taxa

The taxonomic uncertainty outlined for this species related to its morphology, was contrasted with genetic data. The molecular analysis based on the COI gene fragment reveals that all sequences attributed to "*A. dorsalis*" in the study area are distant from those of the Palaearctic *Arctodiaptomus* with a

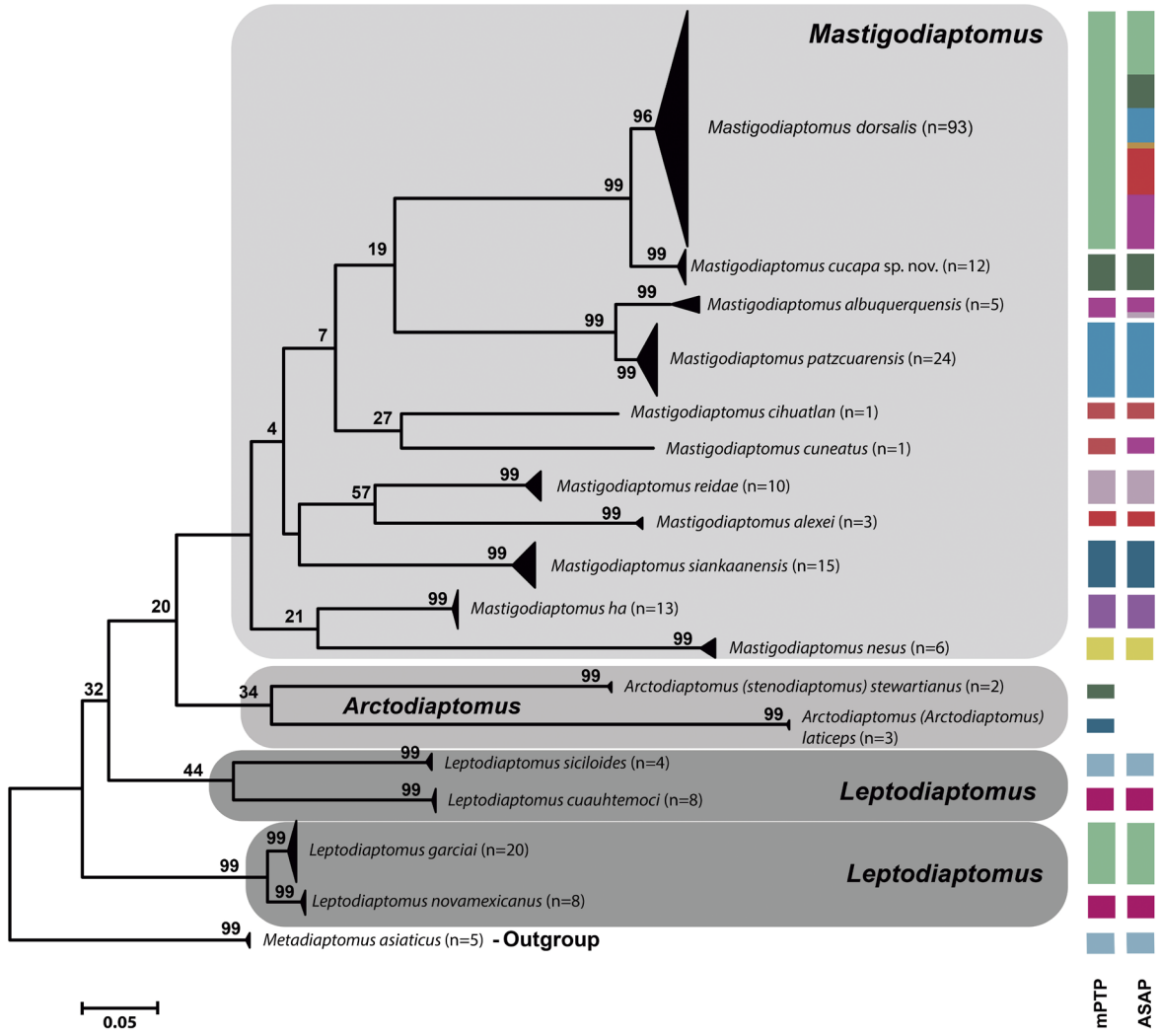


Fig. 2. Maximum Likelihood tree of K2P distances for 222 genetic sequences belonging to the genera *Mastigodiaptomus* Light, 1939, *Leptodiaptomus* Light, 1938, *Arctodiaptomus* Kiefer, 1932 and *Metadiaptomus* Methuen, 1910. Species delimited with mPTP and ASAP models. Each cluster collapsed in a vertical triangle. Horizontal depth indicates the level of genetic divergence within each group; vertical height indicates the sequences analyzed. Values on each branch indicate the node support.

genetic divergence of 27 to 29% (Fig. 2, Table 1), suggesting their distinct generic status. Accordingly, "*A. dorsalis*" is hereafter treated as *Mastigodiaptomus dorsalis* in Figure 2.

The analyzed species of *Leptodiaptomus* were inferred as at least two distinct clades in the ML tree. A weakly supported clade comprises *Leptodiaptomus siciloides* (Lilljeborg, 1889) and *L. cuauhtemoci* (Osorio-Tafall, 1941), whereas a second, well-supported, clade includes *L. garciai* and *L. novamexicanus*. This reconstruction probably reflects a partial resolution for *Leptodiaptomus* because only four species of this genus were considered here. In contrast, *Mastigodiaptomus* was represented by multiple sequences corresponding to 11 of the 16 known species, widely distributed in Mexico.

The mPTP reconstruction (Supp. file 4) recovered two separate clusters within *Leptodiaptomus*. In contrast, the ASAP analysis grouped the four analyzed species of *Leptodiaptomus* into a single genetic cluster (Supp. file 5).

Although the molecular analyses presented here cannot resolve the taxonomy at the subgeneric level within Diaptominae, they suggest that *Arctodiaptomus dorsalis* and *A. cucapa* sp. nov. are better assigned to the heterogeneous genus *Mastigodiaptomus*. In addition, the genetic divergence between the species of Diaptominae considered here and *M. asiaticus* (Paradiaptominae) ranged from 18.78 to 29.48%

Mastigodiaptomus dorsalis is represented by 93 sequences from a broad geographic range, including the southeastern United States, southern and southeastern Mexico, and Guatemala. This group exhibits moderate intraspecific genetic divergence (3.39%) and strong nodal support (bootstrap value = 96%) (Fig. 2, Table 1).

A second, well-supported cluster corresponds to *Mastigodiaptomus cucapa* sp. nov., comprising 12 sequences. This species is clearly differentiated from *M. dorsalis*, with an interspecific genetic distance of 8.7%, and shows low intraspecific divergence (0.31%) (Table 1).

Species delimitation analyses further support this pattern. The mPTP analysis recovered all sequences of *M. dorsalis* as a single species, distinct from *M. cucapa* sp. nov. (Fig. 2; Supp. file 3, Supp. file 4). In contrast, the ASAP analysis identified six groups within the *M. dorsalis* cluster (Supp. file 5). These groups were inferred for the most densely sampled species from the dataset (n = 93) and demonstrate genetic variation within this widely distributed species rather than discrete species-level entities. The specimens included in this group represents multiple localities across the Nearctic, Mexican Transition Zone, and Neotropical regions.

Therefore, we interpret ASAP partitions as reflecting intraspecific genetic and phenetic variability within *M. dorsalis* at the population level, combined with slight morphological variation as described in Table 3. Nevertheless, we do not rule out the possibility that further studies using additional markers are needed to better evaluate this variable species. The most important point is that both methods consistently delimit *M. cucapa* sp. nov. as a distinct species from the large cluster represented by *M. dorsalis*.

Table 1 (continued on next page). Intra- and interspecific genetic divergence percentage of mean K2P with standard deviation of the analyzed barcodes in this study. Genetic percentages of *Mastigodiaptomus dorsalis* (Marsh, 1907) comb. nov. and *Mastigodiaptomus cucapa* sp. nov. are marked in bold. Percentages inside gray box represent instraspecific distances. * = singletons. Locations from represented BINs are listed in Supp. file 1.

	Species	1	2	3	4	5	6	7	8	9	10	11	12	13	14	15	16	17	18	19	20	21	22	23	24	25	26
1	*A. stewartianus* BOLD:ADW9770	**0.2**																									
2	*L. cuauhtemoci* BOLD:AAZ8481	25.7 ± 3.4	**0.1**																								
3	*L. novamexicanus* BOLD:AAB2389	21.7 ± 3.1	18.9 ± 2.6	**0.1**																							
4	*L. siciloides* BOLD:ADM0938	22.4 ± 2.9	17.8 ± 2.4	20.3 ± 2.8	**0.2**																						
5	*L. garciai* BOLD:AAD0924	24.1 ± 3.5	21.0 ± 3.1	4.8 ± 1.1	19.6 ± 2.8	**0.5**																					
6	*A. laticeps* BOLD:AAD8192	25.7 ± 3.4	22.3 ± 3.0	26.0 ± 3.5	26.3 ± 3.6	26.2 ± 3.4	**0**																				
7	*M. albuquerquensis* BOLD:AAC4388, BOLD:AAC4390	24.1 ± 3.3	27.3 ± 3.5	27.1 ± 3.6	23.4 ± 3.0	26.3 ± 3.6	25.4 ± 3.2	**1.5**																			
8	*M. cihuatlan* BOLD:AAJ1590 *	26.8 ± 3.6	26.1 ± 3.5	28.7 ± 4.0	26.1 ± 3.4	25.2 ± 3.5	25.2 ± 3.2	19.7 ± 2.7	–																		
9	*M. patzcuarensis* BOLD:AAC4008, BOLD:ABZ7048	24.5 ± 3.4	23.5 ± 3.0	24.3 ± 3.3	21.0 ± 2.8	24.6 ± 3.3	24.9 ± 3.2	8.2 ± 1.4	21.0 ± 2.9	**1.3**																	
10	*M. reidae* BOLD:AAC8649	25.6 ± 3.4	22.6 ± 2.9	23.5 ± 3.3	23.5 ± 3.0	24.8 ± 3.4	29.1 ± 3.7	24.1 ± 3.1	20.6 ± 2.8	22.8 ± 2.9	**1.2**																
11	*M. siankaanensis* BOLD:AAF1222	25.5 ± 3.5	25.2 ± 3.3	25.7 ± 3.5	24.0 ± 3.1	23.9 ± 3.2	24.6 ± 3.3	20.2 ± 2.8	18.8 ± 2.6	20.2 ± 2.8	18.6 ± 2.6	**0.7**															
12	*M. nesus* BOLD:AAG9522	27.2 ± 3.7	26.8 ± 3.4	24.9 ± 3.4	25.4 ± 3.2	25.8 ± 3.4	25.4 ± 3.3	25.4 ± 3.2	26.8 ± 3.7	26.7 ± 3.3	24.0 ± 3.0	21.9 ± 3.0	**1**														
13	*M. alexei* BOLD:AAF1220	24.7 ± 3.4	22.1 ± 3.1	26.8 ± 3.6	23.2 ± 3.2	28.6 ± 4.0	27.1 ± 3.7	25.3 ± 3.4	22.8 ± 3.1	21.8 ± 3.0	18.2 ± 2.5	20.5 ± 2.9	25.4 ± 3.3	**0.4**													
14	*M. ha* BOLD:AAU1038	25.2 ± 3.4	19.4 ± 2.8	21.6 ± 3.0	18.8 ± 2.6	19.1 ± 2.7	27.1 ± 3.5	21.1 ± 2.9	20.7 ± 3.0	20.0 ± 2.7	19.5 ± 2.8	19.9 ± 2.7	20.5 ± 2.8	20.6 ± 2.9	**0.2**												
15	*M. cuneatus* BOLD:ACX8828 *	27.8 ± 3.7	24.5 ± 3.2	23.7 ± 3.2	20.8 ± 2.8	22.2 ± 3.1	23.0 ± 3.2	20.4 ± 2.7	18.1 ± 2.6	21.7 ± 3.0	22.2 ± 2.8	21.3 ± 2.9	25.6 ± 3.2	23.0 ± 3.2	17.3 ± 2.4	–											
16	***M. dorsalis* BOLD:ACE4750**	29.1 ± 3.9	24.1 ± 3.2	24.0 ± 3.3	23.8 ± 3.1	23.9 ± 3.3	26.3 ± 3.6	22.2 ± 3.0	20.8 ± 3.0	19.4 ± 2.8	23.5 ± 3.1	17.7 ± 2.5	26.2 ± 3.5	22.3 ± 3.1	18.7 ± 2.8	19.6 ± 2.7	**0.3**										
17	***M. dorsalis* BOLD:AAE0729**	30.1 ± 4.0	23.2 ± 3.1	22.3 ± 3.0	24.3 ± 3.1	22.1 ± 3.0	26.0 ± 3.5	23.5 ± 3.2	24.0 ± 3.4	19.6 ± 2.8	25.1 ± 3.4	20.3 ± 2.8	25.7 ± 3.4	23.2 ± 3.2	20.0 ± 3.0	21.7 ± 3.0	**3.87 ± 0.9**	**0.7**									
18	***M. dorsalis* BOLD:AEA6335, BOLD:ABZ3765**	25.9 ± 3.5	24.2 ± 3.1	23.7 ± 3.2	23.5 ± 3.1	22.4 ± 3.1	26.2 ± 3.5	21.0 ± 3.0	21.9 ± 3.0	19.3 ± 2.8	24.9 ± 3.3	19.6 ± 2.7	25.3 ± 3.4	22.6 ± 3.1	19.8 ± 2.8	20.2 ± 2.8	**2.8 ± 0.7**	**3.7 ± 0.8**	**1.1**								

Table 1 (continued). Intra- and interspecific genetic divergence percentage of mean K2P with standard deviation of the analyzed barcodes in this study. Genetic percentages of *Mastigodiaptomus dorsalis* (Marsh, 1907) comb. nov. and *Mastigodiaptomus cucapa* sp. nov. are marked in bold. Percentages inside gray box represent instraspecific distances. * = singletons. Locations from represented BINs are listed in Supp. file 1.

	Species	1	2	3	4	5	6	7	8	9	10	11	12	13	14	15	16	17	18	19	20	21	22	23	24	25	26
19	***M. dorsalis* BOLD:ABA0903**	27.8 ± 3.7	24.1 ± 3.2	23.4 ± 3.3	23.5 ± 3.1	23.1 ± 3.2	28.1 ± 3.9	23.1 ± 3.2	24.9 ± 3.4	20.2 ± 2.9	25.0 ± 3.3	20.2 ± 2.8	24.9 ± 3.3	22.6 ± 3.1	20.5 ± 2.9	20.7 ± 2.8	**3.9 ± 0.9**	**4.7 ± 1.0**	**3.6 ± 0.8**	**1**							
20	***M. dorsalis* BOLD:AEM6544**	27.8 ± 3.8	25.8 ± 3.4	23.8 ± 3.2	23.4 ± 3.1	22.7 ± 3.1	26.3 ± 3.6	22.3 ± 3.1	21.3 ± 3.0	19.9 ± 2.9	24.0 ± 3.1	19.5 ± 2.7	26.0 ± 3.3	22.2 ± 3.1	18.7 ± 2.7	19.1 ± 2.7	**2.1 ± 0.6**	**4.6 ± 1.0**	**3.3 ± 0.8**	**4.7 ± 1.0**	**0.6**						
21	***M. dorsalis* BOLD:ACE4752**	28.5 ± 3.8	23.6 ± 3.1	24.0 ± 3.3	23.8 ± 3.1	24.0 ± 3.3	25.9 ± 3.6	22.0 ± 3.1	22.8 ± 3.2	19.8 ± 2.9	22.9 ± 3.1	18.6 ± 2.6	24.5 ± 3.3	22.2 ± 3.1	20.2 ± 2.9	20.7 ± 2.8	**1.6 ± 0.6**	**3.1 ± 0.9**	**2.1 ± 0.6**	**3.2 ± 0.8**	**2.5 ± 0.7**	**0**					
22	***M. dorsalis* s.str. BOLD:AAV0647**	26.6 ± 3.6	23.6 ± 3.1	21.6 ± 3.0	22.1 ± 3.0	21.2 ± 3.0	25.5 ± 3.5	20.8 ± 3.0	22.8 ± 3.2	18.6 ± 2.8	24.2 ± 3.2	19.7 ± 2.8	23.2 ± 3.1	23.5 ± 3.3	18.6 ± 2.7	20.0 ± 2.8	**3.5 ± 0.9**	**4.1 ± 1.0**	**3.4 ± 0.9**	**4.6 ± 1.0**	**4.1 ± 1.0**	**2.7 ± 0.8**	**0**				
23	***M. cucapa* sp. nov. BOLD:AAF4891, BOLD:AEC2215**	28.0 ± 3.8	24.1 ± 3.2	22.3 ± 3.0	22.2 ± 3.1	22.2 ± 3.0	25.9 ± 3.5	22.3 ± 3.1	20.6 ± 3.0	19.8 ± 2.9	23.5 ± 3.02	18.1 ± 2.6	25.8 ± 3.5	26.5 ± 3.7	18.7 ± 2.7	20.7 ± 2.9	**6.9 ± 1.4**	**9.0 ± 1.7**	**8.3 ± 1.6**	**8.5 ± 1.6**	**8.0 ± 1.5**	**7.6 ± 1.5**	**6.2 ± 1.3**	**0.3**			
24	***M. dorsalis* BOLD:AAE6395**	27.2 ± 3.7	23.6 ± 3.1	23.2 ± 3.2	21.9 ± 3.0	20.8 ± 2.9	25.3 ± 3.4	21.4 ± 3.0	22.9 ± 3.2	19.0 ± 2.7	23.0 ± 18.1	18.6 ± 2.6	23.6 ± 3.1	22.4 ± 3.1	17.0 ± 2.4	19.1 ± 2.7	**4.1 ± 1.0**	**5.2 ± 1.1**	**4.0 ± 1.0**	**4.8 ± 1.0**	**4.6 ± 1.0**	**3.4 ± 0.9**	**3.4 ± 0.9**	**6.2 ± 1.3**	**0.5**		
25	***M. dorsalis* BOLD:AAE6394 ***	29.0 ± 4.0	23.2 ± 3.0	22.0 ± 3.0	23.3 ± 3.1	21.2 ± 3.0	25.9 ± 3.6	20.8 ± 3.0	22.8 ± 3.1	18.3 ± 2.7	22.7 ± 3.0	17.9 ± 2.5	23.2 ± 3.1	21.4 ± 3.0	17.9 ± 2.6	18.5 ± 2.6	**3.0 ± 0.9**	**3.1 ± 0.9**	**3.1 ± 0.8**	**3.9 ± 0.9**	**3.6 ± 0.9**	**2.2 ± 0.7**	**1.8 ± 0.6**	**6.0 ± 1.3**	**2.5 ± 0.7**	–	
26	*L.* c.f. *novamexicanus* BOLD:AAB2390 *	21.2 ± 3.1	21.0 ± 2.9	6.2 ± 1.2	17.9 ± 2.6	6.8 ± 1.4	25.8 ± 3.5	25.0 ± 3.3	24.0 ± 3.2	24.0 ± 3.3	23.3 ± 3.1	22.8 ± 3.0	28.0 ± 3.8	26.9 ± 3.6	19.5 ± 2.7	22.2 ± 3.0	21.1 ± 2.9	20.2 ± 2.9	19.7 ± 2.8	21.0 ± 2.9	20.9 ± 2.9	21.1 ± 2.9	19.6 ± 2.8	20.9 ± 2.3	20.5 ± 2.8	20.7 ± 2.9	–

Taxonomy

Class Copepoda Milne Edwards, 1840
Order Calanoida Sars G.O., 1903
Family Diaptomidae Baird, 1850
Genus *Mastigodiaptomus* Light, 1939

Mastigodiaptomus dorsalis (Marsh, 1907) comb. nov.
Figs 3–17

Diaptomus dorsalis Marsh, 1907: 408, 467–468, pl. XXIII figs 8–9, pl. XXIV, figs 2–3, 5–6.
Diaptomus dampfi Brehm, 1932: 63–66.
"*Diaptomus*" *proximus* Kiefer, 1936: 268–271, abb. 1–8.

Diaptomus dampfi – Brehm 1939: 175–177, 194–195, pl. 35 figs 1–4. — Wilson 1959: 778.
"*Diaptomus*" *proximus* – Light 1939: 476.
Diaptomus dorsalis – Light 1939: 476. — Marsh 1959: 769, fig. 1202. — Wilson 1959: 739, 778, fig. 29.62 a–d.
Diaptomus alter – Herbst 1960: 28–32, abb. 3–7.
Arctodiaptomus dorsalis – Smith & Fernando 1978: 2017–2018, figs 11–13. — Dussart & Defaye 1983: 66, 212. — Collado *et al.* 1984: 91–92, figs 2–4. — Dussart & Fernando 1985: 204–206, figs 28–32. — Reed 1994: 671, 676. — Suárez-Morales *et al.* 1996: 95–100, 107, fig. 18; 2020: 678–679, fig. 21.7b. — Suárez-Morales & Elías-Gutiérrez 2001: 13–15, figs 1–14. — Elías-Gutiérrez *et al.* 2008b: 174, fig. 8. — Reid & Williamson 2010: 832, 835, 857, 861, figs 21.2a, 21.6a, 21.12f–g. — Brandorff 2012: 192–193, 195. — Velazquez-Ornelas *et al.* 2021: 33–34, 104, figs 14–16.

Type material

Syntypes

USA – **Louisiana** • 1 ♀, 1 ♂, permanent slide with partly dissected specimens, incomplete female; Lake Slidell; 24 Oct. 1903; E.A. Birge leg.; USNM 309758 • 7 ♂♂, permanent slide with complete adults in lateral view; Guzman; E.A. Birge leg.; USNM 296403.

Other material examined

GUATEMALA – **Amatitlán** • 6 ♂♂, specimens mounted in semipermanent slides; Lake Amatitlán; 14.131° N, 90.541° W; 5 Jun. 2017; A. Cervantes-Martínez, J.R. Juárez-Pernillo and E.M. Reyes-Solares leg.; ECO-CH-Z-10527, ECO-CH-Z-10662, ECO-CH-Z-10663 • 3 ♀♀; same data as for preceding; ECO-CH-Z-10528, ECO-CH-Z-10529, ECO-CH-Z-10659 • 8 ♀♀; same data as for preceding; ECO-CH-Z-10660, ECO-CH-Z-10661 • 1 ♂; same data as for preceding; ECO-CH-Z-10664. – **Petén** • 2 ♀♀, specimen mounted in semipermanent slide; Lake Petén; 16.981° N, 89.712° W; 4 Jul. 1999; M. Elías-Gutiérrez leg.; ECO-CH-Z-10665, ECO-CH-Z-10669 • 2 ♀♀, 2 ♂♂; same data as for preceding; ECO-CH-Z-10666 • 2 ♂♂; same data as for preceding; ECO-CH-Z-10667 • 3 ♀♀; same data as for preceding; ECO-CH-Z-10668.

MEXICO – **Campeche** • 56 ♀♀, 46 ♂♂, sample preserved with 96% ethanol and a drop of glycerol; Pond 2 Jonuta-Escárcega; 18.063° N, 92.017° W; 26 Jun. 2011; M. Elías-Gutiérrez leg.; BOLD:AAE0729; ECO-CH-Z-10650. – **Guerrero** • 5 ♂♂, specimens mounted in semipermanent slide; pond in Lázaro Cárdenas Highway; 17.987° N, 102.013° W; 19 Sep. 2004; M. Elías-Gutiérrez leg.; ECO-CH-Z-10632 • 4 ♀♀; same data as for preceding; ECO-CH-Z-10633 • 5 ♀♀; same data as for preceding; ECO-CH-Z-10634 • 30 ♀♀, 10 ♂♂; sample preserved with 96% ethanol and a drop of glycerol; same data as for preceding; ECO-CH-Z-10635. – **Quintana Roo** • 5 ♀♀, 15 ♂♂, sample preserved with 96% ethanol and a drop of glycerol; Felipe Carrillo Puerto, lagoon at Km 170; 19.873° N,

97.861° W; 2 Mar. 2001; M. Elías-Gutiérrez leg.; ECO-CH-Z-10520 • 5 ♀♀, specimens mounted in semipermanent slide; same data as for preceding; ECO-CH-Z-10521 • 4 ♀♀; same data as for preceding; ECO-CH-Z-10522, ECO-CH-Z-10523 • 5 ♂♂; same data as for preceding; ECO-CH-Z-10524 • 8 ♂♂; same data as for preceding; ECO-CH-Z-10525, ECO-CH-Z-10656 • 6 ♂♂; same data as for preceding; ECO-CH-Z-10526, ECO-CH-Z-10657, ECO-CH-Z-10658 • 8 ♀♀; same data as for preceding; ECO-CH-Z-10654, ECO-CH-Z-10655 • 30 ♀♀, 30 ♂♂, sample preserved with 96% ethanol and a drop of glycerol; Bacalar, Cocalitos sinkhole; 18.650° N, 88.409° W; 28 Jun. 2015; M. Elías-Gutiérrez leg.; BIN no: BOLD:ACE4750; ECO-CH-Z-10651 • 1 ♀, specimen mounted in semipermanent slide; same data as for preceding; ECO-CH-Z-11619 • 10 ♀♀, 11 ♂♂, sample preserved with 96% ethanol and a drop of glycerol; Bacalar, Cenote Azul; 18°646° N, 88.458° W; 29 May 1997; A. Cervantes-Martínez and M. Gutiérrez-Aguirre leg.; ECO-CH-Z-10535 • 1 ♀, specimen mounted in semipermanent slide; same data as for preceding; 25 Aug. 2008; P. Quiroz-Vázquez and J.A. Cohuo-Collí leg.; ECO-CH-Z-5313 • 2 ♂♂; same data as for preceding; ECO-CH-Z-5314, ECO-CH-Z-5315 • 2 ♀♀, 2 ♂♂, specimens mounted in semipermanent slide; Othón P. Blanco, Laguna Puente Milagros; 18.503° N; 88.451° W; 14 Sep. 2011; M. Elías-Gutiérrez leg.; BIN no: BOLD:ABA0903; ECO-CH-Z-10652 • 2 ♀♀; same data as for preceding; ECO-CH-Z-10653 • 15 ♀♀, 15 ♂♂, sample preserved with 96% ethanol and a drop of glycerol; Othón P. Blanco, Laguna Negra; 18.5° N, 88.394° W; 7 Sep. 2011; M. Elías-Gutiérrez leg.; BIN no: BOLD:ABA0903; ECO-CH-Z-11620. – **San Luis Potosí** • 30 ♀♀, 30 ♂♂, sample preserved with 96% ethanol and a drop of glycerol; San José Dam; 22.150° N, 101.055° W; 8 Jun. 2021; A. Cervantes-Martínez, M.A. Gutiérrez-Aguirre and S. Jaime leg.; ECO-CH-Z-10597 • 6 ♀♀, specimens mounted in semipermanent slide; same data as for preceding; ECO-CH-Z-10598 to ECO-CH-Z-10600 • 12 ♀♀; same data as for preceding; ECO-CH-Z-10601, ECO-CH-Z-10602, ECO-CH-Z-10630 • 5 ♂♂; same data as for preceding; ECO-CH-Z-10603 • 8 ♂♂; same data as for preceding; ECO-CH-Z-10604, ECO-CH-Z-10628 • 5 ♀♀; same data as for preceding; ECO-CH-Z-10629 • 1 ♀, 1 ♂; same data as for preceding; ECO-CH-Z-11618. – **Tabasco** • 20 ♀♀, 36 ♂♂, sample preserved with 96% ethanol and a drop of glycerol; Laguna Vernet; 17.877° N, 92.550° W; 25 May 2011; M. Elías-Gutiérrez leg.; BIN no: BOLD:AAE0729; ECO-CH-Z-10649. – **Veracruz** • 3 ♀♀, 20 ♂♂, sample preserved with 96% ethanol and a drop of glycerol; Lago de Catemaco; 18.371° N, 95.115 ° W; 14 Oct. 1998; M. Elías-Gutiérrez leg.; ECO-CH-Z-10605 • 5 ♀♀, specimens mounted in semipermanent slide; same data as for preceding; ECO-CH-Z-10606 • 5 ♂♂; same data as for preceding; ECO-CH-Z-10607 • 5 ♀♀, 7 ♂♂, sample preserved with 96% ethanol and a drop of glycerol; Km 50 Tampico-Veracruz highway, ephemeral pond; 21.249° N, 95.116° W; 10 Sep. 2005; M. Elías-Gutiérrez leg.; ECO-CH-Z-10530 • 5 ♀♀, specimens mounted in semipermanent slide; same data as for preceding; ECO-CH-Z-10531 • 2 ♀♀; same data as for preceding; ECO-CH-Z-10532 • 3 ♂♂; same data as for preceding; ECO-CH-Z-10533 • 2 ♂♂; same data as for preceding; ECO-CH-Z-10534 • 4 ♀♀; same data as for preceding; ECO-CH-Z-10631. – **Yucatán** • 7 ♀♀, 3 ♂♂, sample preserved with 96% ethanol and a drop of glycerol; Cenote Abalá; 20.645° N, 89.685° W; 4 Aug. 2008; M. Elías-Gutiérrez leg.; ECO-CH-Z-10648.

NICARAGUA – **Managua** • 5 ♀♀, 6 ♂♂, dissected specimens mounted in slide from sample preserved with ethanol; Lake Managua; approx. coordinates 12.16° N; 86.32° W; 23 Mar. 1995; L. Moreno leg.; USNM 243712 • 1 ♂, dissected specimen mounted in slide from sample preserved with ethanol; Lake Masaya; approx. coordinates 11.96° N, 86.12° W; 23 Mar. 1991; L. Moreno leg.; USNM 243704 • 2 ♀♀, 1 ♂, dissected specimens mounted in slide from sample preserved with ethanol; Lake Cociboca; 11.12° N, 85.87° W; 13 Jun. 1997; L. Moreno leg.; USNM 243719.

USA – **Florida** • 4 ♀♀, 5 ♂♂, dissected specimens mounted in slide from sample preserved with ethanol; Pensacola, Santa Rosa Island, Pond 3; 30.32° N, 87.23° W; 15 Apr. 1958; G.E. Walsh leg.; USNM 122758 • 2 ♀♀; same data as for preceding; USNM 204671 • 1 ♀, 2 ♂♂, specimens mounted in two slides; Lake George, stn #3680; 29.214° N, 81.382° W; 21 Mar. 1897; W.C. Kendall leg.; USNM 309760 • 4 ♂♂, 1 ♀, specimens mounted in two slides; same data as for preceding but stn #3681; USNM 309760.

Table 2. Armature of swimming legs 1–4 observed in all the specimens analyzed in this study. Arabic numerals = setae; Roman numerals = spines.

legs	Cx	Bs	Exp	Enp
P1	0-1	0-0	I-1, 0-1, I-3-2	0-1, 0-2-3
P2	0-1	0-0	I-1, I-1, I-3-3	0-1, 0-2, 0-2-3-2
P3	0-1	0-0	I-1, I-1, I-3-3	0-1, 0-2, 0-2-3-2
P4	0-1	0-1	I-1, I-1, I-3-3	0-1, 0-2, 0-2-3-2

Description

Female (character states are shared by all specimens examined in North and Central America. Description based on specimens from Santa Rosa Island, Pensacola, Florida).

Habitus (Fig. 3A–B). Body length of 950–1320 µm excluding caudal setae. Prosome with five pedigers, keel-like projections on fourth pediger, and rounded process on fifth pediger (Figs 3B, 4A–B). Short metasomal wings with two distal spines, slightly asymmetrical (Figs 3A, 4A). A1 reaching end of CR (Fig. 3B). Rostrum with paired spines slightly curved inwards, thick and ending in acute tip (Fig. 3C–D).

Urosome (Fig. 4). Three-segmented, smooth dorsoventrally. Genital double-somite longer than wide, with spine on both margins proximally (Fig. 4A–B). Genital operculum proximally, oval-shaped in ventral view, with rugose free margin (Fig. 4C). Second somite 0.2 times as long as first somite, integument slightly rugose distally in ventral view. Anal somite twice as long as second somite (Fig. 4B, D). CR with setules on both margins and six caudal setae (Fig. 4D).

A1 (Fig. 5A). 25-segmented, setal formula as follows: 1 (1s+1ae), 2 (3s+1ae), 3 (1s+1ae), 4 (1s), 5 (1s+1ae), 6 (1s), 7 (1s+1ae), 8 (1sp+1s), 9 (2s+1ae), 10 (1s), 11 (1s), 12 (1sp+1s+1ae), 13 (1s), 14 (1s+1ae), 15 (1s), 16 (1s+1ae), 17 (1s), 18 (1s), 19 (1s+1ae), 20 (1s), 21 (1s), 22 (2s), 23 (2s), 24 (2s), 25 (5s+1ae).

A2 (Fig. 5B). Cx small with one seta. Bs elongated, with two distal setae. Enp two-segmented; Enp1 with inner row of spines and two outer setae, Enp2 with two lobes, with eight and seven setae, respectively, second lobe with proximal row of minute spines. Exp seven-segmented with setal armature as 1, 3, 1, 1, 1, 1, 1–3.

Md (Fig. 6A). Gnathobase with seven bidented denticles, a spine and outer spiniform seta, inner distal spine on projection. Cx smooth. Bs with four inner proximal setae. Enp three-segmtented, first segment without armature, second segment with four setae, third segment with five setae and two rows of minute proximal spinules. Exp 4-segmented with setal armature as 1, 1, 1, 3.

Mx1 (Fig. 6B). Precoxal arthrite with 14 spiniform setae. Coxal epipodite with nine setae. Basal exite with spine. Basal endite with four setae. Bs with four setae. Enp three-segmented with setal formula as 4, 2, 4; Enp1 with distal setules. Exp with six setae.

Mx2 (Fig. 6C). Praecoxa with two lobes, with five and three setae, respectively. Cx with two lobes bearing three setae each. Allobasis with three setae, distal lobe with single seta. Enp three-segmented with setal formula as 1, 1, 2.

Mxp (Fig. 6D). Praecoxa and Cx fused. Praecoxa with single seta. Cx with tree lobes, first lobe with two setae and setules, second with three setae, third lobe with setules, four spiniform setae and rounded projection with row of spinules. Bs elongated, with setules and three proximal setae. Enp six-segmented, first segment fused to second, with setal formula as 2, 3, 2, 2, 2, 4.

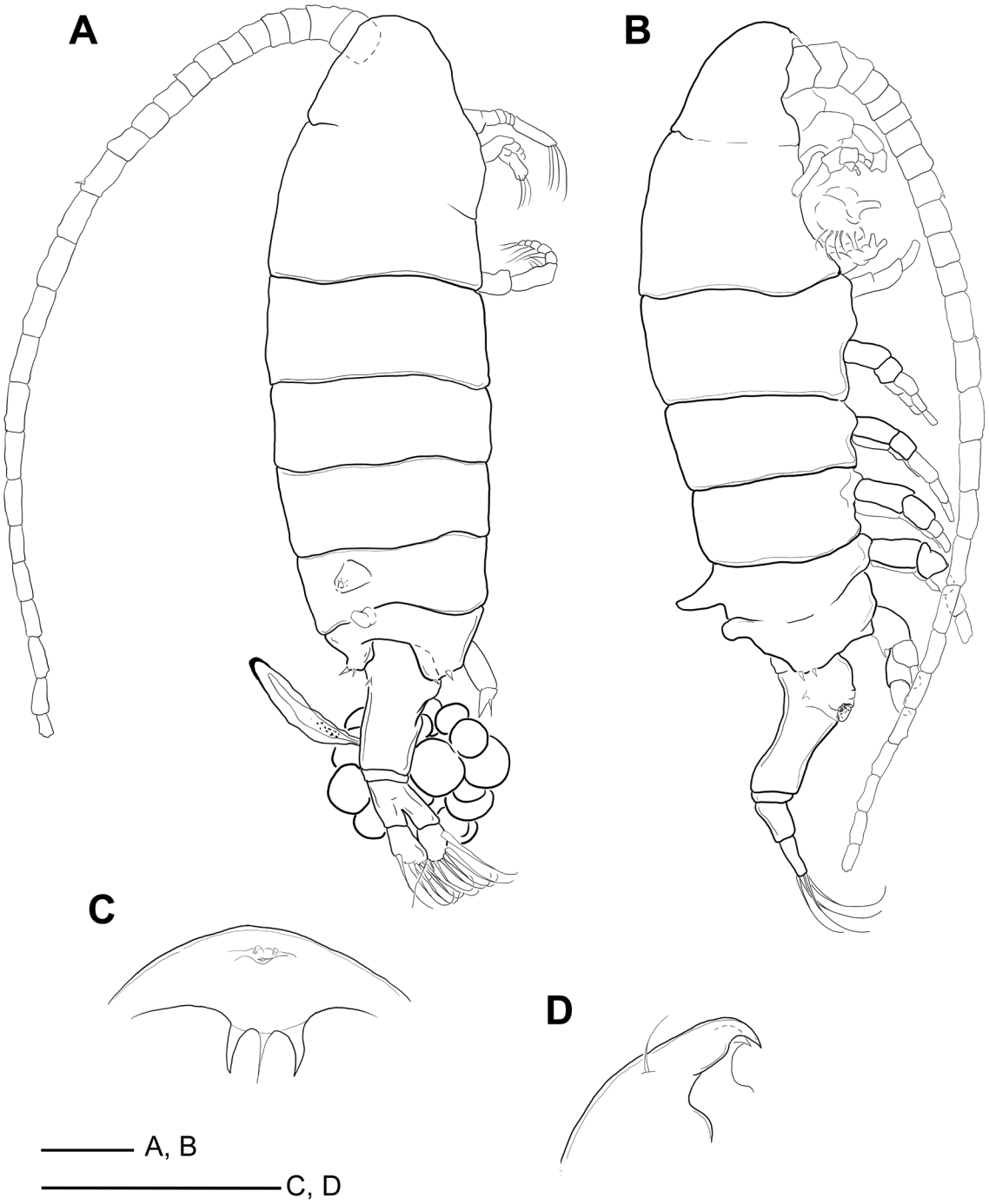


Fig. 3. *Mastigodiaptomus dorsalis* (Marsh, 1907) comb. nov. Adult, ♀ (USNM 122758, Santa Rosa Island, Pensacola, Florida). **A**. Habitus in dorsal view. **B**. Habitus in lateral view. **C**. Rostrum in ventral view. **D**. Rostrum in lateral view. Scale bars = 100 µm.

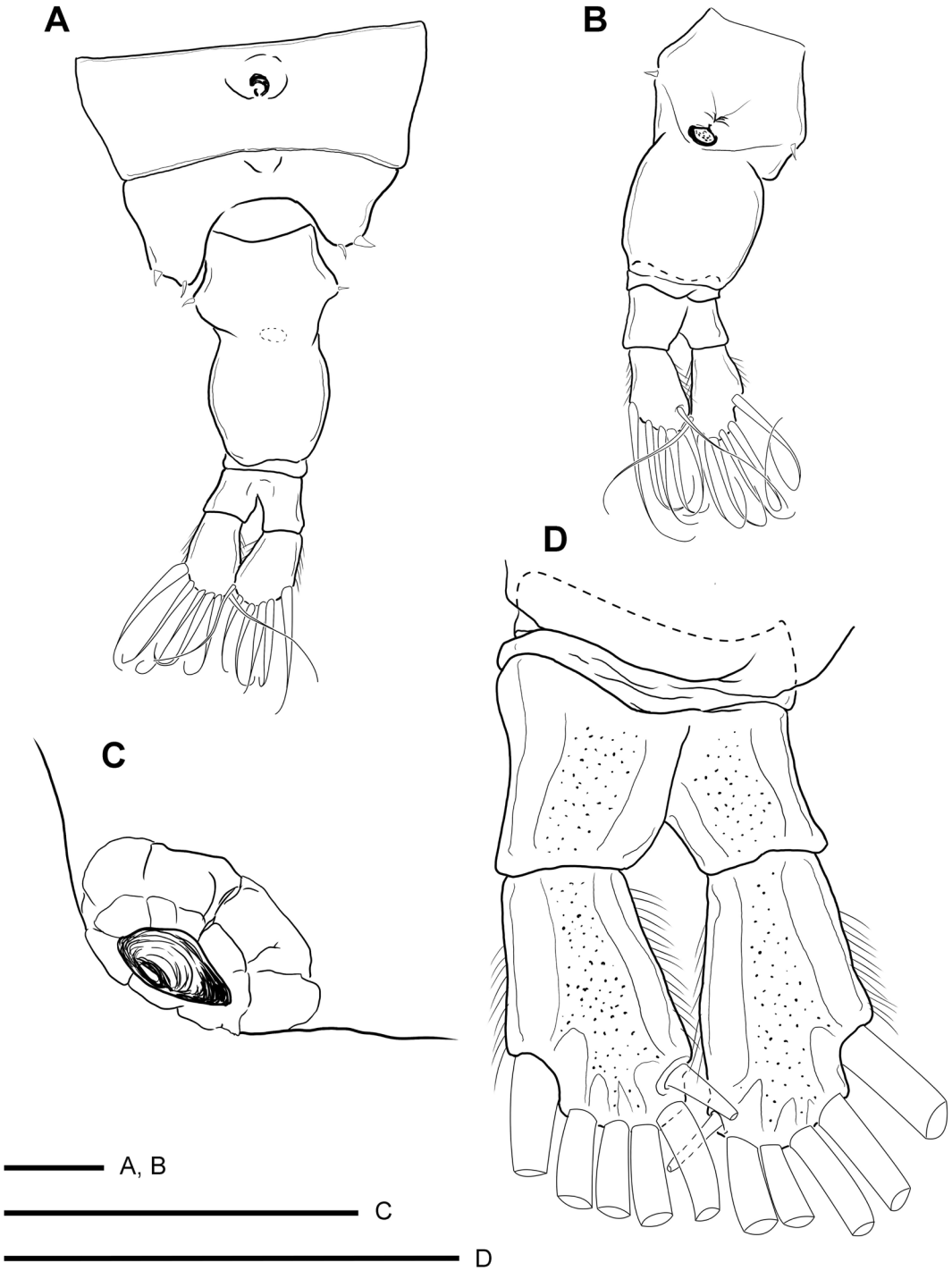


Fig. 4. *Mastigodiaptomus dorsalis* (Marsh, 1907) comb. nov. Adult, ♀ (USNM 122758, Santa Rosa Island, Pensacola, Florida). **A**. Urosome in dorsal view. **B**. Urosome in ventral view. **C**. Genital operculum. **D**. Anal somite and caudal rami in ventral view. Scale bars = 100 µm.



Fig. 5. *Mastigodiaptomus dorsalis* (Marsh, 1907) comb. nov. Adult, ♀ (USNM 122758, Santa Rosa Island, Pensacola, Florida). **A**. Antennule. **B**. Antenna. Asterisks indicate separation of A1 segments. Abbreviations: see Material and methods. Scale bars =100 μm.

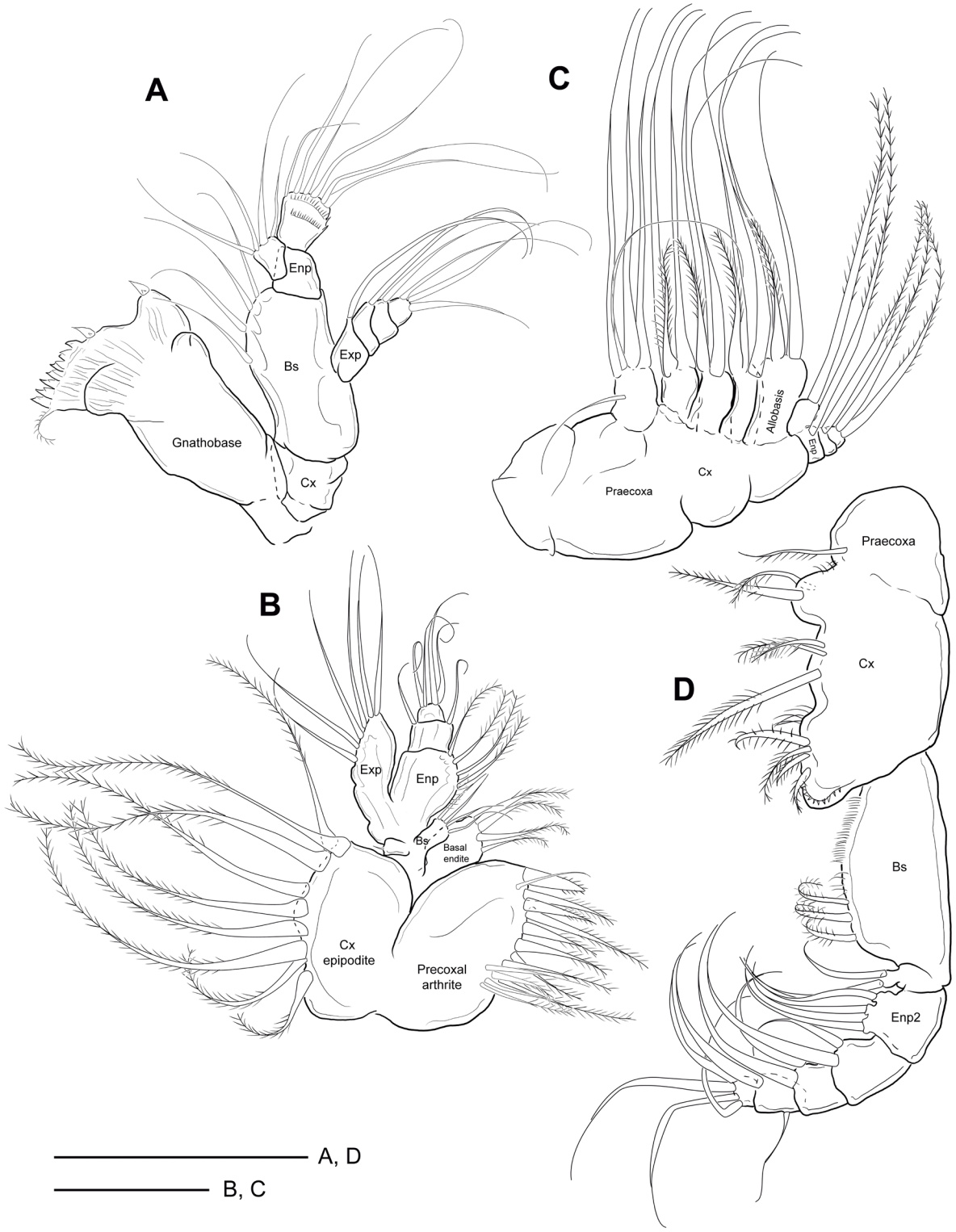


Fig. 6. *Mastigodiaptomus dorsalis* (Marsh, 1907) comb. nov. Adult, ♀ (USNM 122758, Santa Rosa Island, Pensacola, Florida). **A**. Mandible. **B**. Maxillule. **C**. Maxilla. **D**. Maxilliped. Abbreviations: see Material and methods. Scale bars = 100 μm.

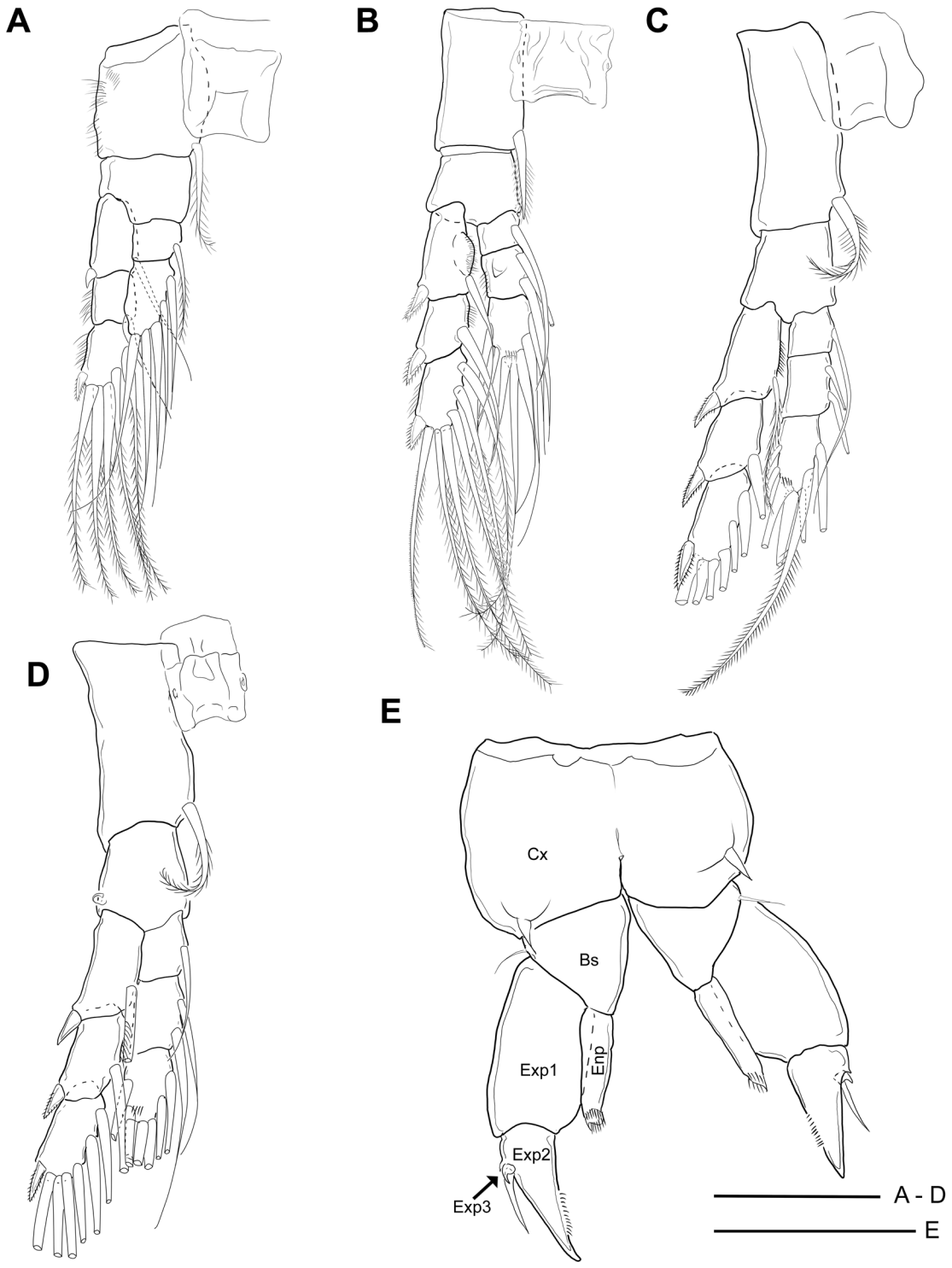


Fig. 7. *Mastigodiaptomus dorsalis* (Marsh, 1907) comb. nov. Adult, ♀ (USNM 122758, Santa Rosa Island, Pensacola, Florida). **A–D**. Swimming legs 1 to 4. **E**. Leg 5, arrow indicates the exopod 3. Abbreviations: see Material and methods. Scale bars = 100 µm.

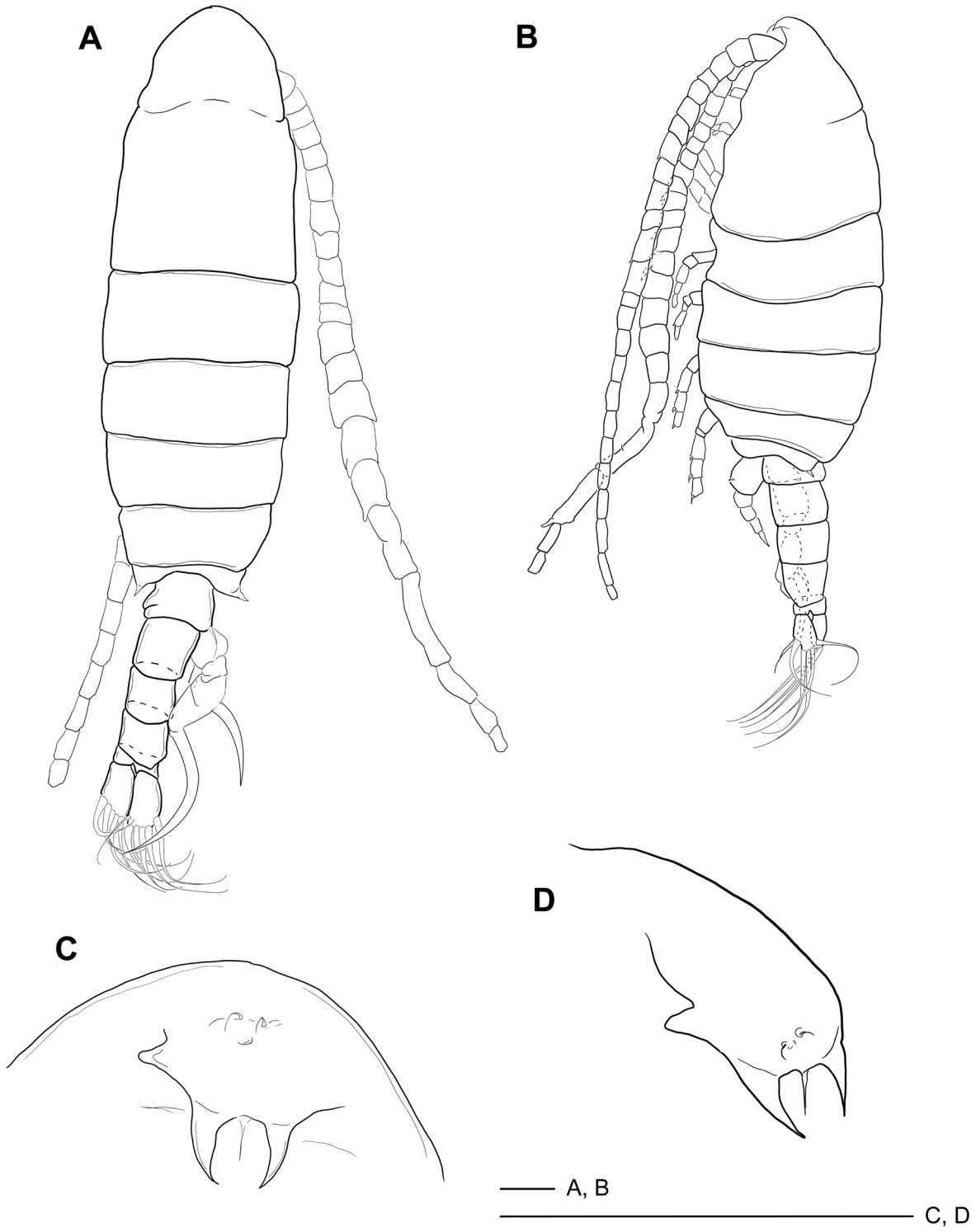


Fig. 8. *Mastigodiaptomus dorsalis* (Marsh, 1907) comb. nov. **A, C**. Adult, ♂ (USNM 122758, Santa Rosa Island, Pensacola, Florida. **B, D**. Syntype, ♂ (USNM 296403, Guzman, Louisiana). **A**. Habitus in dorsal view. **B**. Habitus in lateral view. **C**. Rostrum in ventral view. **D**. Rostrum in oblique view. Scale bars = 100 μm.

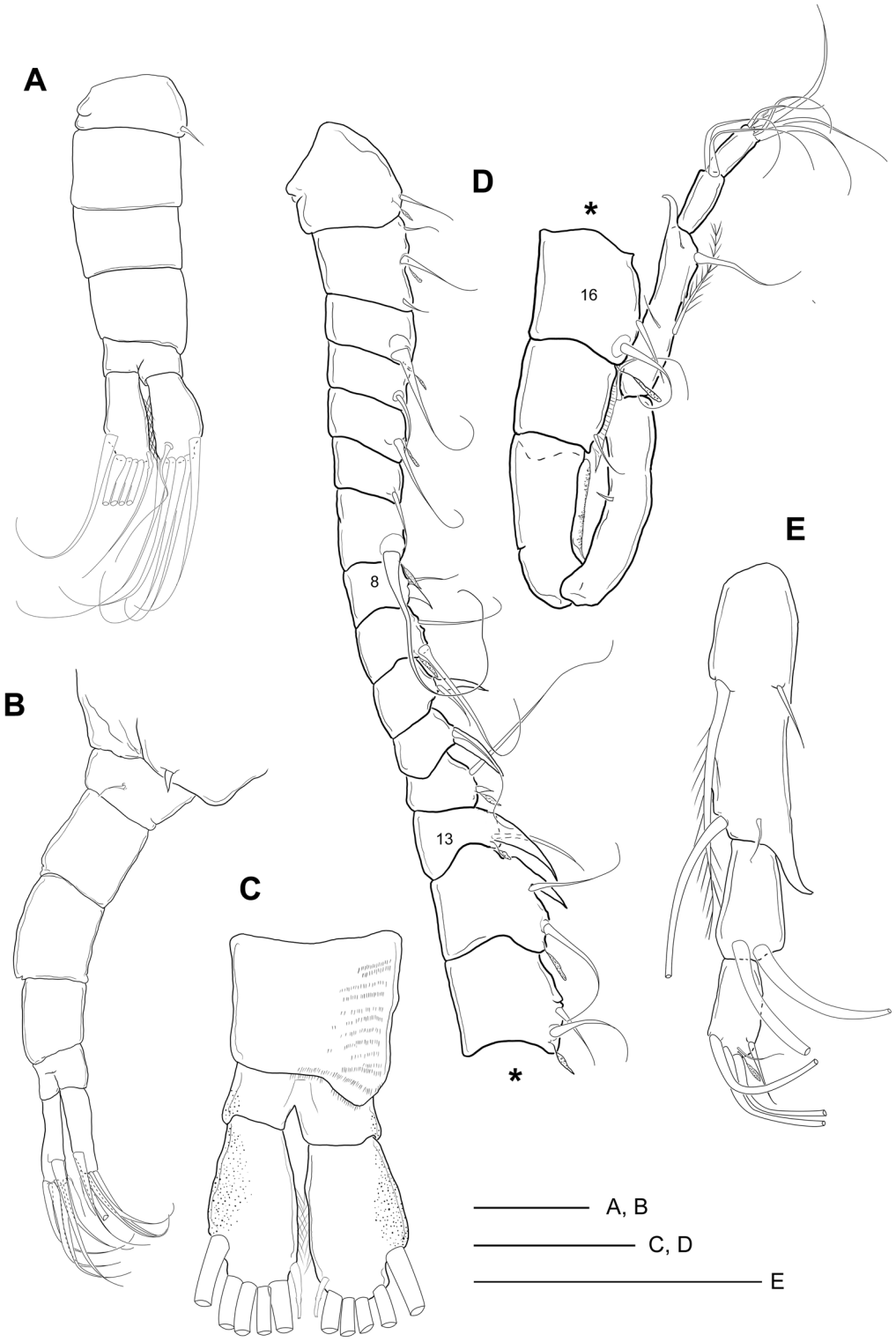


Fig. 9. *Mastigodiaptomus dorsalis* (Marsh, 1907) comb. nov. **A, E**. Adult, ♂ (USNM 122758, Santa Rosa Island, Pensacola, Florida. **B–C**. Syntype, ♂ (USNM 296403, Guzman Lake, Louisiana). **D**. Syntype (USNM 309758, Slidell Lake, Louisiana). **A**. Urosome in dorsal view. **B**. Urosome in lateral view. **C**. Fourth urosomite, anal somite and caudal rami in dorsal view. **D**. Right antennule. **E**. Right antennule segments 20 to 22. Asterisks indicate separation of the segments in the right A1. Scale bars = 100 µm.

Swimming legs (Fig. 7A–D). Spinal and setal armature as presented in Table 2. P1 with setules on Cx. Exp three-segmented, setules along inner margin of Exp1, setules along outer margin on Exp2 and 3. Enp two-segmented, smooth (Fig. 7A). P2 Cx and Bs smooth, Exp three-segmented with protuberance bearing setules on inner margin of Exp1, setules along inner margin of Exp2, setules along outer margin of Exp3; Enp three-segmented with setules along inner margins, Enp2 with Schmeil's lobe in semi-acute tip; Enp3 with spinules apically (Fig. 7B). P3 Cx longer than wide, Cx and Bs smooth, Exp three-segmented, with setules along inner margin of Exp1; Enp three-segmented with spinules apically on Exp3 (Fig. 7C). P4 Cx longer than wide, Cx and Bs smooth; Exp three-segmented, setules along inner margin of Exp 1 and 2; Enp three-segmented with setules along inner margin and spinules apically on Exp3 (Fig. 7D).

P5 (Fig. 7E). Cx with thick distal spine. Bs in triangle-shape with distal outer sensilla, Exp three-segmented; Exp1 longer than wide; Exp2 with minute proximal spiniform process on outer margin and row of spinules on inner margin. Exp3 fused to Exp2, with small spinous process and spine reaching beyond midlength on outer margin of Exp2. Enp one-segmented, as long as inner margin of Exp1, ending in acute tip and two distal spines, with setules subterminally.

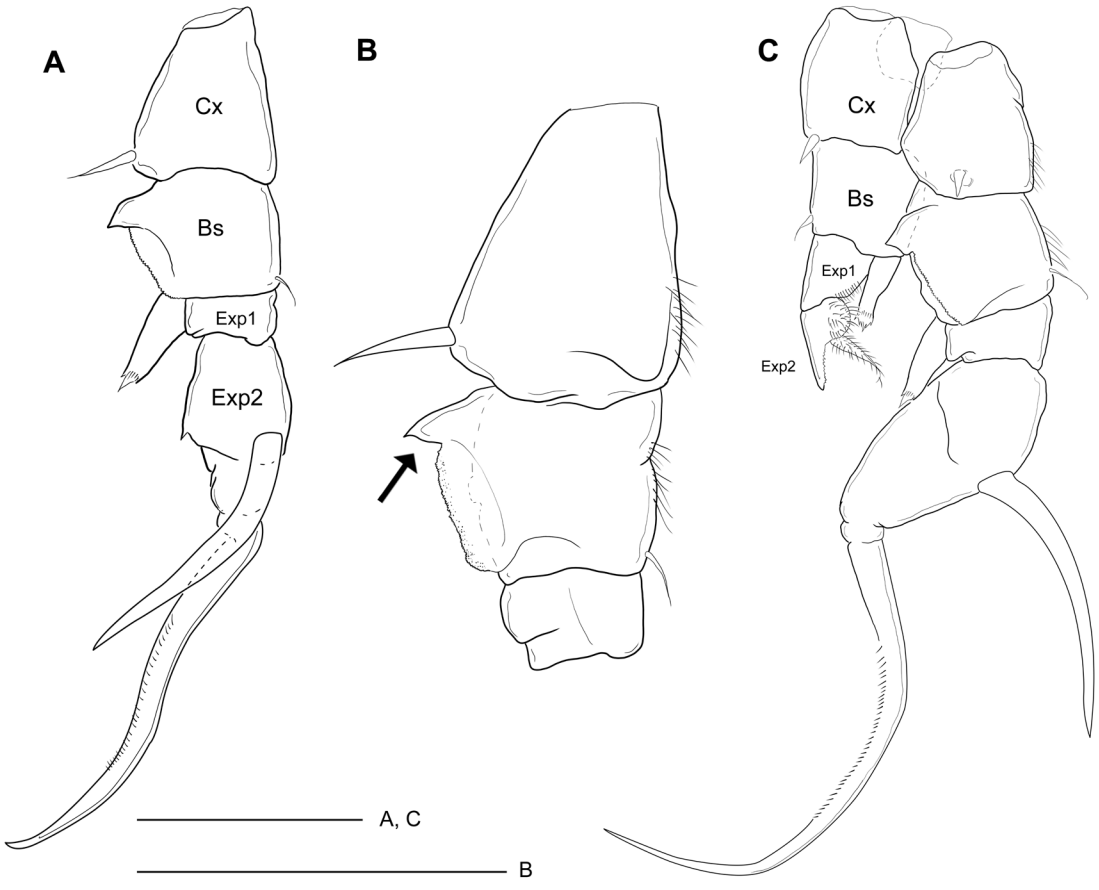


Fig. 10. *Mastigodiaptomus dorsalis* (Marsh, 1907) comb. nov. **A**. Syntype (USNM 309758, Santa Rosa Island, Pensacola, Florida). **B–C**. Syntype, ♂ (USNM 296403, Guzman Lake, Louisiana, **A**. Right leg 5. **B**. Right leg 5 coxa, basis and exopod 1, arrow indicates proximal projection. **C**. P5. Abbreviations: see Material and methods. Scale bars = 100 μm.

Male

Character states are shared by all specimens examined in North and Central America. Description based on specimens from Guzman and Slidell lakes, Louisiana and Santa Rosa Island, Pensacola, Florida.

Habitus (Fig. 8A–B). Total body length of 850–1500 μm excluding caudal setae. Prosome smooth with five pedigers, metasomal wings short, bearing two minute spines distally (Fig. 8A–B). Rostrum with acute rostral spines slightly curved inwards, and left projection proximally (Fig. 8C–D). A1 reaching tip of CR.

Urosome (Fig. 9A–C). Five-segmented. First urosomite with two lobes on left margin and spine on right margin (Fig. 9A). Second to fourth urosomites of about the same length (Fig. 9A–B). Fourth urosomite with rows of spinules in different patterns covering dorsal surface. Anal somite of half the length of preceeding urosomites, covered with papules on surface. CR with inner setules and tubercules on surface, bearing six caudal setae (Fig. 9C).

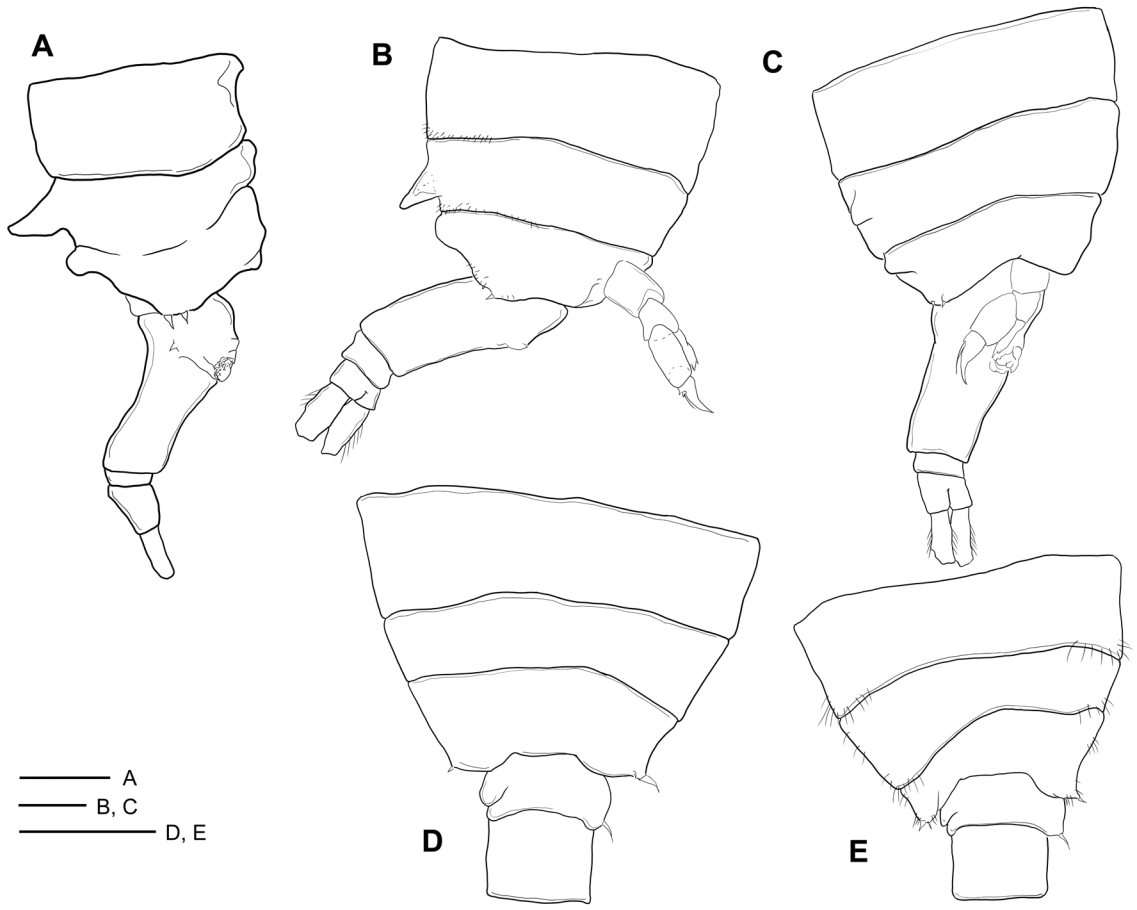


Fig. 11. *Mastigodiaptomus dorsalis* (Marsh, 1907) comb. nov. **A–C**. ♀, pedigers 3–5 in lateral view. **D–E**. ♂, pedigers 3–5 in dorsal view. **A**. Specimen form Pensacola, Florida, USA (USNM 122758). **B**. Specimen from San José Dam, San Luis Potosí, Mexico (ECO-CH-Z-10629). **C**. Specimen from lake Amatitlán, Guatemala (ECO-CH-Z-10660). **D**. Specimen from sinkhole in Km 170, Quintana Roo, Mexico (ECO-CH-Z-10524). **E**. Specimen from Lake Cociboca, Nicaragua (USNM 243719). Scale bars = 100 μm.

RA1 (Fig. 9D–E). 22-segmented. Setal formula as follows: 1 (1s+1ae), 2 (3s+1ae), 3 (1s+1ae), 4 (1s), 5 (1s+1ae), 6 (1s), 7 (1s+1ae), 8 (1sp+1s), 9 (2s+1ae), 10 (1sp+1s), 11 (1sp+1s), 12 (1sp+1s+1ae), 13 (1s+1ae), 14 (2s+1ae), 15 (2s+1ae), 16 (2s+1ae), 17 (1s), 18 (0), 19 (1sp+1s), 20 (4s), 21 (2s), 22 (5s+1ae) (Fig. 9 D). Segments 10, 11, 13–15 with proximal spinous process. Segments 17–19 with dorsal thickening, antepenultimate segment with hook-like distal process (Fig. 9E).

LA1. As in female (based on specimens from Florida).

Buccal appendages. As in females (based on specimens from Florida).

Swimming legs. As in females (based on specimens from Florida).

RP5 (Fig. 10). Cx with thick distal spine. Bs with caudal lamella, proximal pointed projection, hyaline lamella on inner margin, and outer seta distally. Cx and Bs with or without setules along outer margin

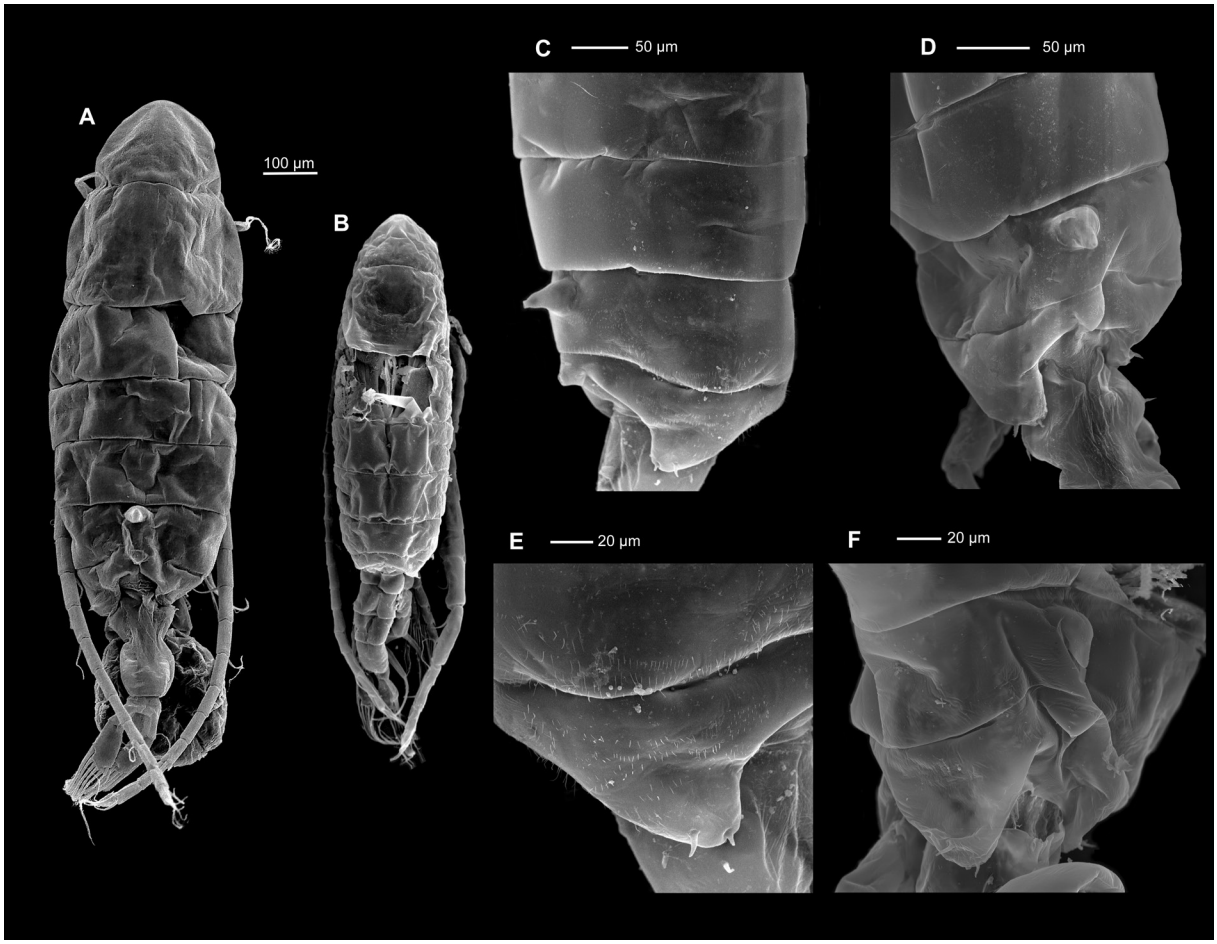


Fig. 12. *Mastigodiaptomus dorsalis* (Marsh, 1907) comb. nov. Scanning Electron Microscopy. **A**. ♀, habitus from San Luis Potosí, Mexico. **B**. ♂, habitus from San José Dam, San Luis Potosí, Mexico (ECO-CH-Z-10597). **C**. ♀, pedigers 2–5 from Lake Catemaco, Veracruz, Mexico (ECO-CH-Z-10605). **D**. ♀, pedigers three to five from sinkhole in Km 170, Quintana Roo, Mexico (ECO-CH-Z-10520). **E**. ♀, metasomal wings from Lake Catemaco, Veracruz, Mexico. **F**. ♀, pedigers four and five from Cenote Azul, Quintana Roo, Mexico (ECO-CH-Z-10535).

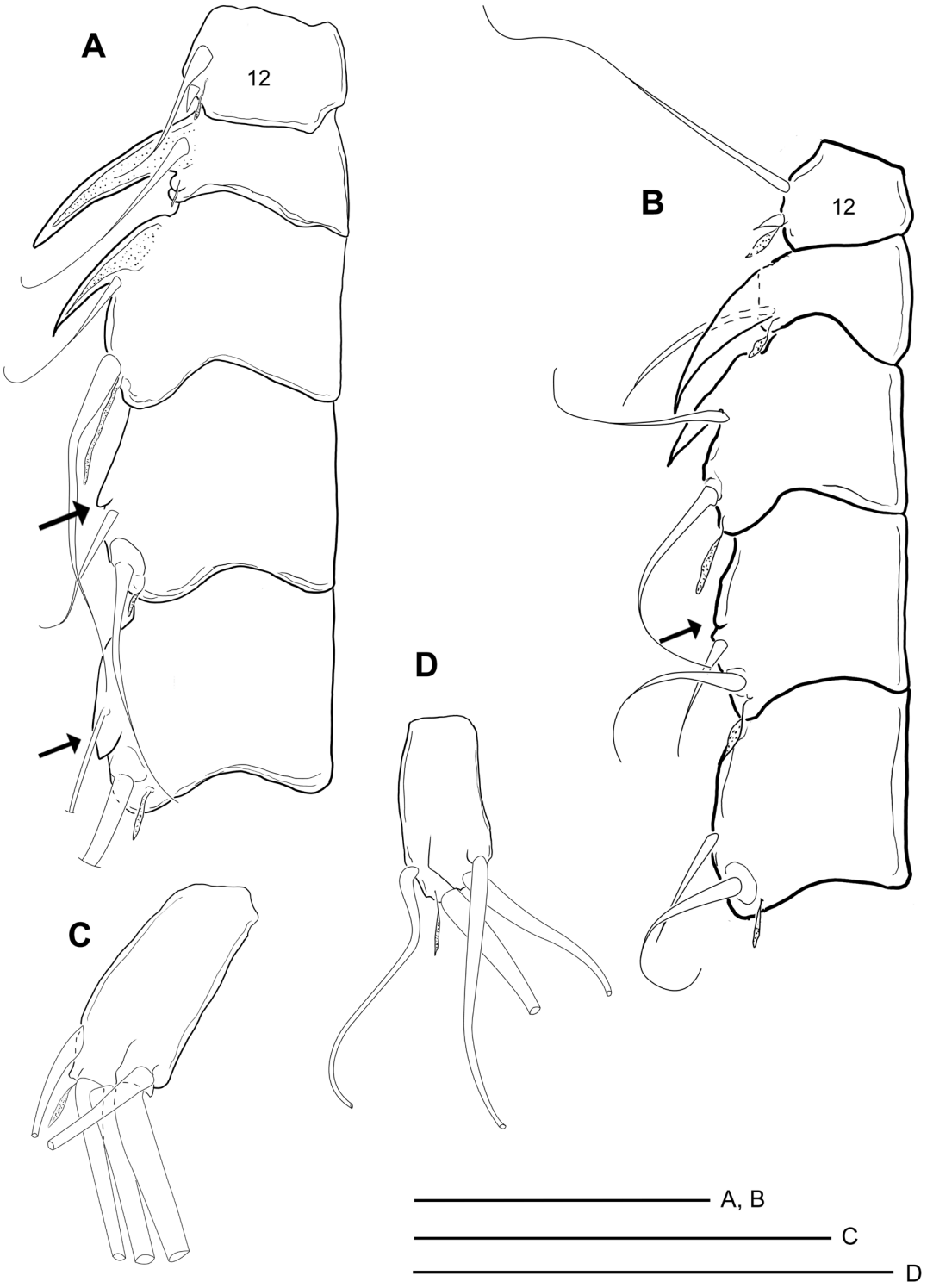


Fig. 13. *Mastigodiaptomus dorsalis* (Marsh, 1907) comb. nov., ♂, right antennule. **A**. Segments 12–16 from San José Dam, San Luis Potosí, Mexico (ECO-CH-Z-10604), arrows indicate the process on segments 15 and 16. **B**. Segments 12–16 from Lake Slidell, Louisiana, USA (syntype USNM 309758), arrow indicates the process on segment 15. **C**. Segment 22 from Lake Slidell. **D**. Segment 22 from San José Dam. Scale bars = 100 µm.

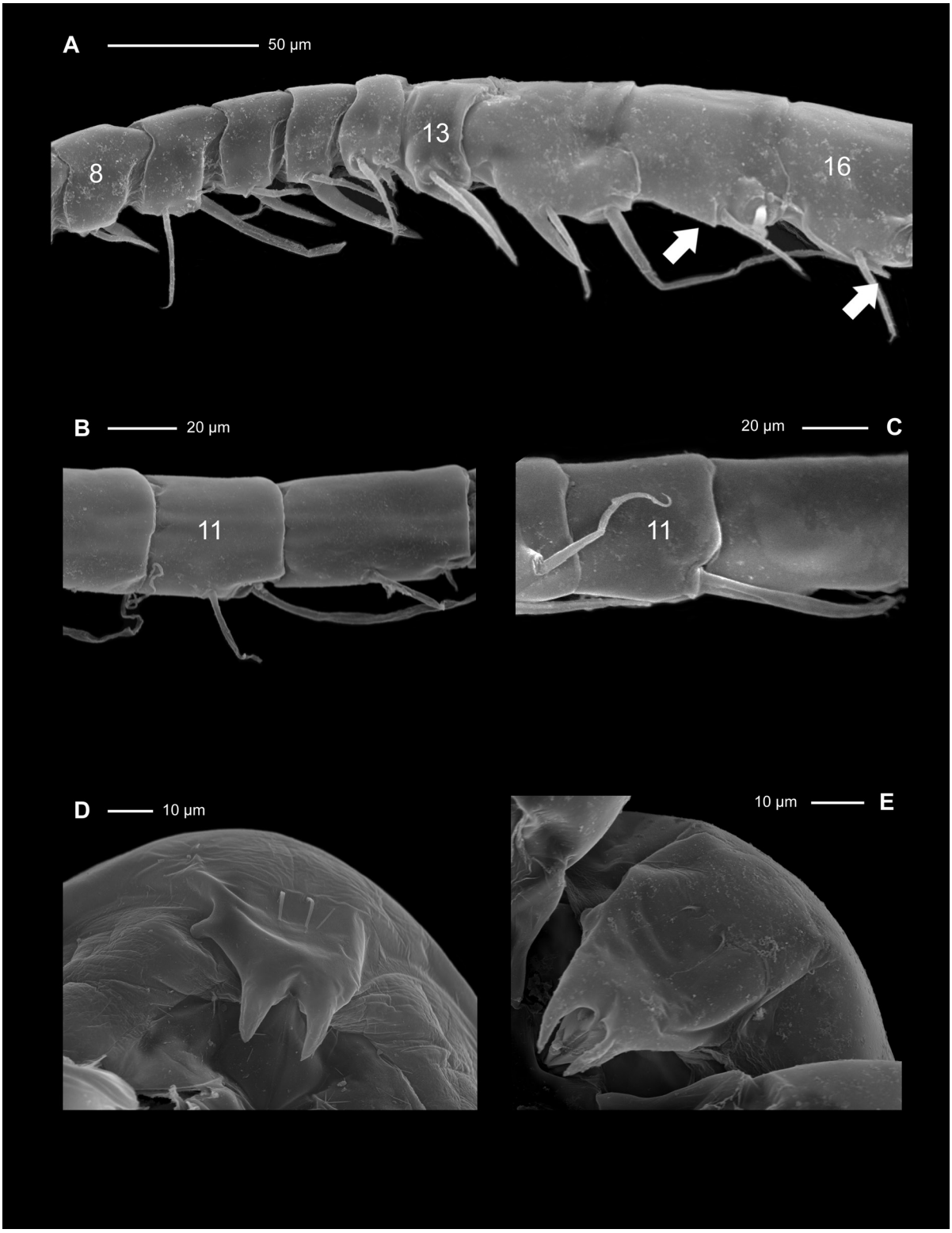


Fig. 14. *Mastigodiaptomus dorsalis* (Marsh, 1907) comb. nov. Scanning Electron Microscopy. **A, C–D**. Specimens from San José Dam, San Luis Potosí, Mexico (ECO-CH-Z-10597). **B, E**. Specimens from Lake Amatitlán, Guatemala (ECO-CH-Z-10663). **A**. ♂, right antennule segments 8–16, arrows indicate the process on segments 15 and 16. **B**. ♀, antennule, segment 11. **C**. ♀, antennule, segment 11. **D**. ♂, rostrum. **E**. ♂, rostrum.

(Fig. 10A–B). Exp two-segmented; Exp1 wider than long, about half the length of Bs, with two lobes on inner margin distally. Exp2 longer than wide, with caudal lamella, aculeus placed at midlength of outer margin, with bent terminal claw, about the length of RP5, with row of spinules along inner margin (Fig. 10A, C).

LP5 (Fig. 10C). Cx with spine on outer margin distally. Bs with seta on outer margin distally. Exp 2-segmented; Exp1 with row of setules on iner margin, tapering terminally. Exp2 about half the length of Exp1, bearing a patch of setules, and tubercles proximally, serrated spinous process apically as long as Exp2 with a spinous seta attached, covered with setules, about the same length of the spinous process.

Remarks

The specimens examined in this study from Florida should be considered as *M. dorsalis* s. str. based on its proximity (~ 300 km) with the type locality in Louisiana, a site which has since disappeared, sharing the same habitat and ecoregion.

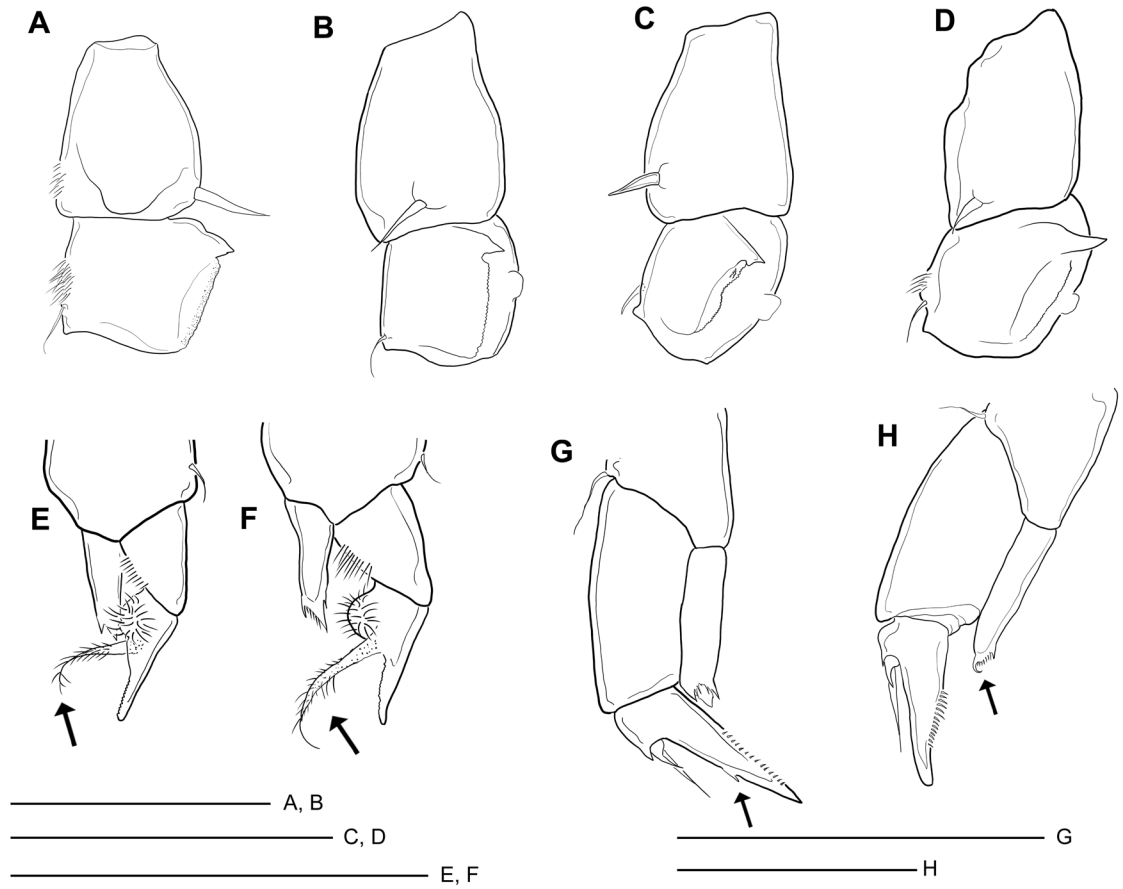


Fig. 15. *Mastigodiaptomus dorsalis* (Marsh, 1907) comb. nov. **A–D**. ♂, right leg 5 coxa and basis. **E–F**. ♂, left leg 5, exopod arrows indicate the spinous seta. **G–H**. ♀, leg 5, arrows indicate spinous process on exopod 2 and endopod, respectively. **A**. Lake Slidell, Louisiana, USA (USNM 30958, syntype). **B**, **F**. Lake Amatitlán, Guatemala (ECO-CH-Z-10664). **C**. Lake Petén, Guatemala (ECO-CH-Z-10667). **D**. Lake Managua, Nicaragua (USNM 243712). **E**. San José Dam, San Luis Potosí, Mexico (ECO-CH-Z-10604). **G**. Lake Amatitlán (ECO-CH-Z-10660). **H**. San José Dam, San Luis Potosí, Mexico (ECO-CH-Z-10629). Scale bars = 100 μm.

This species shows several phenetic (morphological) differences between and within populations across bioregions as presented in Table 3.

Distribution

This species extends to the Eastern NA, in the Alleghany subregion and, particularly, the Austroriparian ecoregion (Escalante *et al.* 2021), where both the type specimens (from Guzman and Slidell lakes in Louisiana) and the sensu stricto specimens from Florida occur; these sites are characterized by large lakes and wetlands.

Several NT populations studied occur in Mexico, Guatemala, and Nicaragua, encompassing large ecoregions such as the Yucatan Peninsula, Pacific Lowlands, and the Veracruzan Province. A record of "*A. dorsalis*" by Torres-Orozco & Zanatta (1998) in Lake Catemaco (Veracruzan Province) was preceded by a more accurate record of the species *Mastigodiaptomus albuquerquensis* reported by Suárez-Morales *et al.* (1986) in the same ecoregion. Other state and locally records from these Mexican bioregions should now be re-evaluated. The NT is also characterized by high species and habitat diversity (Morrone 2019)

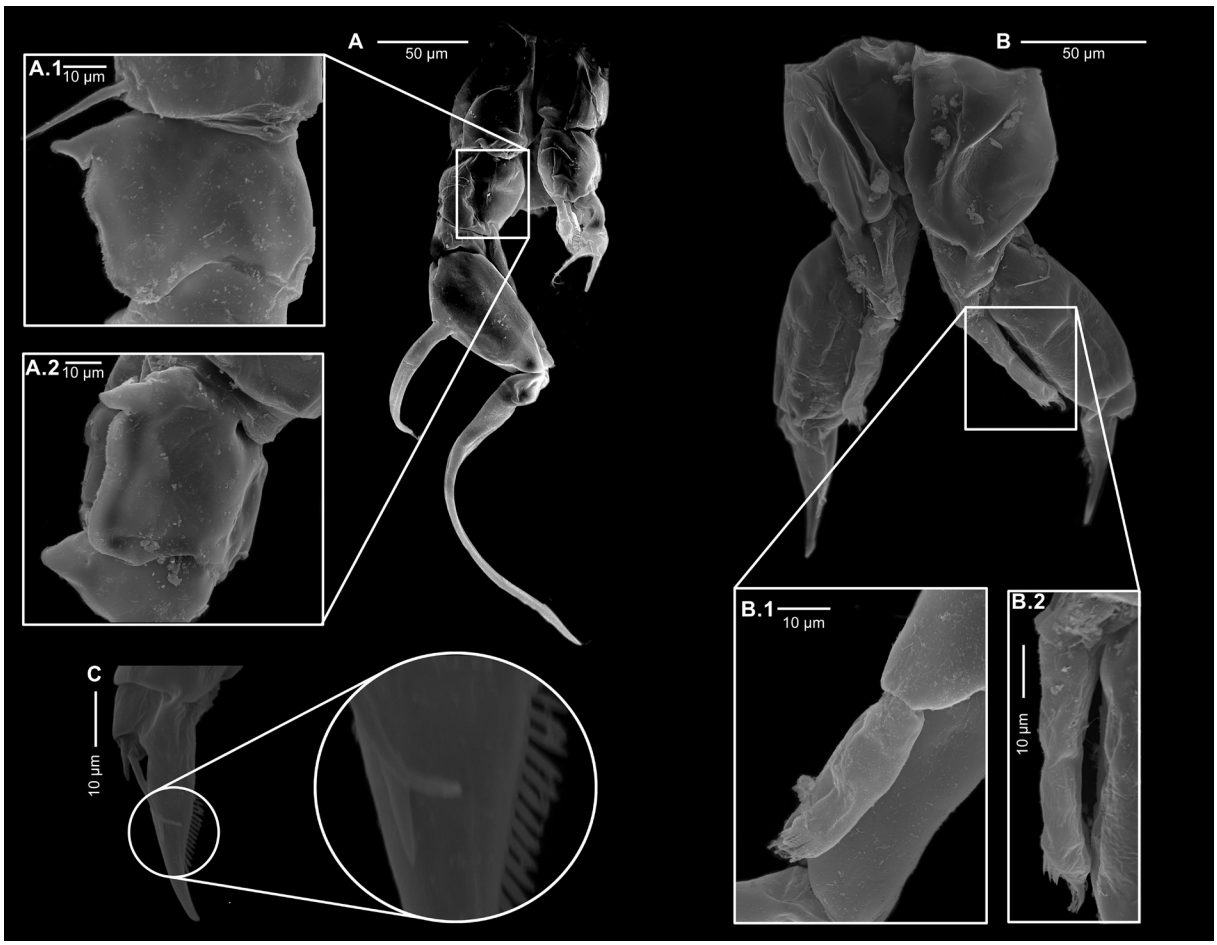


Fig. 16. *Mastigodiaptomus dorsalis* (Marsh, 1907) comb. nov. Scanning Electron Microscopy, leg 5. **A**, **A.1, A.2**. ♂ leg 5. **B, B.1, B.2, C**. ♀ leg 5. **A.1**. Specimen from lake Amatitlán, Guatemala. **A.2**. Specimen from San José Dam, San Luis Potosí, Mexico. **B.1**. Specimen from Cenote Azul. **B.2**. Specimen from San José Dam, San Luis Potosí, Mexico. **C**. Exp2, specimen from Cocalitos sinkhole, Quintana Roo, Mexico.

Table 3. Morphological differences (females and males) of the analyzed specimens of *Mastigodiaptomus dorsalis* (Marsh, 1907), for the two bioregions and the transition zone (marked with *) where this species is distributed. Abbreviations: MTZ: Mexican Transition Zone; NA: Nearctic; NT: Neotropic bioregions.

Character	NA	MTZ*	NT
Prosome pedigers 4–5	Smooth ♀♂ with well-developed projections ♀ (Figs 8A, 11A)	With setules ♀, without setules ♂ (Figs 11B, D, 12C–D) with well-developed projections ♀	These characters combined: smooth or with setules ♀♂ (Fig. 11C, E) with reduced or well-developed projections ♀ (Figs 11C, 12F)
A1 ♀ (left in ♂)	Reaching CR (Fig. 3A–B). Segment 11 with single seta (Fig. 5A). Last segment with 5 setae and 1 ae (Fig. 13C)	Beyond CR by 1 segment (Fig. 12A–B). 19% of populations with 2 setae in segment 11 (as in Fig. 14B–C). Last segment with 4 setae and 1 ae (Fig. 13D)	Beyond CR by 1 segment (as in Fig. 12A–B). 44% of populations with 2 setae in segment 11 (Fig. 14B–C). Last segment with 4 setae and 1 ae (as in Fig. 13D)
RA1 ♂	With spinous processes on segments 13–15 (Fig 13 B).	With spinous processes on segments 13–16 (Figs 13A, 14A)	With spinous processes on segments 13–16 (as in Figs 13A, 14A)
Rostrum ♂	Thick spines (as in Fig. 14D)	Thick spines (Fig. 14D)	Long spines (Fig. 13E)
RP5 ♂	Cx and Bs with or without setules (Fig. 15A). Bs caudal hyaline lamella proximal projection in acute tip (Fig. 15A)	Cx and Bs smooth (Fig. 15B). Bs caudal hyaline lamella proximal projection in curved tip (Figs 15B, 16A.2)	These characters combined: Bs with or without setules (Fig. 15C–D). Bs caudal hyaline lamella proximal projection in slit-shaped or elongated acute tip (Figs 15C–D, 16A.1)
LP5 ♂	Setae of Exp2 as long as the serrated spinous terminal process (as in Fig. 15E)	Setae of Exp2 as long as the serrated spinous terminal process (Fig. 15E)	Setae of Exp2 beyond the length of the serrated spinous terminal process (Fig. 15F)
P5 ♀	Enp reaching the end of inner margin of Exp1, and with terminal spinous process (Fig. 7E).	Enp reaching the end of inner margin of Exp1, and with curved terminal spinous process (Figs 15H, 16B.2)	These characters combined: Enp reaching the end of inner margin of Exp1 or beyond it, with terminal spinous process (Figs 15G, 16B.1). Exp2 with or without minute outer spinous process (arrows in Figs 15G, 16C)

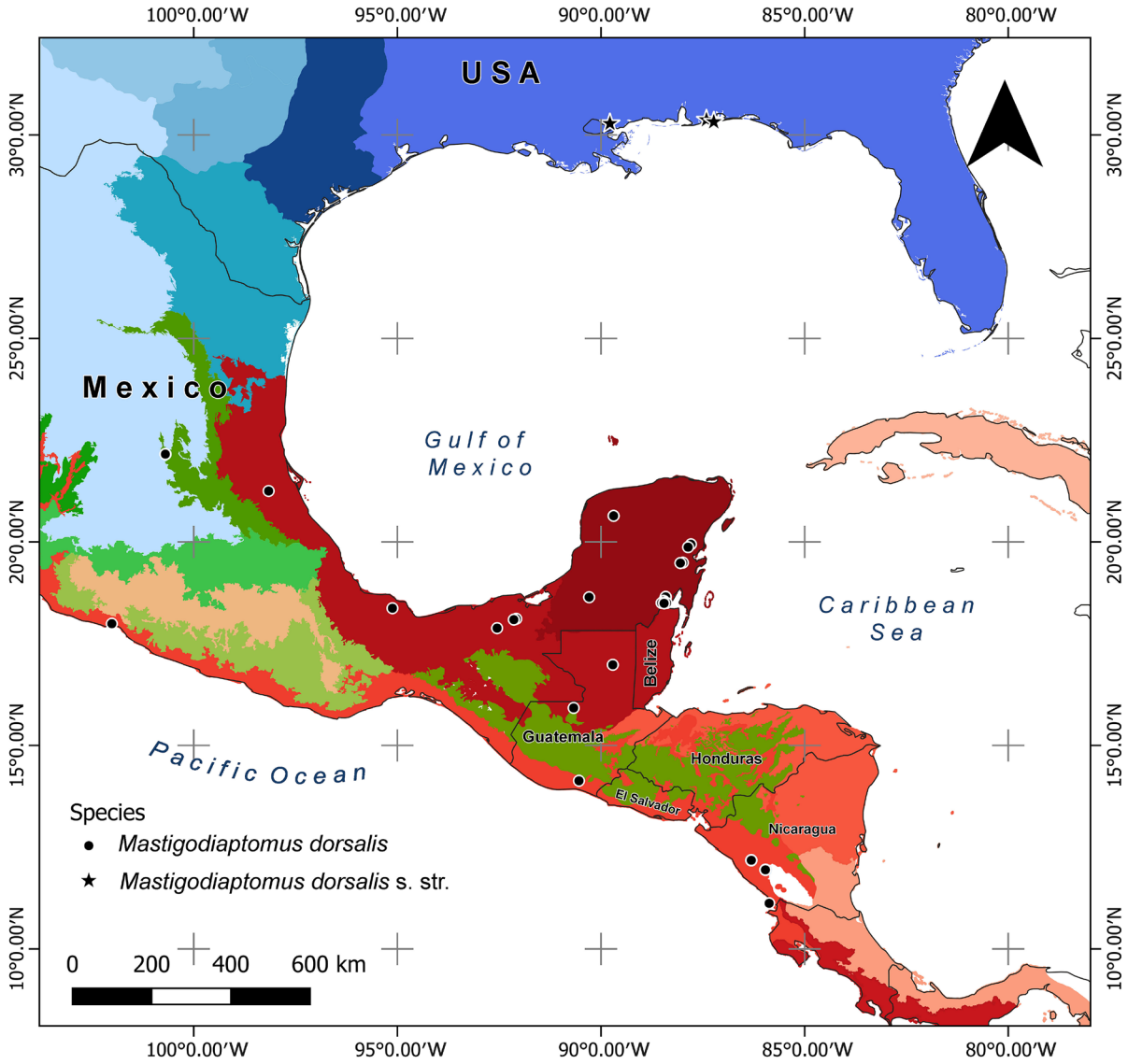


Fig. 17. Geographical distribution of *Mastigodiaptomus dorsalis* (Marsh, 1907) comb. nov. specimens in North and Central America analyzed in this study. Biogeographical representation with ecoregions is based on Morrone (2015, 2017) and Escalante *et al*. (2021) for both bioregions and the Mexican Transition Zone.

and includes the largest anchialine systems worldwide, with a remarkable number of endemic aquatic species (Gutiérrez-Aguirre *et al.* 2024; Jaime *et al.* 2025).

Other records of this species occur in the MTZ, in the Sierra Madre Oriental, e.g., the San Luis Potosí population. This area is characterized by predominantly karstic conditions and an average elevation of 1500 meters above sea level. This region forms the boundary between the NA and NT bioregions (Morrone 2019; Bautista 2023) Therefore, it is likely that *M. dorsalis* comb. nov. is a generalist species inhabiting a wide range of aquatic habitats like wetlands, rivers, man-made lakes and reservoirs, lakes, temporary ponds, and karstic sinkholes with humid and warm climates (Fig. 17). This explains its wide distribution across the Americas.

Mastigodiaptomus cucapa sp. nov.
urn:lsid:zoobank.org:act:689D452B-7F02-404C-9B4A-D26350CC5E5F
Figs 18–25

Diagnosis

Female and male prosome with row of minute spinules on pedigers 3–5 (Figs 18E, 19E, 23B–C). Rostrum elongated and slender, curved inwards (Figs 18C–D, 19C, 22D–E). Exp3 of Md palp with three rows of minute spinules apically (Fig. 21C). Mx1 with proximal setules on praecoxal arthrite (Fig. 21D).

Female metasomal wing slightly asymmetric, left wing longer than right. A1 overreaching CR by three segments (Figs 18A–B, 19A, D). Genital double-somite slightly dilated, CR with setules on outer margin (Fig. 20B–C). P5 Bs with process on outer margin distally (upper arrows in Fig. 20D).

Male A1 reaching tip of CR (Fig. 22A). First urosomite with long and slender spine distally (Fig. 22B). Fourth urosomite with straight row of minute spinules (Figs 22C, 23D). RP5 Bs with caudal lamella bearing a process distally (upper arrow in Fig. 24C). Exp1 with curved outer projection distally (lower arrow in Fig. 24C). LP5 Exp2 with setae covered with minute spinules (arrow in Fig. 24D).

Etymology

The species name is a noun in apposition in reference to the Cucapá people, an almost extinct indigenous community of northwest Mexico, where the type locality is located. The term ‘cucapa’ means ‘people of water’ in the Cucapan language.

Type material

Holotype

MEXICO – **Sonora** • ♀, specimen dissected in semipermanent slide; Mocuzari Dam; 27.231° N, 109.794° W; 30 May 2006; M. Elías-Gutiérrez leg.; BIN no: BOLD:AAF4891; ECO-CH-Z-10636.

Allotype

MEXICO – **Sonora** • ♂; same data as for holotype; ECO-CH-Z-10640.

Paratypes

MEXICO – **Sonora** • 20 ♀♀, 19 ♂♂, specimens preserved with 96% ethanol and a drop of glycerol; same data as for holotype; ECO-CH-Z-10642.

Additional material examined

MEXICO – **Baja California Sur** • 2 ♂♂, specimens mounted in semipermanent slide; La Palma Dam; 23.226° N, 109.079° W; 26 Apr. 2014; S. Hernández-Trujillo leg.; ECO-CH-Z-10536 • 16 ♀♀; same data as for preceding; ECO-CH-Z-10637, ECO-CH-Z-10644, ECO-CH-Z-10645, ECO-CH-Z-10647

• 6 ♀♀, 1 ♂, sample preserved with 96% ethanol and a drop of glycerol; same data as for preceding; ECO-CH-Z-10538 • 4 ♂♂, specimens mounted in semipermanent slide; same data as for preceding; ECO-CH-Z-10643 • 2 ♀♀; same data as for preceding; ECO-CH-Z-10646.

Description

Female

Habitus. Total body length 823–1,335 µm (n = 30) excluding caudal setae. Projections on fourth and fifth pedigers, in keel-like and rounded shape, respectively (Figs 18A–B, 19A–B, D); pedigers three to five with row of minute distal spinules (Figs 18E, 19E). Small metasomal wings, slightly asymmetrical, with two spines distally, left wing longer than right (Figs 18A, 19D). Rostral spines sharp, elongated and slender, curved inwards (Figs 18C–D, 19C). A1 overreaching CR for ultimate three segments (Figs 18A–B; 19A).

Urosome. Three-segmented, smooth dorsoventally. Genital double-somite three times longer than wide, slightly dilated, with a spine on dilatation (Fig. 20B–C); genital operculum rounded, inserted proximally in ventral view. Second somite wider than long and about six times shorter than first genital somite (Fig. 20C). Anal somite shorter than genital somite. CR with setules along outer margins and six caudal setae (Fig. 20B–C).

A1 (Fig. 20A). 25-segmented, with setal formula as follows: 1 (1s+1ae), 2 (3s+1ae), 3 (1s+1ae), 4 (1s), 5 (1s+1ae), 6 (1s), 7 (1s+1ae), 8 (1s+1sp), 9 (2s+1ae), 10 (1s), 11 (1s); 12 (1sp+1s+1ae), 13 (1s), 14 (1s+1ae), 15 (1s), 16 (1s+1ae), 17 (1s), 18 (1s), 19 (1s+1ae), 20 (1s), 21 (1s), 22 (2s), 23 (2s), 24 (2s), 25 (4s).

A2 (Fig. 21A–B). Cx three times shorter than Bs, with one seta. Bs elongated with two setae distally. Enp two-segmented; Enp1 with two setae on inner margin distally and row spines along inner margin proximally; Enp2 with two lobes, first lobe with eight setae, second lobe with seven setae and rounded row of spinules proximally (Fig. 21A). Exp 7-segmented with setal formula as follows: 1, 3, 1, 1, 1, 1, 1-3 (Fig. 21B).

Md (Fig. 21C). Gnathobase with seven bidented denticles and spine on inner margin, spinous setae on outer margin, and projection with spine on inner margin. Cx smooth. Bs longer than wide, with four setae along inner margin. Enp three-segmented; first segment smooth, second with four setae, third with five setae and three rows of spinules. Exp four-segmented, with setal formulaas follows: 1, 1, 1, 3.

Mx1 (Fig. 21D). Precoxal arthrite with nine lateral and five dorsal spinous setae, and setules proximally. Coxal epipodite with nine setae. Coxal endite with four setae. Basal endite with four setae. Basal exite with single spine. Enp three-segmented with setal formula as follows: 4, 4, 3; distal setules on Enp1. Exp with seven setae.

Mx2 (Fig. 21E). Praecoxa with two lobes with five and three setae, respectively. Cx with two lobes, bearing three setae each. Allobasis with four setae. Distal lobe with one seta. Enp three-segmented with setal formula as follows: 1, 1, 2.

Mxp (Fig. 21F). Praecoxa and Cx fused. Praecoxa with one seta. Cx with three lobes; first lobe with setules and two setae, second lobe with setules and three setae, fourth lobe with setules, four setae and rounded proximal projection with spinules. Bs with setules and three proximal setae. Enp six-segmented with the setal formula as follows: 2, 3, 2, 2, 2, 4; Enp1 fused to Enp2.

P1-4. Spinal and setal armature as presented in Table 2. P1 with setules on Cx. Exp three-segmented, setules along inner margin of Exp1, setules along outer margin on Exp2 and 3. Enp two-segmented, smooth. P2 Cx and Bs smooth, Exp three-segmented with protuberance with setules on inner margin of Exp1, setules along inner margin of Exp2, setules along outer margin of Exp3; Enp three-segmented with setules along inner margins, Enp2 with Schmeil's lobe in semi-acute tip; Enp3 with spinules apically.

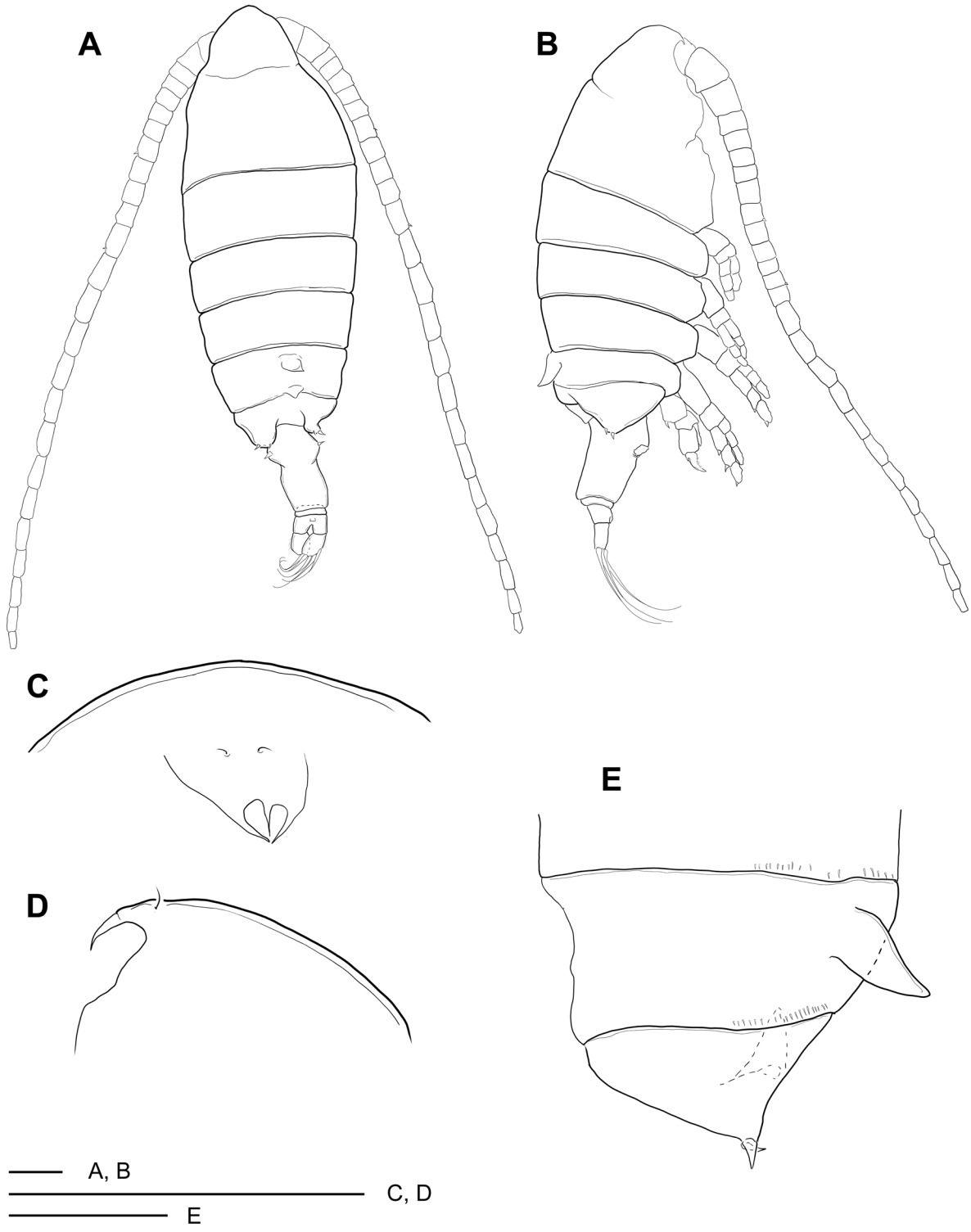


Fig. 18. *Mastigodiaptomus cucapa* sp. nov. **A, C, E**. Holotype, adult, ♀, from Mocuzari Dam, Sonora (ECO-CH-Z-10636). **B, D**. ♂, from La Palma Dam, Baja California Sur (ECO-CH-Z-10643). **A**. Habitus in dorsal view. **B**. Habitus in lateral view. **C**. Rostrum in ventral view. **D**. Rostrum in lateral view. **E**. Pedigers four and five in lateral view. Scale bars = 100 µm.

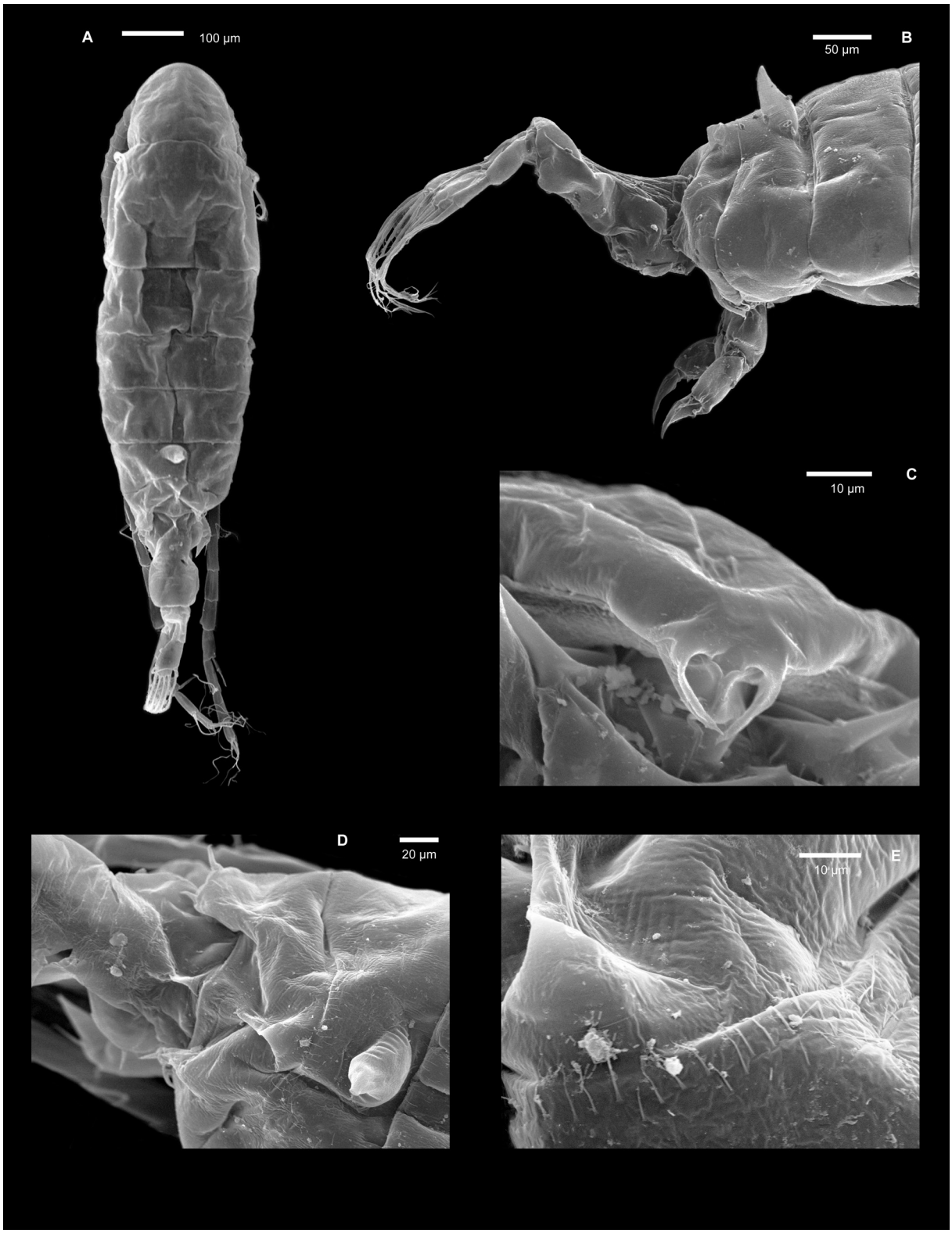


Fig. 19. *Mastigodiaptomus cucapa* sp. nov. Adult, ♀, from La Palma Dam, Baja California Sur, Mexico (ECO-CH-Z-10538). Scanning Electron Microscopy. **A**. Habitus in dorsal view. **B**. Pedigers 3–5 and urosome in lateral view. **C**. Rostrum. **D**. Pedigers 4 and 5 in dorsal view. **E**. Closer view of pediger 4.

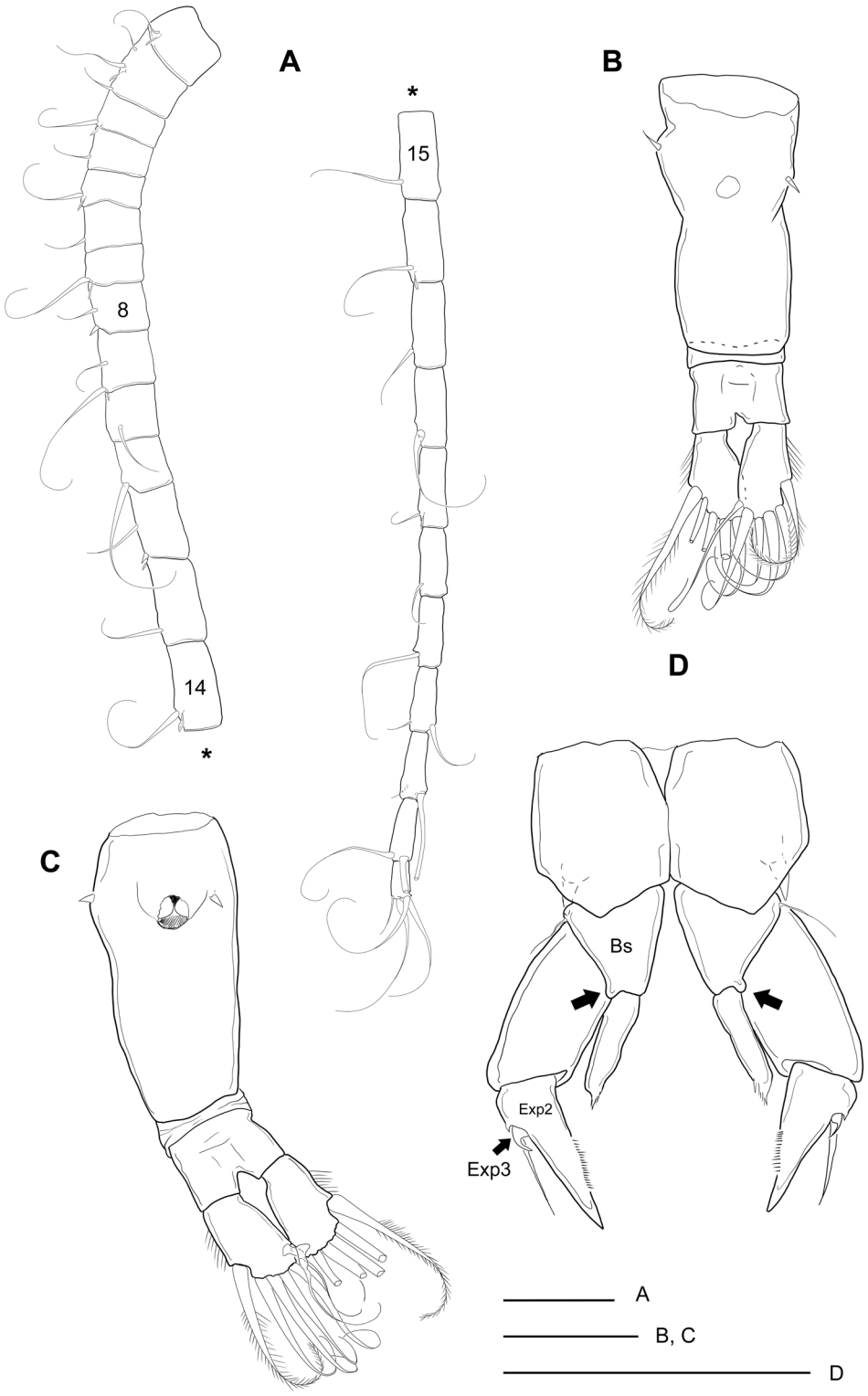


Fig. 20. *Mastigodiaptomus cucapa* sp. nov. **A–B, D**. Holotype, ♀, from Mocuzari Dam, Sonora (ECO-CH-Z-10636). **C**. ♀, adult, from La Palma Dam, Baja California Sur (ECO-CH-Z-10647).**A**. Antennule. **B**. Urosome in dorsal view. **C**. Urosome in ventral view. **D**. Leg 5, upper arrows indicate distal processes, lower arrow indicates exopod 3. Asterisks indicate separation of A1 segments. Abbreviations: see Material and methods. Scale bars = 100 μm.

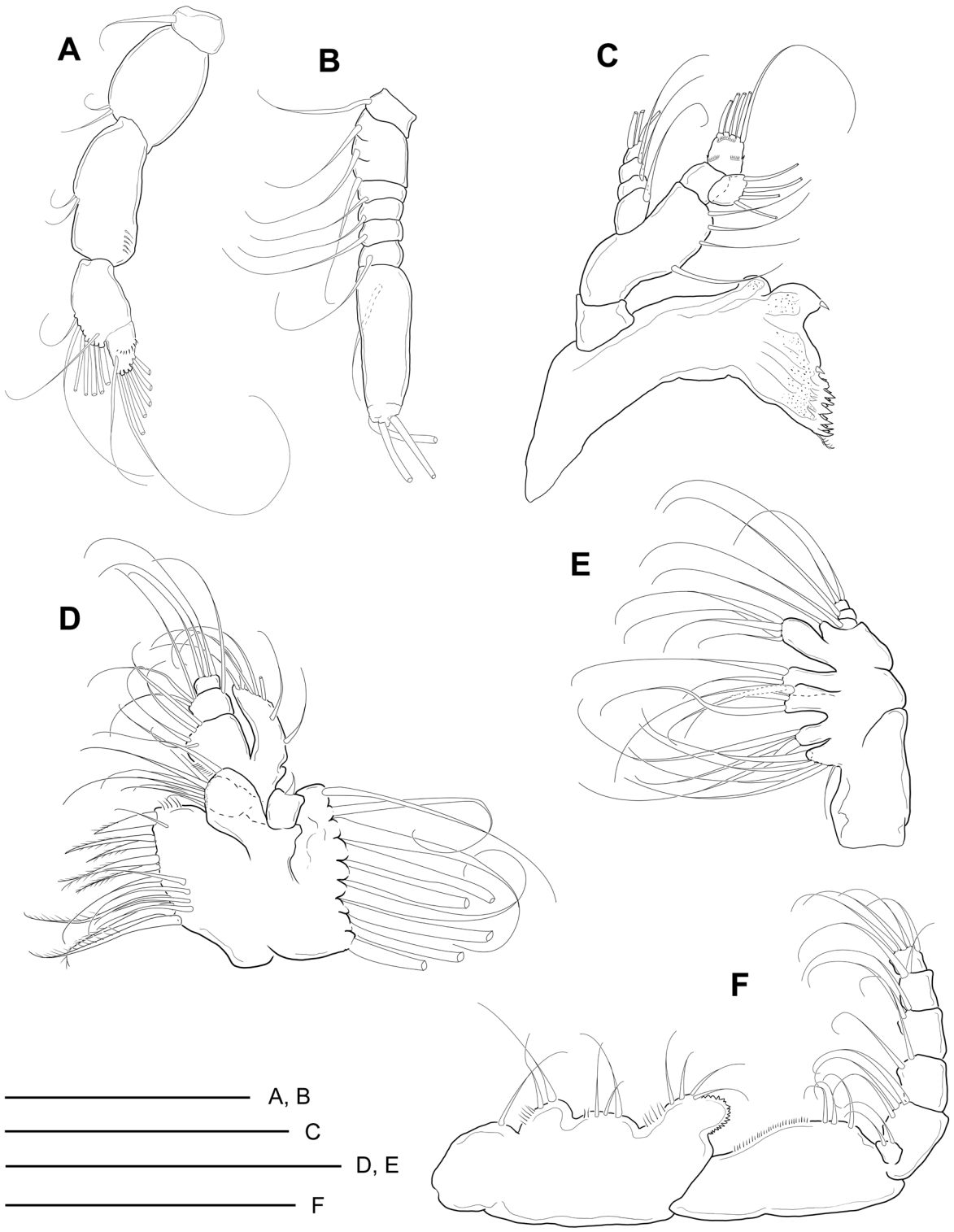


Fig. 21. *Mastigodiaptomus cucapa* sp. nov. **A-C, F**. Holotype, ♀, from Mocuzari Dam, Sonora (ECO-CH-Z-10636). **D–E**. Allotype, ♂, from Mocuzari Dam, Sonora (ECO-CH-Z-10640). **A**. Coxa, basis and endopod of antenna. **B**. Exopod of antenna. **C**. Mandible. **D**. Maxillule. **E**. Maxilla. **F**. Maxilliped. Scale bars = 100 μm.

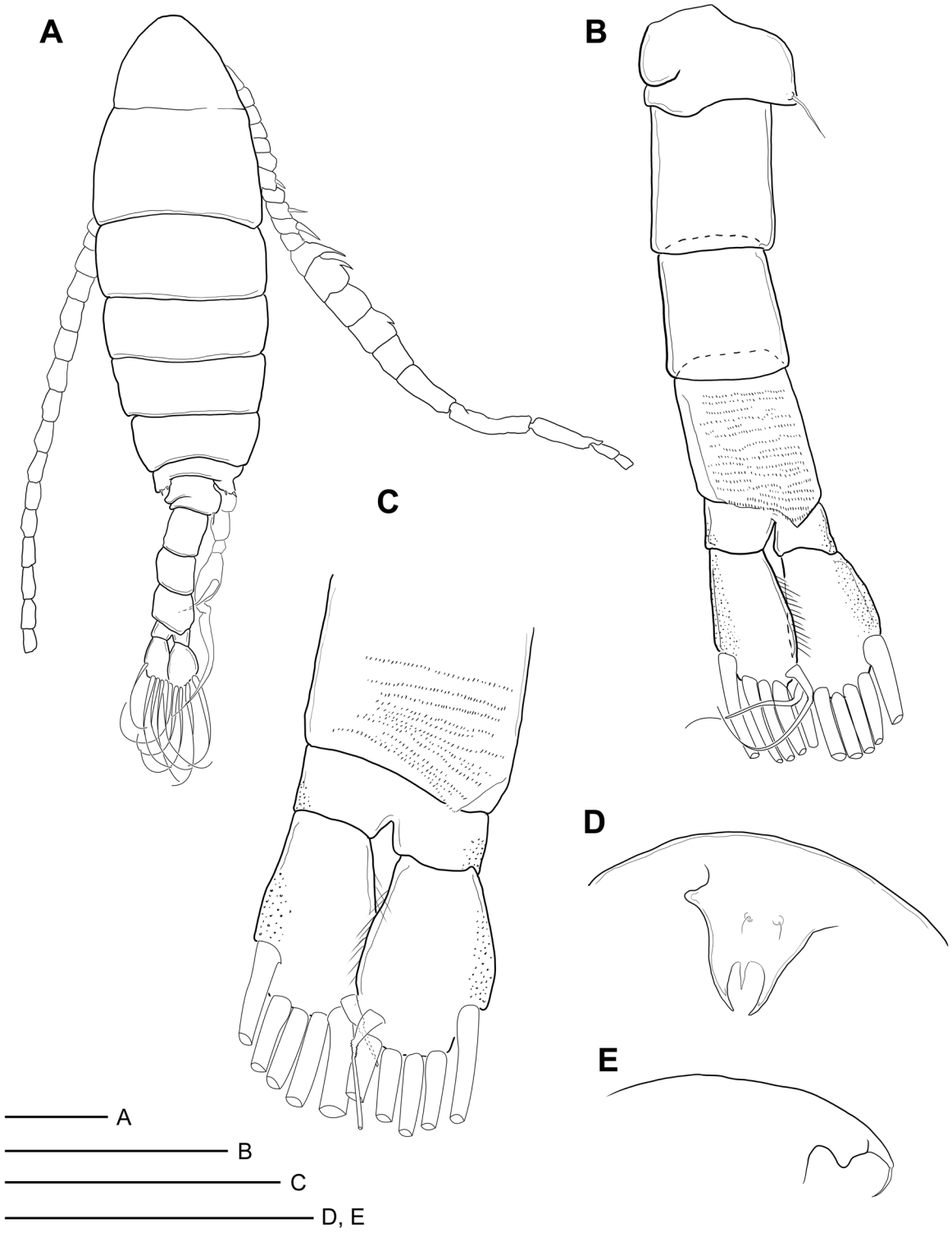


Fig. 22. *Mastigodiaptomus cucapa* sp. nov., allotype, adult, ♂ (ECO-CH-Z-10640, from Mocuzari Dam, Sonora). **A**. Habitus in dorsal view. **B**. Urosome in dorsal view. **C**. Fourth urosomite, anal somite and caudal rami. **D**. Rostrum in ventral view. **E**. Rostrum in lateral view. Scale bars = 100 μm.

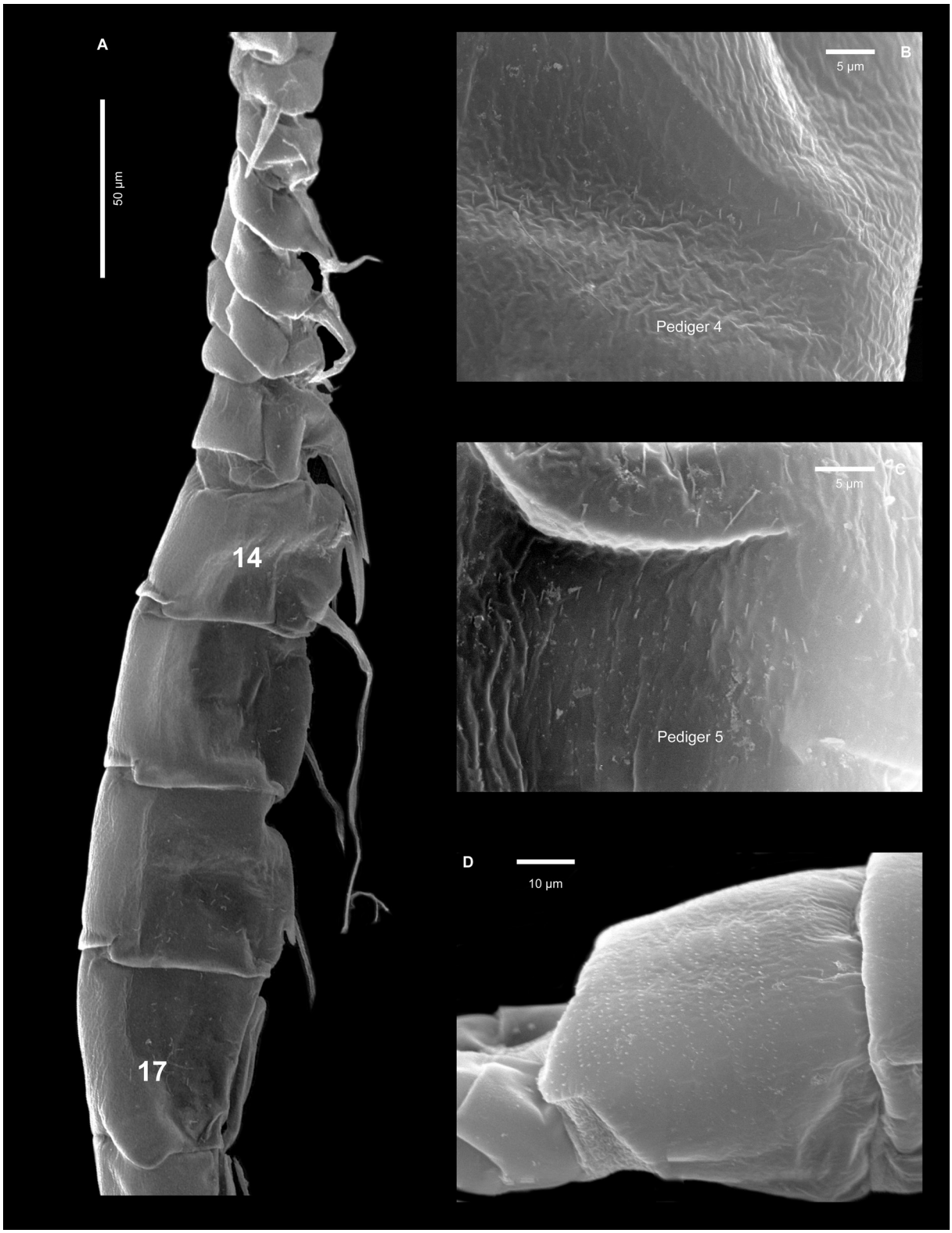


Fig. 23. *Mastigodiaptomus cucapa* sp. nov., adult, ♂, from La Palma Dam, Baja California Sur, Mexico (ECO-CH-Z10538). Scanning Electron Microscopy. **A**. Antennule, segments 8–17. **B**. Pediger 4. **C**. Pediger 5. **D**. Fourth urosomite in lateral view.

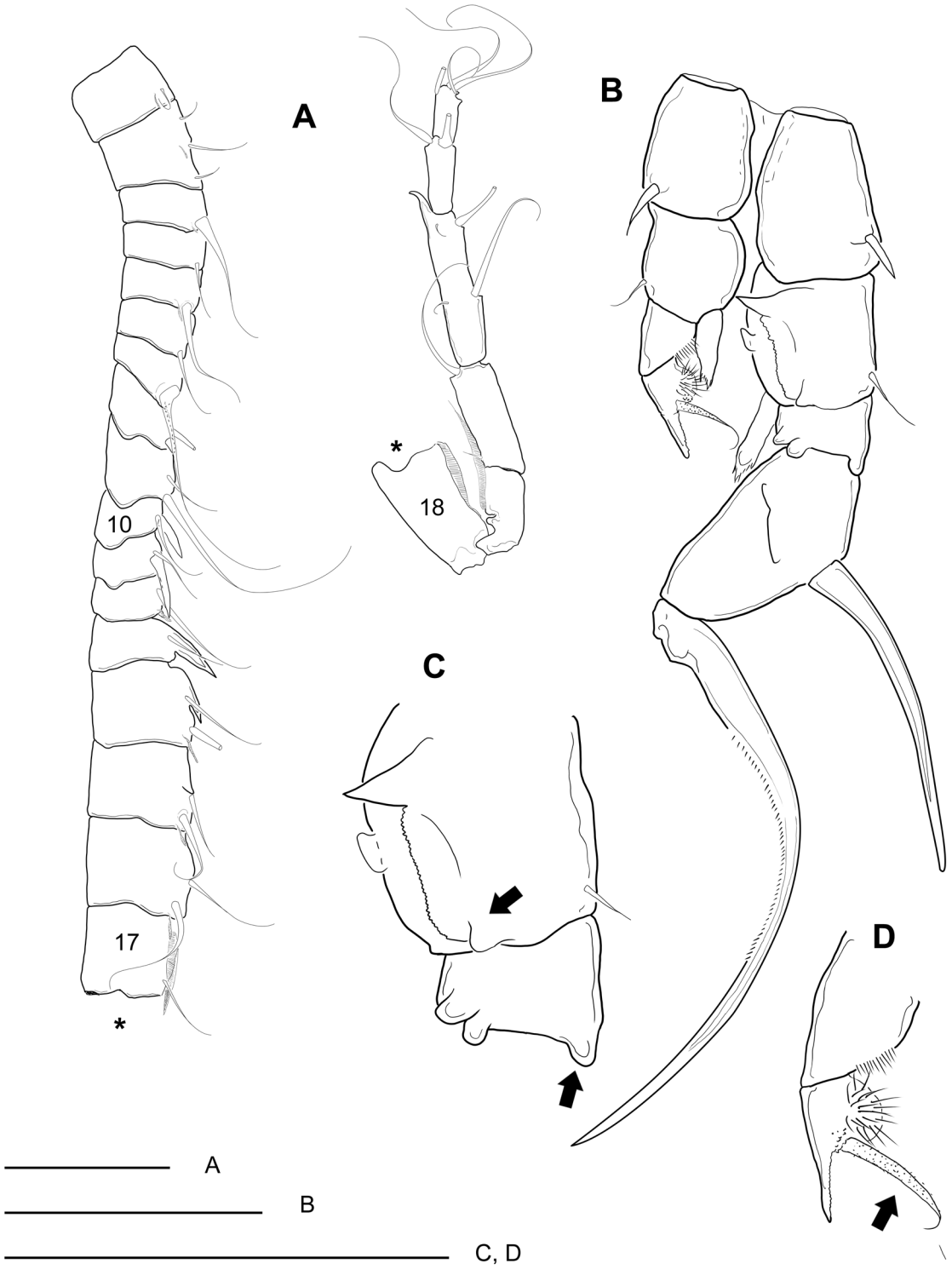


Fig. 24. *Mastigodiaptomus cucapa* sp. nov. **A**. ♂, from La Palma Dam, Baja California Sur ECO-CH-Z-10643). **B–D**. Allotype, adult, ♂, from Mocuzari Dam, Sonora (ECO-CH-Z-10640). **A**. Antennule. **B**. Leg 5. **C**. Basis and Exp1 of right leg 5, arrows indicate distal projection, respectively. **D**. Exopods 1 and 2 of left leg 5, arrow indicate details on spinous seta. Asterisks indicate segmental separation of the right A1. Scale bars = 100 µm.

P3 Cx longer than wide, Cx and Bs smooth, Exp three-segmented, with setules along inner margin of Exp1; Enp three-segmented with spinules apically on Exp3. P4 Cx longer than wide, Cx and Bs smooth; Exp three-segmented, setules along inner margin of Exp 1 and 2; Enp three-segmented with setules along inner margin and spinules apically on Exp3.

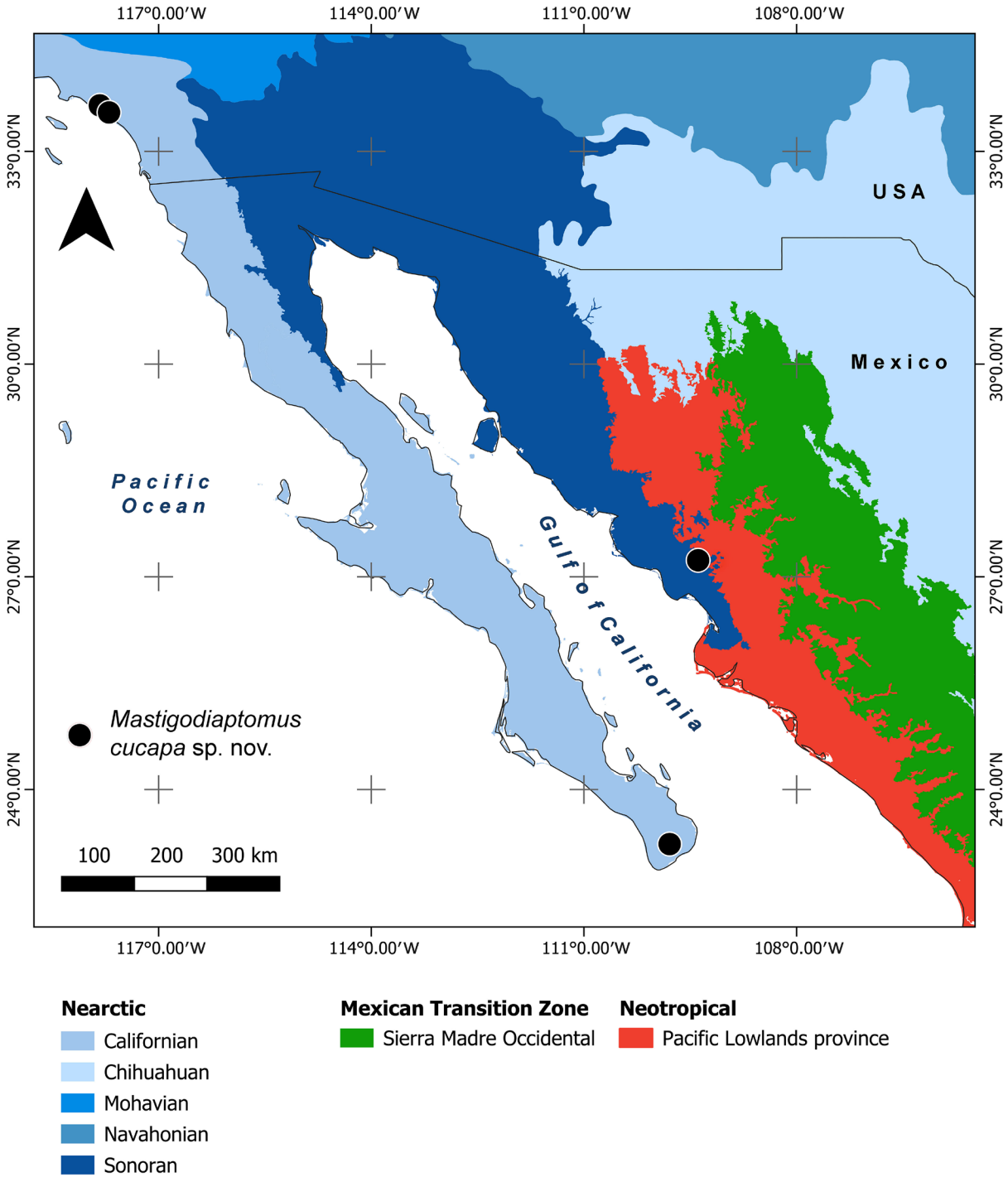


Fig. 25. Geographical distribution of *Mastigodiaptomus cucapa* sp. nov. in the Nearctic bioregion recorded in this study. Biogeographical representation with ecoregions following Morrone (2017, 2019) and Escalante *et al*. (2021).

P5 (Fig. 20D). Cx with thick spine distally. Bs with seta proximally and outer projection distally on outer margin (upper arrows in Fig. 20D). Exp three-segmented; Exp1 longer than wide, Exp2 with outer small spinous projection and row of minute spinules along inner margin. Exp3 small, with curved spinous process and spine almost reaching the end of Exp2 (lower arrows in Fig. 20D). Enp one-segmented, as long as inner margin of Exp1, ending in acute spinous process with spinules subtertminally and terminally.

Male

Habitus (Fig. 22A). Total body length 950–1280 µm (n = 24) excluding caudal setae. Pedigers four and five with row of minute spinules distally (Fig. 23B–C). Short metasomal wings, slightly asymmetrical, with two distal minute spines distally (Fig. 22A). Rostral spines elongated, slender and curved inwards (Fig. 22D–E). A1 reaching tip CR.

Urosome (Figs 22B–C, 23D). Five-segmented. First segment wider than long, with two lobes on left and right, long and slender spine on right side. Urosomites two to four about the same length, longer than wide (Fig. 22B). Fourth urosomite covered with spinules in straight lines transversally (Figs 22C, 23D). Anal somite about half the length of preceding urosomites, covered with tubercles laterally. CR longer than wide, with tubercles, inner setules and six setae (Fig. 22B–C).

RA1 (Figs 23A, 24A). 22-segmented, with setal formula as follows: 1 (1s), 2 (3s + 1ae), 3 (1s + 1ae), 4 (1s), 5 (1s + 1ae), 6 (1s), 7 (1s + 1ae), 8 (1s + 1ae), 9 (2s), 10 (1sp + 1s), 11 (1sp + 1s), 12 (1sp + 1s + 1ae), 13 (1s), 14 (2s + 1ae), 15 (2s + 1ae), 16 (2s + 1ae), 17 (1s), 18 (0), 19 (1sp + 1s), 20 (4s), 21 (2s), 22 (4s). Segments 13–16 with spinous process. Segments 17–19 with with dorsal thickening. Segment 19 with pseudosegmentation. Antepenultimate segment with distal hook-like process.

LA1. As in female.

Mouthparts. As in female.

P1–P4. As in female.

RP5 (Fig. 24B–C). Cx with thick spine distally. Bs with hyaline lamella on inner margin; caudal lamella with projection proximally, ending in acute spinous process and distal projection (upper arrow in Fig. 24C), and distal outer setae. Exp 2-segmented; Exp1 wider than long, with two lobes along inner margin and rounded process on outer margin (lower arrow in Fig. 24C); Exp2 longer than wide, with inverted "3" shaped lamella, bent aculeus inserted at midlength of outer margin, terminal claw about the same length as RP5, with minute spinules on inner face. Enp one-segmented reaching lamella of Exp2, ending in acute tip and setules.

LP5 (Fig. 24B, D). Cx with thick spine distally, Bs with seta on outer margin distally. Exp two-segmented; Exp1 with row of setules along inner margin tapering distally; Exp2 with rounded patch of setules on inner margin, and tubercles proximally, strong serrated spinous process terminally, with setae on inner margin covered with minute spinules (Fig. 24D). Enp one-segmented, reaching midlength of Exp2, ending in acute tip and setules.

Remarks

Morphological comparisons of *M. dorsalis* allowed us to identify a new species as previously hypothesized by Elías-Gutiérrez *et al.* (2008a, 2008b). This species is herein described as *Mastigodiaptomus cucapa* sp. nov., which resembles the nominal *M. dorsalis*, including projections on pedigers 4 and 5 and a one-segmented female P5 Enp. Males of both species have a pincer-like LP5 Exp2. However, several diagnostic characters allow a clear differentiation in *M. cucapa* sp. nov: 1) in

both sexes, the prosome bears rows of minute spinules on pedigers 3 to 5, the rostrum is elongated, slender, and curved inwards, the Md palp Exp3 possesses three rows of apical minute spinules, and the Mx1 praecoxal arthrite features proximal setules. 2) The female is characterized by slightly asymmetric metasomal wings with the left one longer than the right, A1 overreaching the CR by three segments, genital double-somite is slightly dilated, CR with setules on the outer margin, and a P5 Bs with a process on the distal outer margin. 3) The male is distinguished by an A1 reaching the tip of the CR, a first urosomite with a long and slender distal spine, a fourth urosomite with a straight row of minute spinules, a RP5 Bs caudal lamella bearing a distal process, an RP5 Exp1 with a curved distal outer projection, and LP5 Exp2 setae densely covered with minute spinules.

Distribution

This species was recorded in the Western NA subregion (Fig. 25), particularly within the Californian and Rocky Mountain dominions, encompassing the Californian and Sonoran ecoregions (Escalante *et al.* 2021). These regions are located in northern Mexico and the southern USA and are characterized mainly by arid environments with vegetation from temperate forests (Morrone 2019). Although this region has a mean annual precipitation deficit of 500–600 mm, it contains permanent, ephemeral, saline, freshwater and occasionally alkaline epicontinental water bodies.

Key to the species of Mastigodiaptomus

The key is modified from the key based on morphological analysis proposed by Wilson (1959), Elías-Gutiérrez *et al.* (2008b), Gutiérrez-Aguirre & Cervantes-Martínez (2013, 2016), Gutiérrez-Aguirre *et al.* (2014, 2020), Suárez-Morales *et al.* (2020) and Elías-Gutiérrez *et al.* (2023).

Females

1. Setules only on medial margin of CR 2
– Setules on both medial and lateral margins of CR 4

2. Symmetric or asymmetric genital double-somite, dilated proximally or bulbose, with short spines on both margins 3
– Symmetric genital double-somite, almost parallel lateral margins, with short spines on both margins ..... ***M. purpureus*** Marsh, 1907 [Cuba]
3. Slightly asymmetric genital double-somite, bulbose lateral margins, with short spines on both margins; P5 Enp two-segmented, reaching midlength of inner margin of Exp 1; Bs with rounded process projecting over Enp; prosome smooth, without projection on pedigers 4 and 5 .... ***M. reidae*** Suárez-Morales & Elías-Gutiérrez, 2000 [Campeche, Mexico]
– Symmetric genital double-somite, slightly dilated proximally, lateral margins with short spines, P5 Enp one-segmented, reaching the end of inner margin of Exp1, Bs with rounded outer distal process; prosomites 3–5 with row of minute spinules, with processes on pedigers 4 and 5 .... ***M. cucapa*** sp. nov. [Sonora, Baja California Sur – Mexico; California, Indiana – USA]

4. Slightly symmetric genital double-somite, almost parallel margins; one- or two-segmented Enp of P5 5
– Asymmetric genital double-somite, bulbose margins or dilated proximally; one- or two-segmented Enp of P5 9

5. Left thoracic wing slightly shorter than right wing; A1 reaching proximal third of genital double-somite ..... ***M. maya*** Suárez-Morales & Elías-Gutiérrez, 2000 [Campeche, Mexico]
– Left thoracic wing slightly longer than right wing; A1 reaching beyond distal margin of genital double-somite 6

6. A1 extending beyond CR by last one or two segments; lateral margins of genital double-somite parallel: right and left spines placed at the same level 7
– A1 reaching anal somite or CR; genital double-somite asymmetric: right spine placed more proximal than left spine 8

7. Genital double-somite 1.5 times as long as wide; A1 without setules on medial margin .... ***M. texensis*** Wilson M.S., 1953 [Texas, USA; Southeastern Mexico].
– Genital double-somite 1.0–1.1 times as long as wide; A1 with setules on medial margin ....***M. siankaanensis*** Mercado-Salas *et al.*, 2018 [Quintana Roo, Mexico]

8. A1 reaching half the length of anal somite; widest region of the body on first pediger of prosome; length/width ratio of rostral spines = 2.0–2.1; genital double-somite 1.6–1.7 times as long as wide ... . ***M. ha*** Cervantes-Martínez, 2020 [Quintana Roo, Mexico]
– A1 reaching distal margin of CR; widest region of the body between second and third pedigers of prosome; length/width ratio of rostral spines = 2.5–2.6; genital double-somite 1.7–1.8 times as long as wide .....***M. alexei*** Elías-Gutiérrez, 2020 [Veracruz, Mexico]

9. One or two urosomites with a chitinous protuberance in the right posterolateral corner 10
– Urosomites with straight posterior margins, without protuberances in the right posterolateral corner 11

10. Second urosomite with one acute protuberance in the right posterolateral corner; P5 Enp one-segmented ..... ***M. amatitlanensis*** (Wilson M.S., 1941) [Lake Amatitlán, Guatemala]
– Genital double-somite and second urosomite with chitinous protuberance in the right posterolateral corner; P5 Enp two-segmented .... ***M. cuneatus*** Gutiérrez-Aguirre & Cervantes-Martínez, 2016 [Sinaloa, Mexico]

11. Genital double-somite distal half laterally swollen or curved and wrinkled on the right lateral margin 12
– Genital double-somite distal half straight or dilated on the right lateral margin 14

12. Second and third urosomites fused ventrally, usoromite two-segmented ventrally and three-segmented dorsally, plus CR .....***M. cihuatlan*** Gutiérrez-Aguirre, 2020 [Guerrero, Mexico]
– Urosomites unfused, urosomite three-segmented dorsoventrally, plus CR 13

13. P5 Enp as long as medial margin of Exp1; distal half of genital double-somite curved and wrinkled on the right lateral margin .... ***M. suarezmoralesi*** Gutiérrez-Aguirre & Cervantes-Martínez, 2013 [Chiapas, Mexico]
– P5 Enp shorter than the half the length of medial margin of Exp1; distal half of genital double-somite swollen on the right lateral margin .....***M. montezumae*** (Brehm, 1955) [Central Mexico]

14. Very small spines arranged in parallel rows on dorsal and anal plate; lateral spines of genital double-somite inserted at the same level; ventral spine of right wing if fifth pediger of prosome directed to the posterior region of the body .....***M. nesus*** Bowman, 1986 [Mexico, Central America]
– Dorsal and anal plate bare; right spine of genital double-somite inserted more proximally than left; ventral spine of right wing of fifth pediger of prosome directed to the dorsal region of the body 15

15. A1 24-segmented, fourth pediger of prosome with large blunt process on dorsal surface ....***M. galapagoensis*** Elías-Gutiérrez *et al.*, 2023 [Galapagos Island]
– A1 25-segmented, fourth pediger of prosome with blunt or keel-like process on dorsal surface 16

16. Fourth pediger of prosome with keel-like process and rounded projection of fifth pediger on dorsal surface; P5 Enp one-segmented as long as medial margin of Exp1 ..... ***M. dorsalis*** (Marsh, 1907) [Easter region of USA and Mexico, Central America]
– Fourth pediger of prosome with blunt process on dorsal surface; P5 Enp two-segmented reaching half the length of lateral margin of Exp1 17
17. Short spines of rostrum: 1.5–3.6 times as long as wide; cuticular surface of pedigers smooth (or at most, extremely small setae on ventrolateral surfaces); 1.4–1.8 mm of body length, including CR .. ***M. albuquerquensis*** (Herrick,1985) [Northern Mexico, Southern USA]
– Long spines of rostrum: 3.6– 4.0 times as long as wide; setules on ventral and distal margins from 2–5 pedigers (continuous or discontinuous rows); 0.9–1.3 mm of body length, including CR ..... ***M. patzcuarensis*** (Kiefer, 1938) [Michoacan, Mexico]

Males

1. RA1 with spiniform process on segment 16 well-developed, almost as long as its segment width; RP5 Bs with one subrectangular protuberance on medioproximal margin ..... ***M. reidae*** Suárez-Morales & Elías-Gutiérrez, 2000
– RA1 spiniform process reduced or absent; RP5 Bs with rounded basal protuberance on medioproximal margin 2

2. RP5 Bs with only one lobular protuberance on medioproximal margin, no chitinous lamella (in caudal view) 3
– RP5 Bs with chitinous lamella or lamellae and with or without protuberance on medioproximal margin 4

3. RP5 Bs with large protuberance; Exp2 with two semicircular transverse lamellae and one longitudinal Y-shaped ridge; RA1 antepenultimate segment with fang-like process ..... ***M. montezumae*** (Brehm, 1955)
– RP5 Bs with short protuberance; Exp2 with one low, rounded protuberance on outer margin; RA1 antepenultimate segment with wide knob-like process ..... ***M. maya*** Suárez-Morales & Elías-Gutiérrez, 2000

4. RP5 Bs with one chitinous lamella (or hyaline membrane) 5
– RP5 Bs with more than one chitinous lamella (or hyaline membrane) 13

5. RP5 Bs with chitinous semicircular lamella 6
– RP5 Bs with chitinous, cuneiform, transversal, longitudinal or semitriangular lamella 10

6. RP5 Exp2 caudal surface smooth, without lamellae ..... ***M. ha*** Cervantes-Martínez, 2021
– RP5 Exp2 caudal surface ornamented with sclerotization, lamellae, hyaline membranes or ridge 7

7. RP5 Exp2 caudal surface with two short semicircular lamellae: one medial and one lateral; aculeus length of half the length of its segment; RA1 with short spiniform process on segment 14 ..... ***M. purpureus*** (Marsh, 1907)
– RP5 Exp2 caudal surface with one sclerotization; aculeus length over half of its segment; RA1 with long spiniform process on segment 14 8

8. Urosomites two to four with rows of tiny spines on dorsal surfaces; LP5 Exp2 triangular, attenuated distally (with only setules); RP5 Exp2 with a long, straight ridge ..... ***M. nesus*** Bowman, 1986
– Urosomites with smooth dorsal surfaces; LP5 Exp2 truncated or tapering distally, with apical denticles (plus setules) 9

9. RP5 Exp2 1.6 times as long as wide, with one elongated hyaline membrane ..... ***M. siankaanensis*** Mercado-Salas, Khodami, Kihara, Elías-Gutiérrez & Martínez-Arbizu, 2018
– RP5 Exp2 1.7–1.8 times as long as wide, with a narrow crescent-shaped sclerotization ..... ***M. alexei*** Elías-Gutiérrez, 2020

10. RA1 spine on segment 8 enlarged, unarticulated, modified into a strong spiniform process; PR5 Exp2 caudal surface with two sclerotized projections plus one sclerotized longitudinal line ..... ***M. cihuatlan*** Gutiérrez-Aguirre, 2020
– RA1 articulate spine of segment 8 extremely small, or with single seta; RP5 Exp2 caudal surface nude or with simple ornament 11

11. RA1 segment 8 with single seta; RP5 Exp2 with shallow longitudinal groove ....***M. galapagoensis*** Elías-Gutiérrez, Steinitz-Kannan, Suárez-Morales & López, 2023
– RA1 segment 8 with small spine; RP5 caudal surface nude or with simple ornament 12

12. RP5 Exp2 with naked surface; Bs caudal surface with triangular protuberance on distal margin and one rounded protuberance on medioproximal margin .... ***M. cuneatus*** Gutiérrez-Aguirre & Cervantes-Martínez, 2016
– RP5 Exp2 with straight ridge; obliquely directed; Bs caudal surface without protuberances, almost rectangular ..... ***M. amatitlanensis*** (Wilson M.S., 1941)

13. LP5 Exp2 distally truncated and denticulated; aculeus inserted subterminally into the RP5 Exp2 ....***M. texensis*** Wilson M.S., 1953
– LP5 Exp2 distally attenuated (triangular); aculeus inserted into the second third of the RP5 Exp2 14

14. Aculeus shorter than the length of RP5 Exp2, with long spinules on medial margin; two short semi-cuticular lamellae on medial margin of Exp2; second to fourth urosomites with denticules on dorsal surfaces ..... ***M. suarezmoralesi*** Gutiérrez-Aguirre & Cervantes-Martínez, 2013
– Aculeus subequal or longer than the length of RP5 Exp2, with short spinules on medial margin, or bare; one long, curved hyaline lamella on Exp2; dorsal surfaces of urosomites nude or with minute spinules on dorsal surface of fourth urosomite 15

15. RP5 Bs with butterfly-like caudal lamella; nude urosomites 16
– RP5 Bs with proximal process on caudal lamella; fourth urosomite with minute spinules on dorsal surface 17

16. Short rostral spines: 2.2–3.0 times as long as wide; cuticular surfaces of prosomites nude; 1.37–1.82 mm body length, including CR .....***M. albuquerquensis*** (Herrick, 1895)
– Long rostral spines: 3.5–5.0 times as long as wide; setules on ventral and distal margins from second to fifth prosomites (continuous or discontinuous rows); 0.9–1.1 mm body length, including CR ....***M. patzcuarensis*** (Kiefer, 1938)

17. First urosomite with right slender spine distally; RP5 Exp1 with curved outer projection; LP5 Exp2 distal spiniform seta covered with minute spinules .....***M. cucapa*** sp. nov.
– First urosomite with regular distal spine; RP5 Exp1 without outer projection; LP5 Exp2 distal spiniform seta covered with minute setules ..... ***M. dorsalis*** (Marsh 1907)

Discussion

History of the generic assignment

The historical nomenclature treatment of "*Arctodiaptomus dorsalis*" reveals persistent taxonomic uncertainty for decades, particularly regarding its generic placement and species limits. Since its original description by Marsh (1907), the species has been repeatedly reassigned and compared with morphologically similar taxa, reflecting the difficulty of interpreting diagnostic characters for this species.

For instance, the resemblance of "*Arctodiaptomus dorsalis*" with *Prionodiaptomus* Light, 1939 have been mentioned by Collado *et al.* (1984), without further clarification and without including a formal synonymy for this species. The main generic differences between "*A. dorsalis*" and *Prionodiaptomus*, can be found in Dussart & Defaye's (1995) generic descriptions.

The major inconsistency is its generic delimitation, and somehow its specific status: despite the fact that *A.* (*H.*) *kurilensis* and *A.* (*R.*) *arapahoensis* are American species traditionally assigned to *Arctodiaptomus*, in our opinion they do not fully conform to the diagnostic features of the genus. Probably, the reason why Dussart & Defaye (1983) and Reddy (1994) remarked that their position within the genus *Arctodiaptomus* was doubtful, was because generic morphological characters differ from those presented for the Palaearctic *Arctodiaptomus*.

In addition, Light (1939) excluded *Diaptomus dorsalis* from *Mastigodiaptomus*, and tentatively suggested that this species and its congeners (*D. floridanus*, *D. asymmetricus*, and *D. saltillinus*) might be more appropriately placed in *Arctodiaptomus*. However, he also recognized that the available evidence was insufficient to confirm this relocation. Later, Dussart & Defaye (1983) clarified that these American species do not correspond to the diagnostic characters of *Arctodiaptomus*, thereby rejecting Light´s (1939) proposal.

In that sense, the exclusion of "*A. dorsalis*" from the genus *Arctodiaptomus* stems from morphological inconsistencies with the genus diagnosis, assigned after Dussart & Fernando (1985). According to Kiefer (1932), Reddy (1994), Dussart & Defaye (1995), the genus *Arctodiaptomus* is characterized by the female with wide metasomal wings, antennule segment 11 bearing two setae, P5 Enp short, bearing only a tuft of apical setules, or subapical row of setules on the anterior aspect. Males exhibit a RP5 Bs with hyaline lamella and plug-like lobe, and LP5 Exp2 forming a distinct 'pincer' with an elongated digitiform process and terminal seta, and RA1 with spines on segments 10, 11, 13, sometimes on segments 14, 15.

None of these morphological characters were observed in the specimens analyzed herein. Contrastingly, they exhibit morphological characters consistent with *Mastigodiaptomus* s. str. as defined by Kiefer (1932), Light (1939), Wilson (1959), Dussart & Defaye (1995), such as: males RA1 with spiniform processes on segments 10, 11, 13, 14, 15 and sometimes on 16; antepenultimate segment with a small extension. RP5 with caudal hyaline membrane. LP5 with Exp1 tapering gradually, Exp2 ending with process and inner spiniform seta. Females P5 Exp3 with long spiniform seta and vestigial seta, Enp ending in two curved rows of setules and subapical setae. These characters support the reassignment of "*A. dorsalis*" to *Mastigodiaptomus dorsalis*.

Chronicle of synonyms

Regarding the synonym species assigned to "*A. dorsalis*", Brehm (1932, 1939), stated that the main difference between *D. dampfi* and *D. dorsalis* was the absence of the typical keel-like dorsal processes on the female's pediger. Nevertheless, revising material from the type locality (lake Petén, Guatemala), we found specimens with very reduced processes, variation in the dorsal process was also reported by Suárez-Morales & Elías-Gutiérrez (2001), who synonymized *A. dampfi* with "*A. dorsalis*".

On the other hand, Herbst (1960) described *D. alter* with characters resembling "*A. dorsalis*" without performing a formal species comparison. After revising several specimens from Nicaragua, including the type locality (lake Managua), we found slight morphological differences observed in other *M. dorsalis* populations (see Figs 11, 15; Table 3). Although we did not revise material of *D. proximus*, this species was synonymized with *D. alter* and subsequently with *D. dorsalis* by Dussart & Fernando (1985). They concluded that probably all these synonymies are the result of the material preparation and compression of the structures between the slide and coverslip, thus, they suggest to revise especially male's P5 in three dimensions. Nevertheless, slight morphological differences could be related to phenotypic variations, such as the reported for *M. ha* Cervantes, 2020 (Cervantes-Martínez *et al.* 2021).

Differentiation of *M. cucapa* sp. nov.

Females of *M. cucapa* sp. nov. can be distinguished from *M. dorsalis* by their A1 extending beyond CR by three segments (vs antenules reaching tip of CR or beyond it only by 1 segment in *M. dorsalis*), a slightly dilated genital double-somite, CR with setules on outer margin (vs setules on both CR margins in *M. dorsalis*), and Bs of P5 with rounded process distally. Additional differences include: three rows of spinules on the mandible Enp3, setules on the precoxal arthrite margin of Mx1, and long, slender rostral spines.

Males of *M. cucapa* sp. nov. have a long spine distally on the first urosomite, RP5 Bs with a process distally on the caudal lamella, Exp1 with a curved projection on the outer margin, and LP5 Exp2 setae covered with minute spinules. These characters are different in *M. dorsalis*, which lacks Bs and Exp1 projections distally and the LP5 Exp2 setae are setulate.

Genetic divergence of the analyzed taxa

The intergeneric divergences between *Mastigodiaptomus*, *Leptodiaptomus*, and *Arctodiaptomus* ranged from 27–30% (Table 1) which are consistent with values reported in other calanoid copepods (Bucklin *et al.* 2003). The *COI* barcode analysis revealed that all specimens historically identified as "*A. dorsalis*" can be allocated to a single, well-supported group showing some affinities with the genus *Mastigodiaptomus* (Fig. 2). Interspecific divergence within *Mastigodiaptomus* species found in this study, is also in agreement with previous findings (Mercado-Salas *et al.* 2018; Gutiérrez-Aguirre *et al.* 2020).

The *COI* gene exhibits relatively high mitochondrial substitution rates, and calanoid copepods in particular exhibit accelerated molecular evolution, which can result in deep divergences even among closely related taxa. In this group, interspecific distances exceeding 20% have been reported (Thum & Derry 2008), along with a wide range of intergeneric divergence between 9 and 25% (Bucklin *et al.* 2003). This overlap indicates that, in rapidly evolving taxa, species with a low evolutionary rate may exhibit genetic distances comparable to those observed among more recently diversified genera. For instance in species with allopatric or parapatric speciation in a short period of time as observed for diaptomids (Mercado-Salas *et al*. 2018). Conversely, divergence thresholds alone may be insufficient for distinguishing taxonomic levels in these groups.

Furthermore, mt*COI* has been widely used as a complementary tool for species delimitation and taxonomic identification across several taxa (Hebert *et al.* 2003; Kochanova *et al.* 2021). Nevertheless, single-marker mitochondrial analyses are generally less informative for resolving relationships at higher taxonomic levels, such as subfamilies or families (Elías-Gutiérrez *et al.* 2026). This inadequacy of the *COI* marker could also apply to genus complexes of more ancient origin, like the *Leptodiaptomus*/*Mastigodiaptomus* complex, and it could be one of the reasons for the low bootstrap support values found in our analysis (Fig. 2).

In any case, the analyzed *COI* fragment proved useful in highlighting – alongside the morphological analysis – to suggest the placement of *M. dorsalis* within *Mastigodiaptomus*, as well as for supporting the recognition of *M. cucapa* sp. nov., particularly because the analysis included sequences representing 11 of the 16 currently recognized species of the genus.

The pattern recovered for *Leptodiaptomus* with the ML tree may also reflect the effects of partial taxon sampling within Diaptominae, considering that only four representatives of this widespread genus were included in the analysis. A limited sampling effort, coupled with the genetic divergence observed in *L. novamexicanus* could be one of the contributing factors to the separation into at least two distinct clades. Similar patterns of unresolved or incomplete sorting in mitochondrial gene trees have been documented in arthropods, with about 26% of unsolved groups at different taxa levels (Funk & Omland 2003), as well as in freshwater (Elías-Gutiérrez *et al.* 2026) and marine copepods (Blanco-Bercial *et al.* 2014).

Accordingly, *Mastigodiaptomus dorsalis* shows moderate instraspecific genetic divergence (see Fig. 2, Table 1), which is consistent with the slight morphological variation observed from different localities in the Neotropics and the Mexican Transition Zone (Table 3; Figs 11–16). Similar patterns of intra- and interpopulation variability have been documented in other diaptomid copepods, including *Mastigodiaptomus montezumae* (Brehm, 1955), *Leptodiaptomus sicilis* (S.A. Forbes, 1882) and *Tropodiaptomus vicinus* (Kiefer, 1930) (Mercado-Salas *et al.* 2018; Ortega-Mayagoitia *et al.* 2022; Saetang *et al.* 2022).

Due to the high sampling density of *M. dorsalis* (93 *COI* sequences), the ASAP analysis inferred an increased number of genetic partitions within this cluster, likely resulting in oversplitting. As sampling intensity increases, the probability of detecting higher intraspecific genetic divergence also rises (Gaytán *et al.* 2020).

Furthermore, widely distributed species such as *M. dorsalis* are expected to exhibit considerable intraspecific genetic and phenetic variability. This variability is often associated with genetic isolation by distance, as documented in some moth species (Gaytán *et al*. 2020), or with phenotypic plasticity in response to environmental heterogeneity, as observed in tropical cichlids (Barrientos-Villalobos *et al*. 2018). Similar patterns have also been reported in other diaptomids such as *L. sicilis* (Barrera-Moreno *et al*. 2015), as well as in systems influenced by continental-island isolation (Cervantes-Martínez *et al*., 2021).

Thus, the ML tree in combination with mPTP results supports the interpretation that the partitions inferred by ASAP represents geographically structured subgroups within *M. dorsalis*, rather than discrete species-level entities.

Furthermore, the ML tree and species delimitation analyses (mPTP and ASAP) consistently support the recognition of *M. cucapa* sp. nov. as a distinct species separated from *M. dorsalis* (Fig. 2). The genetic divergence between these taxa (8.07%, Table 1) falls within the range commonly reported for closely related species in diaptomid copepods (Bucklin *et al*. 2003; Elías-Gutiérrez *et al*. 2026). Comparable values have been documented for sibling species such as *M. patzcuarensis* and *M. albuquerquensis* (~4%, Gutiérrez-Aguirre *et al.* 2014) as well as *L. garciai* and *L. novamexicanus* (6.04%, Montiel-Martínez *et al.* 2008). In these cases, species boundaries were supported by integrative evidence, including morphological differentiation and geographic distribution, highlighting the importance of combining multiple lines of evidence when addressing similar species.

The *COI* gene has been widely used to analyze taxon identification mainly in the Americas, related to zooplankters such as rotifers, cladocerans, copepods, and acarii (Cervantes-Martínez *et al*. 2023),

compared with the use of other molecular markers (Mercado-Salas *et al.* 2018; Gutiérrez-Aguirre *et al.* 2020; García-Morales *et al.* 2021; Elías-Gutiérrez *et al.* 2026). In combination with species delimitation methods, along with detailed morphological and distributional assessments, these analyses can provide a robust framework for integrative taxonomical analysis (Kochanova *et al.* 2021; Saetang *et al.* 2022), as presented in this study.

Nevertheless, due to the high substitution rate of the *COI* gene and relatively short fragment length (~650 bp), this marker has limited resolution for deeper phylogenetic inference. More conservative markers, such as 18S or 28S rRNA genes, are better suited for reconstructing evolutionary relationships at higher taxonomic levels (Miracle *et al.* 2013; Mookkaiah & Ravichandran 2016; Kochanova *et al.* 2021; Mayor *et al.* 2024). Therefore, future studies integrating multiple molecular markers will be essential to further resolve phylogenetic relationships within Diaptomidae in the Americas.

Distributional patterns

The relocation of "*A. dorsalis*" to the genus *Mastigodiaptomus* is further supported by geographic distribution. *Mastigodiaptomus* is primarily Neotropical, with 16 known species in America, but largely endemic to Mexico with nine species (Gutiérrez-Aguirre *et al.* 2020; Elías-Gutiérrez *et al.* 2023). This distribution pattern matches that of *M. dorsalis* (Suárez-Morales & Elías-Gutiérrez 2001; Suárez-Morales 2003; Reid 2007). Whereas species of *Leptodiaptomus* are mainly distributed in the Nearctic region, with 22 known species (Silva-Briano & Suárez-Morales 2010), which includes seven species recorded for the Mexican territory. These genera are the most diverse among epicontinental copepods in America and in our study area (Cervantes-Martínez *et al.* 2023). In contrast, species of *Arctodiaptomus* are largely Palearctic (Reddy 1994; Błędzki & Rybak 2016).

The bioregional separation of both species surveyed here reinforces their taxonomic distinction. *Mastigodiaptomus cucapa* sp. nov. inhabits arid and semi-arid environments in the western Nearctic, while *M. dorsalis* is found in humid regions across the NT and NA bioregions, including records in the MTZ (Morrone 2017, 2019; Escalante *et al.* 2021). Although reproductive isolation was not tested for both species, the combination of morphological, genetic and biogeographic evidence supports the recognition of *M. cucapa* and validates its separation from the nominal *M. dorsalis*.

In conclusion, the distinctive morphological characters and biogeographic distribution, supported by *COI* barcodes, allowed us to reclassify this longstanding taxonomical uncertainty. This highlights the key role of integrative taxonomy in effectively solving cryptic diversity of diaptomid copepod taxa.

The generic status of *A. floridanus*, *A. saltillinus*, and *A. asymmetricus* should be re-evaluated with integrative taxonomy; it is likely that they are not members of the genus *Arctodiaptomus*, according to the stated in this study.

In the same way, further studies are needed to clarify the identity of "*A. dorsalis*" populations reported from the Philippines (Papa *et al.* 2012; Metillo *et al.* 2014; de Leon *et al.* 2020) and Hawaii (Hairston *et al.* 2025), which may represent populations of *M. dorsalis* or *M. cucapa* sp. nov. In case that the "*A. dorsalis*" populations are attributed to the genus *Mastigodiaptomus*, then, it will be a new record of extended range of this genus outside their known distribution mainly for the Neotropics (Gutiérrez-Aguirre *et al.* 2020), and the fifth record of a species of *Mastigodiaptomus* inhabiting island environments (Cervantes-Martínez *et al.* 2021), in addition to *M. galapagoensis* Elías-Gutiérrez, Steinitz-Kannan, Suárez-Morales & López, 2023, *M. ha*, *M. nesus* and *M. purpureus* (Marsh, 1907). Further studies are necessary to confirm the identities of these island populations.

Acknowledgments

The first author thanks the National Council of Humanity, Science and Technology (CONAHCYT) with the SNI-III Assistant Program, her scholarship graduate studies from the Ministry of Science, Humanities, Technology and Innovation (SECIHTI), with the Number 1012891, and the Edward B. and Phyllis E. Reed Fellow program held at the Smithsonian Institution National Museum of Natural History (NMNH-SI), for financial support. Sergio Hernández-Trujillo collected samples from La Palma Dam, Baja California Sur, Mexico; Julio Juárez-Pernillo and Elena Reyes-Solares collected samples from Lake Amatitlán, Guatemala. ECO-CH-Z specimen consultation and SEM work were possible thanks to the facilities of El Colegio de la Frontera Sur (ECOSUR-Chetumal). Mexican and Guatemalan specimens were cataloged by José Ángel Cohuo-Collí (ECOSUR). Karen Osborn and Chad Walter from the NMNH provided valuable support with USNM type material, facilities, organization, and bibliography during the fellow tenure of the first author. We are grateful to Martín de Jesús Islas Castro for his careful revision of the English language in this manuscript. Anonymous reviewers made valuable comments on an earlier version of this manuscript.

References

Bautista F. 2023. *El Karst de México*. Asociación Mexicana de Estudios sobre el Karst, Ciudad de México.

Blanco-Bercial L., Cornils A., Copley N. & Bucklin A. 2014. DNA barcoding of marine copepods: assessment of analytical approaches to species identification. *PLoS Currents Tree of Life* 1. https://doi.org/10.1371/currents.tol.cdf8b74881f87e3b01d56b43791626d2

Barrera-Moreno O.A., Ciros-Pérez J., Ortega-Mayagoitia E., Alcántara-Rodríguez A. & Piedra-Ibarra E. 2015. From local adaptation to ecological speciation in copepod populations from neighboring lakes. *PLoS ONE* 10 (4): e0125524. https://doi.org/10.1371/journal.pone.0125524

Barrientos-Villalobos J., Schmitter-Soto J.J. & de los Monteros A.J.E. 2018. Several subspecies or phenotypic plasticity? A geometric morphometric and molecular analysis of variability of the Mayan cichlid *Mayaheros urophthalmus* in the Yucatan. *Copeia* 106 (2): 268–278. https://doi.org/10.1643/CI-17-657

Błędzki L.A. & Rybak J.I. 2016. Characteristics of orders and families with a list of European genera and species. *In:* Błędzki L.A. & Rybak J.I. (eds) *Freshwater Crustacean Zooplankton of Europe*: 453–473. Springer International Publishing, Switzerland. https://doi.org/10.1007/978-3-319-29871-9_16

Brandorff G.O. 2012. Distribution of some Calanoida (Crustacea: Copepoda) from the Yucatán Peninsula, Belize and Guatemala. *Revista de Biología tropical* 60 (1): 187–202. https://doi.org/10.15517/rbt.v60i1.2751

Brehm V. 1932. Notizen zur Süβwasserfauna Guatemalas und Mexikos. *Zoologischer Anzeiger* 91: 63–66.

Brehm V. 1939. La fauna microscópica del Lago Petén, Guatemala. *Anales de la Escuela Nacional de Ciencias Biológicas* 1: 174–203.

Bucklin A., Frost B.W., Brandford-Grieve J., Allen L.D. & Copley N.J. 2003. Molecular systematic and phylogenetic assessment of 34 calanoid copepod species of the Calanidae and Clausocalanidae. *Marine Biology* 142: 333–343. https://doi.org/10.1007/s00227-002-0943-1

Cervantes-Martínez A., Gutiérrez-Aguirre M.A., Suárez-Morales E. & Jaime S. 2021. Phenetic and genetic variability of continental and island populations of the freshwater copepod *Mastigodiaptomus ha* Cervantes, 2020 (Copepoda): A case of dispersal? *Diversity* 13 (6): 11. https://doi.org/10.3390/d13060279

Cervantes-Martínez A., Durán-Ramírez C., Elías-Gutiérrez M., García-Morales A.E., Gutiérrez-Aguirre M., Jaime S., Macek M., Maeda-Martínez A.M., Martínez-Jerónimo F., Mayén-Estrada R., Medina-Durán J.H., Montes-Ortiz L., Olvera-Bautista J.F.Y., Romero-Niembro V.M. & Suárez-Morales E. 2023. Freshwater diversity of zooplankton from Mexico: Historical review of some of the main groups. *Water* 15 (858): 1–22. https://doi.org/10.3390/w15050858

Collado C., Defaye D., Dussart B.H. & Fernando C.H. 1984. The freshwater Copepoda (Crustacea) of Costa Rica with notes on some species. *Hydrobiologia* 119 (2): 89–99. https://doi.org/10.1007/BF00011948

Dussart B. & Defaye D. 1983. *Répertoire mondial des Crustacés Copépodes des Eaux intérieures. I. Calanoïdes*. Centre National de la Recherche Scientifique, Paris.

Dussart B.H. & Defaye D. 1995. Copepoda. *In*: Dummont H.J. (ed.) *Guides to the Identification of the Microinvertebrates of the Continental Waters of the World 7*: 1–277. SPB Academic Publishing, The Hague.

Dussart B.H. & Fernando C.H. 1985. Tropical freshwater Copepoda from Papua, New Guinea, Burma, and Costa Rica, including a new species of *Mesocyclops* from Burma. *Canadian Journal of Zoology* 63: 202–206. https://doi.org/10.1139/z85-031

Elías-Gutiérrez M., Martínez-Jerónimo F., Ivanova N.V., Valdez-Moreno M. & Hebert P.D.N. 2008a. DNA barcodes for Cladocera and Copepoda from Mexico and Guatemala, highlights and new discoveries. *Zootaxa* 1839: 1–42. https://doi.org/10.11646/zootaxa.1839.1.1

Elías-Gutiérrez M., Suárez-Morales E., Gutiérrez-Aguirre M., Silva-Briano M., Granados-Ramírez J.G. & Garfias-Espejo T. 2008b. *Cladocera y Copepoda de las Aguas continentales de México. Guía ilustrada*. Universidad Autónoma de México, México.

Elías-Gutiérrez M., Steinitz-Kannan M., Suárez-Morales E. & López C. 2023. *Mastigodiaptomus galapagoensis* n. sp. (Crustacea: Copepoda: Diaptomidae), a possibly extinct copepod from a crater lake of the Galapagos archipelago. *PeerJ* 11. https://doi.org/10.7717/peerj.15807

Elías-Gutiérrez M., Suárez-Morales E., García-Morales A.E. & Cohuo-Collí J.A. 2026. DNA barcoding of North American freshwater copepods (Diaptomidae and Cyclopoida): an overview after 20 years with emphasis in the Mexican fauna, the transition between the Nearctic and Neotropics. *PeerJ* 14: e20989. https://doi.org/10.7717/peerj.20989

Escalante T., Rodríguez-Tapia G. & Morrone J.J. 2021. Toward a biogeographic regionalization of the nearctic region: Area nomenclature and digital map. *Zootaxa* 5027 (3): 351–375. https://doi.org/10.11646/zootaxa.5027.3.3

Funk D.J. & Omland K.E. 2003. Species-level paraphyly and polyphyly: Frequency, causes and consequences, with insights from animal mitochondrial DNA. *Annual Review of Ecology, Evolution, and Systematics* 34: 397–423. https://doi.org/10.1146/annurev.ecolsys.34.011802.132421

García-Morales A.E., Domínguez-Domínguez O. & Elías-Gutiérrez M. 2021. Uncovering hidden diversity: Three new species of the *Keratella* genus (Rotifera, Monogononta, Brachioinidae) of high altitude water systems from Central Mexico. *Diversity* 13 (12): 676. https://doi.org/10.3390/d13120676

Gaytán A., Bergsten J., Canelo T., Pérez-Izquierdo C., Santoro M. & Bonal R. 2020. DNA Barcoding and geographical scale effect: The problems of undersampling genetic diversity hotspots. *Ecology and Evolution* 10: 10754–10772. https://doi.org/10.1002/ece3.6733

Gutiérrez-Aguirre M.A. & Cervantes-Martínez A. 2013. Diversity of freshwater copepods (Maxillopoda: Copepoda: Calanoida, Cyclopoida) from Chiapas, Mexico with a description of *Mastigodiaptomus suarezmoralesi* sp. nov. *Journal of Natural History* 47 (5–12): 479–498. https://doi.org/10.1080/00222933.2012.742587

Gutiérrez-Aguirre M.A. & Cervantes-Martínez A. 2016. A new species of *Mastigodiaptomus* Light, 1939 from Mexico, with notes of species diversity of the genus (Copepoda, Calanoida, Diaptomidae). *ZooKeys* 2016 (637): 61–79. https://doi.org/10.3897/zookeys.637.10276

Gutiérrez-Aguirre M.A., Cervantes-Martínez A. & Elías-Gutiérrez M. 2014. An example of how barcodes can clarify cryptic species: The case of the calanoid copepod *Mastigodiaptomus albuquerquensis* (Herrick). *PLoS ONE* 9 (1): e85019. https://doi.org/10.1371/journal.pone.0085019

Gutiérrez-Aguirre M.A., Cervantes-Martínez A., Elías-Gutiérrez M. & Lugo-Vázquez A. 2020. Remarks on *Mastigodiaptomus* (Calanoida: Diaptomidae) from Mexico using integrative taxonomy, with a key of identification and three new species. *PeerJ* 8:e8416. https://doi.org/10.7717/peerj.8416

Gutiérrez-Aguirre M.A., Cervantes-Martínez A. & Suárez-Morales E. 2024. Ecological indicators and estimators of fish and crustacean diversity in the Yucatan Peninsula. *Diversity* 17 (1): 5. https://doi.org/10.3390/d17010005

Hairston N.G., Wilkins R.L., Ka'uhane Lupenui C. & Ellner S.P. 2025. An abundant non-native freshwater copepod, *Arctodiaptomus dorsalis*, on the Island of Hawai'i: distribution, dominance, dispersal, and diapause. *Biological Invasions* 27: 136. https://doi.org/10.1007/s10530-025-03585-6

Hebert P.D.N., Ratnasingham S. & de Waard J. 2003. Barcoding animal life: cytochrome c oxidase subunit 1 divergences among closely related species. *Proceedings of The Royal Society B* 270: S96–S99. https://doi.org/10.1098/rsbl.2003.0025

Herbst V.H.V. 1960. Copepods (Crustacea, Entomostraca) from Nicaragua and southern Peru. *Gewässer und Abwässer* 27: 27–54.

Huys R. & Boxall G.A. 1991. *Copepod Evolution*. The Ray Society, London.

Jaime S., Cervantes-Martínez A., Gutiérrez-Aguirre M.A., Hernández-Flores G., González-Herrera R.A., Sánchez-Rivera G., Enseñat-Soberanis F. & Delgado-Blas V.H. 2025. Toward an integrative overview of stygobiotic crustaceans for aquifer delimitation in the Yucatan Peninsula, Mexico. *Diversity* 17 (2): 77. https://doi.org/10.3390/d17020077

Kapli P., Lutreropp S., Zhang J., Kobert K., Pavlidis P., Stamatakis A. & Flouri T. 2017. Multi-rate Poisson tree processes for single-locus species delimitation under maximum likelihood and Markov chain Monte Carlo. *Bioinformatics* 33 (11): 1630–1638. https://doi.org/10.1093/bioinformatics/btx025

Kiefer F. 1932. Versuch eines Systems der Diaptomiden (Copepoda Calanoida). *Zoologische Jahrbücher, Abteilung für Systematik, Ökologie und Geographie der Tiere* 63 (4): 451–520.

Kiefer F. 1936. Freilebende Süß- und Salzwassercopepoden von der Insel Haiti. *Archiv für Hydrobiologie* 18 (IX): 263–317.

Kimura M. 1980. A Simple method for estimating evolutionary rates of base substitutions through comparative studies of nucleotide sequences. *Journal of Molecular Evolution* 16: 111–120. https://doi.org/10.1007/BF01731581

Kochanova E., Nair A., Sukhikh N., Väinölä R. & Husby A. 2021. Patterns of cryptic diversity and phylogeography in four freshwater copepod crustaceans in European lakes. *Diversity* 13: 448. https://doi.org/10.3390/d13090448

de Leon J.R., Guinto S.K.P., Tordesillas D.T. & Papa R.D.S. 2020. Depth and productivity as predictive parameters for the widespread invasion of *Arctodiaptomus dorsalis* (Marsh, 1907) (Copepoda: Calanoida) in tropical lakes in the Philippines. *Journal of Crustacean Biology* 40 (5): 512–519. https://doi.org/10.1093/jcbiol/ruaa052

Light S.F. 1939. New American subgenera of *Diaptomus* Westwood (Copepoda, Calanoida). *Transactions of the Americal Microscopical Society* 58 (4): 473–484. https://doi.org/10.2307/3222789

Marsh C.D. 1907. A revision of the North American species of *Diaptomus*. *Wisconsin Academy of Sciences, Arts, and Letters* 15: 381–515. https://doi.org/10.5962/bhl.title.9932

Marsh C.D. 1959. Copepoda. *In*: Ward H.B. & Whipple G.C. (eds) *Fresh-water Biology*: 741–789. John Wiley & Sons; Chapman & Hall, New York; London.

Mayor T.Y., Chaban O.A., Kaskova K.A. & Sukhikh N.M. 2024. Biodiversity assessment of *Eucyclops* Claus, 1893 (Copepoda: Crustacea) in the Baikal region using genetic methods. *Acta Biologica Sibirica* 10: 1269–1291. https://doi.org/10.5281/zenodo.14029856

Mercado-Salas N.F., Khodami S., Kihara T.C., Elías-Gutiérrez M. & Arbizu P.M. 2018. Genetic structure and distributional patterns of the genus *Mastigodiaptomus* (Copepoda) in Mexico, with the description of a new species from the Yucatan Peninsula. *Arthropod Systematics and Phylogeny* 76 (3): 487–507. https://doi.org/10.3897/asp.76.e31965

Metillo E.B., Masorong A.M., Macabangkit S.A.N., Licayan J.R.U., Tordesillas D.T. & Papa R.D.S. 2014. First record of the invasive *Arctodiaptomus dorsalis* (Marsh, 1907) (Copepoda: Calanoida: Diaptomidae) in Lake Lanao (Mindanao Is., Philippines). *Acta Manilana* 62: 19–23. https://doi.org/10.53603/actamanil.62.2014.pkhk5338

Miracle M.R., Alekseev V., Monchenko V., Sentandreu V. & Vicente E. 2013. Molecular-genetic-based contributions to the taxonomy of the *Acanthocyclops robustus* group. *Journal of Natural History* 47 (5–12): 863–888. https://doi.org/10.1080/00222933.2012.744432

Montiel-Martínez A., Ciros-Pérez J., Ortega-Mayagoitia E. & Elías-Gutiérrez M. 2008. Morphological, ecological, reproductive and molecular evidence for *Leptodiaptomus garciai* (Osorio-Tafall 1942) as a valid endemic species. *Journal of Planckton Research* 30 (10): 1079–1093. https://doi.org/10.1093/plankt/fbn067

Mookkaiah G.J. & Ravichandran R. 2016. Phylogenetic information of freshwater copepod (*Diaptomus sicilis*) with special reference to 18S rRNA. *International Journal of Biological Research* 4 (1): 25–28. https://doi.org/10.14419/ijbr.v4i1.5836

Morrone J.J. 2015. Biogeographical regionalisation of the world: A reappraisal. *Australian Systematic Botany* 28 (3): 81–90. https://doi.org/10.1071/SB14042

Morrone J.J. 2017. *Neotropical Biogeography Regionalization and Evolution*. CRC Press, Taylor & Francis Group, LLC, Boca Raton, Florida. https://doi.org/10.1201/b21824

Morrone J.J. 2019. Biogeographic regionalization and biotic evolution of Mexico: Biodiversity's crossroads of the New World. *Revista mexicana de Biodiversidad* 90 (4): 1–68. https://doi.org/10.22201/ib.20078706e.2019.90.2980

Ortega-Mayagoitia E., Alcántara-Rodríguez J.A., Urbán-Olivares J., Campos J.E. & Ciros-Pérez J. 2022. Genomic signatures of adaptative divergence in lacustrine copepods. *Freshwater Biology* 67 (6): 1045–1062. https://doi.org/10.1111/fwb.13900

Papa R.D.S., Li H., Tordesillas D.T., Han B. & Dumont H.J. 2012. Massive invasion of *Arctodiaptomus dorsalis* (Copepoda, Calanoida, Diaptomidae) in Philippine lakes: A threat to Asian zooplankton biodiversity? *Biological Invasions* 14 (12): 2471–2478. https://doi.org/10.1007/s10530-012-0250-9

Puillandre N., Brouillet S. & Achaz G. 2020. ASAP: Assemble Species by Automatic Partitioning. *Molecular Ecology Resources* 21: 609–620. https://doi.org/10.1111/1755-0998.13281

Reddy Y.R. 1994. Copepoda: Calanoida: Diaptomidae: key to the genera *Heliodiaptomus*, *Allodiaptomus*, *Neodiaptomus*, *Phyllodiaptomus*, *Eodiaptomus*, *Arctodiaptomus* and *Sinodiaptomus*. *In*: Dummont H.J. (ed.) *Guides to the Identification of the Microinvertebrates of the Continental Waters of the World 5*: 1–221. SPB Academic Publishing, The Hague.

Reed E.B. 1994. *Arctodiaptomus novosibiricus* Kiefer, 1971 in Alaska and Northwest territories, with notes on *A. arapahoensis* (Dodds, 1915) a key to the new world species of *Arctodiaptomus* (Copepoda: Calanoida). *Proceedings of the Biological Society of Washington* 107 (4): 666–679. Available from https://www.biodiversitylibrary.org/page/35515311 [accessed 15 Apr. 2026]

Reid J.W. 2007. *Arctodiaptomus dorsalis* (Marsh): A case history of copepod dispersal. *Banisteria* 1860 (30): 3–18.

Reid J.W. & Williamson C.E. 2010. Copepoda. *In*: Thorp J.H. & Covich A.P. (eds) *Ecology and Classification of North American Freshwater Invertebrates. 3rd Edition*. Academic Press, Amsterdam. https://doi.org/10.1016/B978-0-12-374855-3.00021-2

Saetang T., Marrone F., Vecchioni L. & Maiphae S. 2022. Morphological and molecular diversity patterns of the genus *Tropodiaptomus* Kiefer, 1932 (Copepoda, Calanoida, Diaptomidae) in Thailand. *Scientific Reports* 12: 2218. https://doi.org/10.1038/s41598-022-06295-4

Silva-Briano M. & Suárez-Morales E. 2010. Illustrated record of the freshwater copepod *Leptodiaptomus dodsoni* (Calanoida, Diaptomidae) from central Mexico with comments on the distribution of the genus. *Biota Neotropica* 10 (2): 409–414. https://doi.org/10.1590/S1676-06032010000200039

Smith K. & Fernando C.H. 1978. The freshwater calanoid and cyclopoid copepod Crustacea of Cuba. *Canadian Journal of Zoology* 56 (9): 2015–2023. https://doi.org/10.1139/z78-271

Suárez-Morales E. 2003. Historical biogeography and distribution of the freshwater calanoid copepods (Crustacea: Copepda) of the Yucatan Peninsula, Mexico. *Journal of Biogeography* 31 (7): 1051–1063. https://doi.org/10.1111/j.1365-2699.2003.00958.x

Suárez-Morales E. & Elías-Gutiérrez M. 2001. On the taxonomical status of *Arctodiaptomus dampfi* Brehm (Crustacea: Copepoda: Diaptomidae) with comments on *A. dorsalis* (Marsh). *Journal of Limnology* 60 (1): 11–18. https://doi.org/10.4081/jlimnol.2001.11

Suárez-Morales E., Segura L. & Fernández A.M. 1986. Diversidad y abundancia del plancton en la laguna de Catemaco, Veracruz durante un ciclo anual. *Anales del Instituto de Ciencias del Mar y Limnología de la Universidad Nacional Autónoma de México* 13 (3): 313–316.

Suárez-Morales E., Reid J.W., Illiffe T.M. & Fiers F. 1996. *Catálogo de los copépodos (Crustacea) continentales de la Península de Yucatán, México*. El Colegio de la Frontera Sur (ECOSUR) & Comisión Nacional para el Conocimiento y uso de la Biodiversidad (CONABIO), Chetumal.

Suárez-Morales E., Gutiérrez-Aguirre M.A., Gómez S., Perbiche-Neves G., Previattelli D., Dos Santos-Silva N., da Rocha C.E.F., Mercado-Salas N.F., Manriquez T.M., Cruz-Quintana Y. & Santana-Piñeros A.M. 2020. Class Copepoda. *In*: Damborenea C., Rogers C.D. & Thorp J. (eds) *Thorp and Covich's Freshwater Invertebrates: Volume 5: Keys to Neotropical and Antarctic Fauna*: 1046. Elsevier Science Publishing Co Inc. San Diego https://doi.org/10.1016/B978-0-12-804225-0.00021-6

Thum R.A. & Derry A.M. 2008. Taxonomic implications for diaptomid copepods based on contrasting patterns of mitochondrial DNA sequence divergences in four morphospecies. *Hydrobiologia* 614: 197–207. https://doi.org/10.1007/s10750-008-9506-x

Torres-Orozco R.E. & Zanatta S.A. 1998. Species composition, abundance and distribution of zooplankton in a tropical eutrophic lake: Lake Catemaco, México. *Revista de Biología tropical* 46 (2): 2511–5500.

Velázquez-Ornelas K.E., Suárez-Morales E. & Ayón-Parente M. 2021. *Catálogo de los Copépodos (Crustacea Copepoda Calanoida y Cyclopoida) de Cuerpos de Agua temporales del Estado de Jalisco, México: Taxonomía y Distribución*. El Colegio de la Frontera Sur, Chetumal.

Walter T.C. & Boxshall G. 2021. World of Copepods database. *Arctodiaptomus* Kiefer, 1932. Available from https://www.marinespecies.org/copepoda/aphia.php?p=taxdetails&id=346777 [accessed 15 Apr. 2026].

Wilson M.S. 1959. Calanoida. *In*: Edmondson W.T. (ed.) *Fresh-water Biology. Second edition*: 738–794. John Wiley & Sons, Inc., Seattle.

The members of the *EJT* consortium are: Muséum national d'Histoire naturelle, Paris, France; Royal Museum for Central Africa, Tervuren, Belgium; Royal Belgian Institute of Natural Sciences, Brussels, Belgium; Meise Botanic Garden, Meise, Belgium; Natural History Museum of Denmark, Copenhagen, Denmark; Naturalis Biodiversity Center, Leiden, the Netherlands; Museo Nacional de Ciencias Naturales-CSIC, Madrid, Spain; Leibniz Institute for the Analysis of Biodiversity Change, Bonn – Hamburg, Germany; National Museum of the Czech Republic, Prague, Czech Republic; The Steinhardt Museum of Natural History, Tel Aviv, Israel.

Supplementary material

Supp. file 1. Barcode material analyzed in this study, including sequences of Mexican *Mastigodiaptomus* Light, 1939, *Leptodiaptomus* Light, 1938, two species of *Arctodiaptomus* Kiefer, 1932 and *Metadiaptomus asiaticus* (Uljanin, 1875). * = represent material from the same ecoregion of the syntypes of *Mastigodiaptomus dorsalis* (Marsh, 1907) comb. nov.
https://doi.org/10.5852/ejt.2026.1120.3355.14693

Supp. file 2. Biological material revised in this study, in the Colección de Zooplancton (ECO-CH-Z) and Invertebrate Zoology Collection (USNM). * = syntypes. Samples labeled as *Arctodiaptomus dorsalis* (Marsh, 1907) and *Diaptomus dorsalis* Marsh, 1907 in the table, correspond to *Mastigodiaptomus dorsalis* (Marsh, 1907) comb. nov. as proposed in this study.
https://doi.org/10.5852/ejt.2026.1120.3355.14694

Supp. file 3. mPTP species delimitation groupings for the analyzed sequences of *Mastigodiaptomus* Light, 1939, *Leptodiaptomus* Light, 1938, *Arctodiaptomus* Kiefer, 1932, and *Metadiaptomus asiaticus* (Uljanin, 1875) selected as outgroup. https://doi.org/10.5852/ejt.2026.1120.3355.14695

Supp. file 4. mPTP species delimitation tree for the analyzed sequences of *Mastigodiaptomus* Light, 1939, *Leptodiaptomus* Light, 1938 and *Arctodiaptomus* Kiefer, 1932.
https://doi.org/10.5852/ejt.2026.1120.3355.14696

Supp. file 5. ASAP species delimitation tree. https://doi.org/10.5852/ejt.2026.1120.3355.14697